

Andreas Wolfsgruber, BSc

# Exploratory Studies in the Imino- and Carbasugar Area

## MASTER'S THESIS

to achieve the university degree of

Diplom-Ingenieur

Master's degree programme: Technical Chemistry

submitted to

**Graz University of Technology**

Supervisor

Ao.Univ.-Prof. Dipl.-Ing. Dr.techn. Arnold E. Stütz

Institute of Organic Chemistry, Graz University of Technology

2<sup>nd</sup> Supervisor

Prof. Gary B. Evans, PhD

Ferrier Research Institute, Victoria University of Wellington

## **AFFIDAVIT**

I declare that I have authored this thesis independently, that I have not used other than declared sources/resources, and that I have explicitly indicated all material which has been quoted either literally or by content from the sources used. The text document uploaded to TUGRAZonline is identical to the present master's thesis.

---

Date

---

Signature

*Für meine verstorbene Oma*

*Karoline Hattinger*

*Ever tried. Ever failed. No matter. Try Again. Fail again. Fail better.*

-Samuel Beckett

## **Acknowledgments / Danksagung**

*Mein erster und besonderer Dank gebührt Herrn Professor Arnold Stütz für die Möglichkeit, im Zuge meiner Masterarbeit ein weiteres Mal Teil seiner großartigen Arbeitsgruppe sein zu dürfen. Lieber Arnold, danke für den Glauben an mich sowie für alles, was ich von dir lernen durfte!*

*Mein herzlicher Dank gilt außerdem Frau Professor Tanja Wrodnigg für ihre Hilfsbereitschaft und Freundlichkeit. Liebe Tanja, danke für deinen Einsatz, mich zu fördern sowie für die lustigen Stunden im Kreise der Arbeitsgruppe. Ich freue mich, dass ich in den nächsten 3 Jahren mit dir zusammenarbeiten darf!*

*Großer Dank gilt auch meinen beiden „Mentoren“ Michael Schalli und Patrick Weber. Ich danke euch für eure unendliche Unterstützung, die guten Ratschläge und Tipps sowie für die lustigen Abende.....hoffentlich werden es noch mehr.*

*Weiters bedanke ich mich bei Martin Thonhofer und Manuel Zoidl für die praktischen Tricks und Tipps sowie für die großartige Zeit inner- und außerhalb des Labors. Außerdem möchte ich mich bei meinen Institutskolleginnen und –kollegen Astrid Thonhofer-Nauta, Peter Plachota, Peter Urdl, Carina Illaszewicz-Trattner und Prof. Hansjörg Weber für die gute Zusammenarbeit bedanken.*

*Ich durfte während meines Studiums viele Personen kennenlernen, die ich heute zu meinen Freunden zähle: Andi, Carina, Cori, Hanna, Mani, Peter, Silvan, Stefan und Tom, ihr habt die letzten Jahre unvergesslich gemacht. Nicht zu vergessen meine Volleyball-Runde: Bianca, Clemens, Christopher, Hanna (schon wieder), Julia, Juliane, Karin, Michi und Sebastian...danke für die lustigen Abende.*

*Außerordentlich dankbar bin ich für Annika. Ich danke dir für dein Verständnis, deine Ermutigungen und dafür, dass du nie von meiner Seite weichst.*

*Besonderer Dank gilt auch meinen Eltern für das Vertrauen und den Rückhalt in all den Jahren. In diesem Zusammenhang danke ich auch meiner Schwester Eva und ihrer Familie für das Engagement während meines Neuseeland-Aufenthaltes.*

*Furthermore, I would like to thank all members of the Ferrier Research Institute in Lower Hutt, New Zealand. I owe special thanks to my two supervisors Gary Evans and Peter Tyler for their encouragement and kindness. I also wish to thank Chris, Dan, Farah, Herbert, Karl, Keith, Lawrence, Li, Olga, Rachael and Ralf for your support and everything I have learned from you.*

## Abstract

Infections caused by RNA viruses such as the Human Immunodeficiency Virus, Hepatitis C virus, Ebola virus and Zika virus, continue to exist as global threats. The replication of RNA viruses relies on RNA-dependent RNA polymerases (RdRp) and therefore exhibits a high error frequency due to low fidelity and a lack of proofreading ability. Because of the lower accuracy, phosphorylated anti-viral nucleosides are utilized by the viral RNA polymerase which results in either the termination of chain elongation or apoptosis. Since the efficacy of such active agents depends strongly on the stepwise addition of phosphate groups through cellular kinases, techniques such as the ProTide technology from McGuigan have been discovered. The target of the first project was the preparation of potential anti-viral agents based on the iminoribitol-*C*-nucleoside scaffold. In addition, differences in the biological activities between the “free” nucleoside and the corresponding prodrug were investigated. Biological studies are currently ongoing.

Lysosomal storage diseases (LSDs) are a series of metabolic disorders with deficiencies of lysosomal enzymes caused by mutations of specific genes, responsible for their biosynthesis. Interestingly, 25 % of these enzymes are involved in the chemical manipulation of *N*-acetyl-*D*-glucosaminyl or *N*-acetyl-*D*-galactosaminyl residues from degradation-bound polysaccharides and glycoconjugates. Thus, the second project was focused on the synthesis of new powerful hexosaminidase inhibitors, for the treatment of lysosomal storage diseases by chaperon-mediated therapy. Starting from commercially available *N*-acetyl-*D*-glucosamine, two potential inhibitors, based on the carbafuranose scaffold, were synthesized. One of these structures turned out to be a powerful inhibitor of *N*-acetyl- $\beta$ -hexosaminidase (SpHex) with values of  $K_i = 1$  nM and  $IC_{50} = 9.4$  nM.

## Kurzfassung

Infektionskrankheiten wie z.B. das Hepatitis-C-Virus, das Ebola-Virus oder das Zika-Virus, die durch RNA-Viren entstehen, stellen nach wie vor eine Gefahr für die globale Gesundheit dar. Die Replikation von RNA-Viren beruht auf den RNA-abhängigen RNA-Polymerasen (RdRp), die aufgrund von geringer Genauigkeit und fehlender Korrekturfähigkeit eine hohe Fehlerquote aufweisen. In Folge dieser Ungenauigkeiten werden phosphorylierte anti-virale Nucleoside, welche das natürliche Substrat nachahmen, von der viralen RNA-Polymerase verwendet. Dadurch kommt es entweder zu einem Abbruch der Kettenverlängerung oder zum Zelltod. Da die Wirksamkeit solcher anti-viralen Nucleoside von der schrittweisen Phosphorylierung durch zelluläre Kinasen abhängig ist, wurden Techniken wie die ProTide-Technologie von McGuigan entwickelt. Das Ziel des ersten Projekts bestand in der Synthesisierung von potentiellen antiviralen Substanzen auf Basis des Iminoribitol-C-Nucleosid Gerüsts. Zusätzlich, wurden Unterschiede in den biologischen Aktivitäten zwischen dem "freien" Nucleosid und dem entsprechenden Prodrug untersucht. Die entsprechenden biologischen Studien sind noch nicht abgeschlossen.

Lysosomale Speicherkrankheiten sind Stoffwechselerkrankungen die durch Mutationen bestimmter Gene verursacht werden. Im Zuge dessen kommt es zu Fehlern in der Biosynthese von lysosomalen Enzymen. Rund ein Viertel dieser Enzyme sind am chemischen Abbau von *N*-Acetyl-D-Glucosaminy- oder *N*-Acetyl-D-Galactosaminy-Resten von Polysacchariden und Glycokonjugaten beteiligt. Aus diesem Grund, konzentrierte sich das zweite Projekt auf die Synthese von wirksamen Hexosaminidaseinhibitoren, die zur Behandlung von lysosomalen Speicherkrankheiten durch die „Chaperon-Therapie“ eingesetzt werden können. Ausgehend von kommerziell erhältlichem *N*-Acetyl-D-Glucosamin, erfolgte die Synthese von zwei potentiellen Hexosaminidaseinhibitoren welche auf dem Carbafulranose-Gerüst basieren. Eine dieser Strukturen erwies sich bereits als wirksamer Inhibitor von *N*-Acetyl- $\beta$ -hexosaminidase (SpHex) und erzielte Werte von  $K_i = 1$  nM und  $IC_{50} = 9.4$  nM.

## Table of Contents

1	Introduction .....	1
1.1	Carbohydrates.....	1
1.1.1	Monosaccharides .....	2
1.1.2	Oligo- and polysaccharides .....	3
1.2	Carbohydrate processing enzymes .....	4
1.2.1	Hydrolase mechanisms .....	6
1.2.2	Glycosidase inhibitors .....	8
1.2.3	Glycosphingolipids .....	14
1.2.4	Lysosomal storage diseases .....	16
1.3	Nucleoside processing enzymes .....	18
1.3.1	Iminosugars .....	18
1.3.2	Nucleoside- and nucleotide analogues.....	19
1.3.3	RNA viruses .....	23
2	Problem statement and aim of this work.....	25
2.1	Iminosugar nucleoside analogues as potential anti-viral agents .....	25
2.2	Furanoid carbasugars as GH 20 hexosaminidase inhibitors .....	26
3	Results and discussion.....	27
3.1	Iminoribitol-C-nucleosides .....	27
3.1.1	Synthesis of acetonitrile adducts .....	27
3.1.2	Synthesis of isothiazole-C-nucleosides .....	30
3.1.3	Synthesis of pyrrole-C-nucleosides .....	31
3.1.4	Synthesis of phosphorochloridates.....	32
3.1.5	Synthesis of pyrrole-C-nucleoside prodrug.....	32
3.1.6	Biological evaluation.....	33
3.2	Synthesis of <i>N</i> -substituted 3-acetamido-4-amino-5-hydroxymethylcyclopentanetriols .....	34
3.2.1	Synthesis of 2-acetamido-3- <i>O</i> -benzyl-2-deoxy- <i>D</i> -glucopyranoside .....	34
3.2.2	Conversion of the 6-hydroxy group into the corresponding alkyl halide .....	35
3.2.3	Reductive ring opening and [2+3] cycloaddition .....	36
3.2.4	Hydrogenolysis.....	36
3.2.5	<i>N</i> -Alkylation.....	37
3.2.6	Biological evaluation.....	38
4	Conclusion and Outlook .....	39



5	Experimental .....	41
5.1	General Methods.....	41
5.2	Iminoribitol- <i>C</i> -Nucleosides <sup>s</sup> .....	43
5.2.1	Synthesis of acetonitrile adduct.....	43
5.2.2	Synthesis of isothiazole- <i>C</i> -nucleosides .....	44
5.2.3	Synthesis of pyrrole- <i>C</i> -nucleosides .....	45
5.2.4	Synthesis of the phosphoramidate compound .....	48
5.2.5	Synthesis of pyrrole- <i>C</i> -nucleoside prodrug.....	48
5.3	Synthesis of <i>N</i> -Substituted 3-Acetamido-4-amino-5-hydroxymethylcyclopentane-1,2,6-triols .....	50
5.3.1	Synthesis of 3-Acetamido-4-amino-5-hydroxymethylcyclopentanetriol .....	50
5.3.2	<i>N</i> -Alkylated products .....	54
5.3.3	Synthesis of <i>N</i> -benzylhydroxylamine .....	55
6	References.....	56
7	Appendix .....	60
7.1	Abbreviations .....	60
7.2	List of publications.....	62
7.3	Curriculum vitae .....	63

# 1 Introduction

From the beginning of human kind, people have tried to heal injuries and illnesses. Since prehistoric time, medicine men have applied leaves, oils, roots and extracts from the surrounding flora and fauna as a cure.<sup>1</sup> The traditional Chinese phytochemistry, for example, is based upon the mulberry (*Morus alba*), a fruit which was also the major component of European's Haarlem oil. Haarlem oil was the first medication produced on an industrial scale and was used against diabetes in the 17<sup>th</sup> century. The active agent of the white mulberry is the so called 1-deoxynojirimycin (DNJ) (**1**) (**Figure 1**), a carbohydrate structure where the endocyclic oxygen is replaced by a trivalent nitrogen atom.<sup>2</sup> I. Sangster, a co-worker of H. Paulsen, was the first to synthesize DNJ in 1966 without knowledge of its biological properties. It was not until 1976 when DNJ was isolated from nature and its medical potential was revealed.<sup>3</sup> Nowadays, chemists still try to copy and modify naturally occurring carbohydrate structures in order to use them as active agent. These compounds are called "Carbohydrate mimetics". Since their biological activity has been discovered, the interest in this research area has grown significantly.

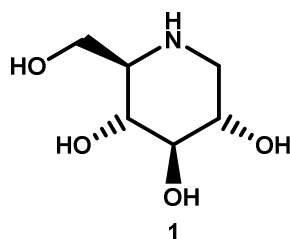


**Figure 1:** 1-deoxynojirimycin (DNJ).

## 1.1 Carbohydrates<sup>4,5</sup>

Carbohydrates, also known as sugars, are the most frequently occurring organic structures in nature. With more than 50 %, they account for the largest share of biomass on earth with cellulose leading as the major final product of photosynthesis. But, they are not only an effective biological energy source, in fact, carbohydrates perform numerous roles in living organisms. According to today's state of knowledge, they are part of structural frameworks as well as are responsible for the regulation and sustainability of various metabolic pathways.

The first carbohydrate chemists defined the empirical formula as  $C_n(H_2O)_n$ , which indicates a ratio of hydrogen to oxygen of 2:1 and therefore, not much structural diversity would be assumed in the first place. But as a result of the high number of stereochemical relations, several positions to introduce hetero atoms such as sulfur and nitrogen and various options

to connect carbohydrate units, carbohydrate chemistry provides a challenging playground for every researcher.

In general, carbohydrates can be categorized by their number of repeating units. The smallest structure is called monosaccharide which consists of just one sugar unit. Moreover, there are disaccharides (2 units), oligosaccharides (3 to 9 units) and polysaccharides (more than 9 units). Furthermore, homo and hetero saccharides can be distinguished. If a saccharide is formed by the identical carbohydrate motifs, it is called homo oligo- or homo polysaccharide. When the connection takes place between different monosaccharides, the structure is named hetero oligo- or hetero polysaccharide.

### 1.1.1 Monosaccharides

Monosaccharides can be classified by several criteria like the position of the carbonyl group (aldose at C-1 and ketose mainly at C-2), the number of carbon atoms (3 C = triose, 4 C = tetrose, 5 C = pentose, 6 C = hexose, et cetera) or the different configurations of the stereo centers, for example: D-manno or D-gluco. The simplest monosaccharide, glyceraldehyde, a triose (3 C), belongs to the group of aldehydes since its carbonyl group exists in form of an aldehyde at position C-1. Furthermore, the aldotriose contains of one stereo center, therefore two stereo isomers are possible, namely the (R)-configured D-glyceraldehyde and the (S)-configured L-glyceraldehyde (**2**). These two epimers were used by Emil Fischer for the historic determination of D/L-sugars. If using the Fischer projection for looking at the molecule, the last chiral carbon atom (furthest from the carbonyl group) is either on the right side (D) or on the left side (L) (**Figure 2**). In original, this nomenclature refers to the optical rotation of glyceraldehydes when they are exposed to polarized light. If the light was turned to the right, the structure was labeled with the Latin term *dexter* and if the other case occurred, it was named *laevo* (left). This, on rotation based convention just accidentally was similar with the configuration in the Fischer projection.

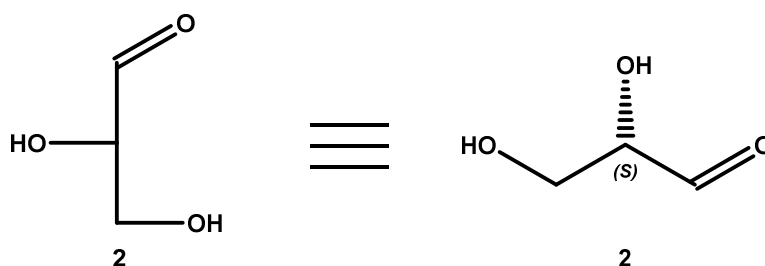


**Figure 2:** Fischer projection (left) and skeletal formula (right) of L-glyceraldehyde (**2**).

Due to thermodynamic reasons, monosaccharides rarely exists as open-chain structures. Instead, they form hemiacetals using the oxygen of a hydroxy group and the carbonyl

function on C-1 in an intramolecular fashion. Hexoses, for example, are able to form stable five- and six-membered ring systems, depending on the hydroxy group which is involved in the hemiacetal formation. This spontaneous cyclisation creates an additional stereo center at the former carbonyl carbon position, called anomeric center. The two possible isomers on the anomeric carbon are referred to as the  $\alpha$ - or  $\beta$ -form, depending on whether the absolute configuration is different or similar to the anomeric reference atom. In **Figure 3**, all possible pyranoid and furanoid forms of D-glucose (**3**) are shown.

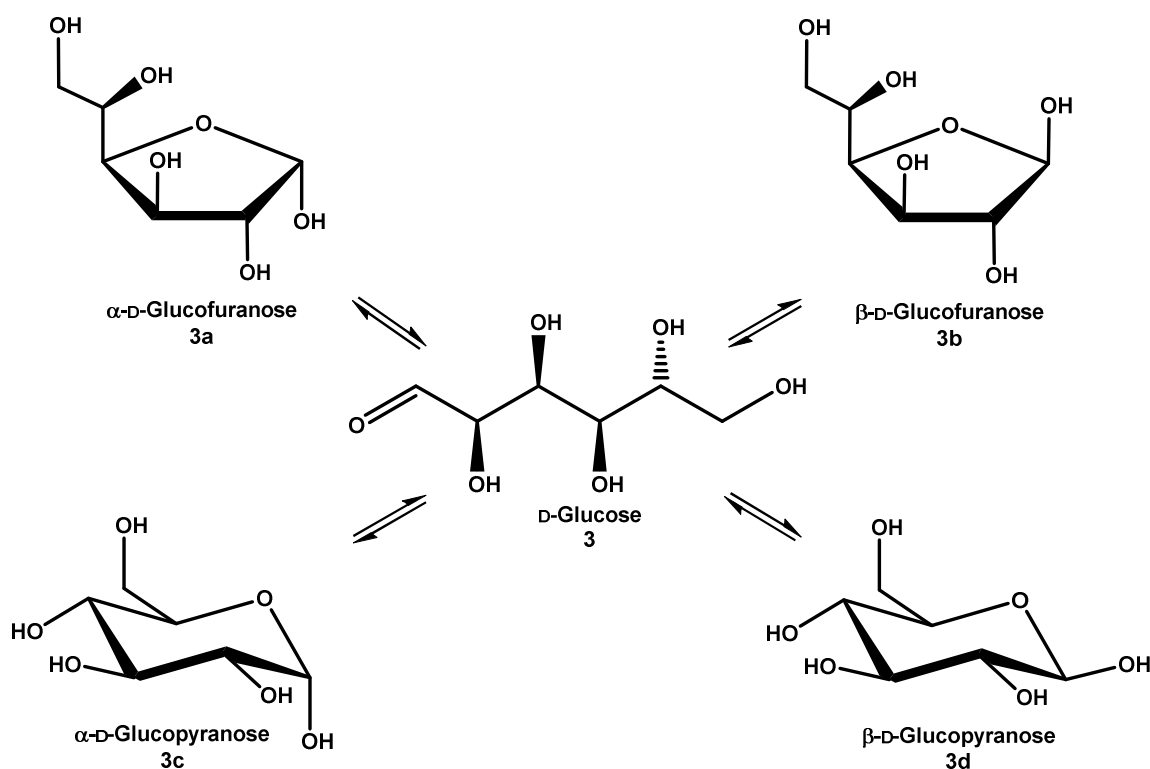


**Figure 3:** Possible forms of D-glucose.

### 1.1.2 Oligo- and polysaccharides

Linked monosaccharides are called oligo- or polysaccharides. They can occur as linear chains like cellulose, as branched structures like amylopectin or as cyclic moieties called cyclodextrins. Furthermore, there are various possibilities of the connection of monomers. A D-glucopyranose molecule, for example, has four hydroxy groups, which can be linked to another D-glucopyranose molecule at the anomeric center via a so called O-glycosidic bond, which can either have a  $\alpha$ - or  $\beta$ -configuration. Additionally, bonds between the anomeric centers can be made, either in form of an  $\alpha$ - $\alpha$ ,  $\beta$ - $\beta$  or  $\alpha$ - $\beta$  linkage. Gentiobiose (**4**), which is incorporated into the chemical structure of crocin (gives saffron its colour<sup>6</sup>), is an example for a  $\beta(1\rightarrow6)$  linkage, while trehalose (**5**), for the first time isolated from rye<sup>7</sup>, is an  $\alpha(1\rightarrow1)$  glycosidically linked disaccharide. The chemical structures of gentiobiose (**4**) and trehalose (**5**) are visualized in **Figures 4 and 5**.

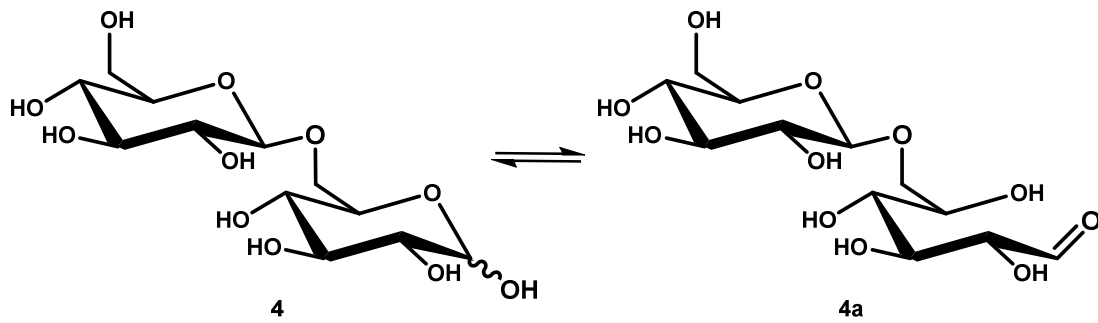


**Figure 4:** Gentiobiose as an example for a reducing sugar.

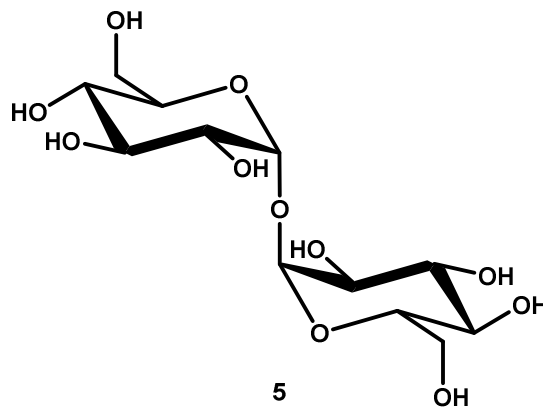


**Figure 5:** Trehalose as an example for a non-reducing sugar.

A further difference between the disaccharides shown in **Figures 4 and 5** is the hemiacetal function in gentiobiose (**4**) as opposed to the acetal in trehalose (**5**). The remaining aldehyde of gentiobiose (**4**) can act as a reducing agent, while undergoing oxidation to the carboxylic acid. In terms of biological and chemical properties of carbohydrate structures this reducing end becomes interesting.

## 1.2 Carbohydrate processing enzymes

As a result of the ongoing research in carbohydrates, various enzymes were found that are responsible either for the degradation or the synthesis of carbohydrates. The formation of glycosidic bonds is achieved by glycosyltransferases, in which sugar donors with a lipid- or nucleoside-bound phosphate leaving group are utilized. Glycosyltransferases are essential in many biological processes like cell wall biosynthesis and cell signalling. They act in prokaryotic and in eukaryotic cells. In the latter case they mainly exist as membrane proteins of the Golgi apparatus<sup>8</sup>. The selective cleavage of glycosidic bonds is performed by glycosyl hydrolases which are also known as glycosidases. They are important for the degradation of oligo- and polysaccharides as well as for the cleavage of glycosphingolipids and glycosaminoglycans.

The reaction principle of glycosyl hydrolases is depicted in **Figure 6**.

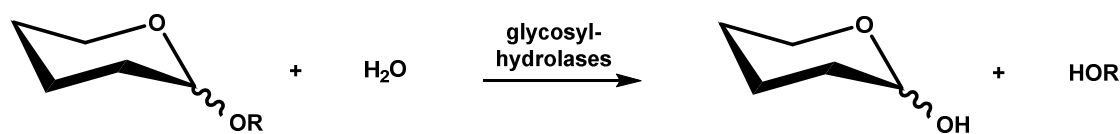


**Figure 6:** General principle of glycosyl hydrolases.

### Classification using enzyme commission number (EC)<sup>9</sup>

The Enzyme commission number classifies enzymes according to the catalysed chemical reaction. If different enzymes catalyse the same reaction, they have the same EC number. For example, enzymes that hydrolyse (EC 3.x) glycosidic bonds (EC x.2) are taken together as glycosyl hydrolases (EC 3.2). Additionally, they can be divided into further classes like *O*- and *S*- glycosidic cleaving hydrolases (EC 3.2.1) and *N*-glycosidic hydrolases (EC 3.2.2).

### Sequence-based classification

Since the EC system is not reflecting all structural features of an enzyme, the sequence based classification has been established. In this process, glycoside hydrolases have been divided into more than 100 families and 14 clans by using algorithmic methods. To do this, at least parts of the amino acid or nucleotide sequence must be known. Each glycosyl hydrolase family (GH) has related characteristics in terms of structural and mechanistic properties.<sup>15</sup>

### Classification as *exo*- or *endo*-glycosidases

The difference between *exo*- and *endo* glycosidases relates to the capability of the enzyme to cleave the substrate either at the non-reducing end, which signifies this specific enzyme as an *exo*-glycosidase, or cleaving at some point in the middle of the substrate chain, which classifies this enzyme as an *endo* glycosidase. While the most *exo*-glycosidases are acting at the non-reducing end, some exceptions for reducing end *exo*- glycosidases are noted.<sup>10</sup> An overview is given in **Figure 7**.

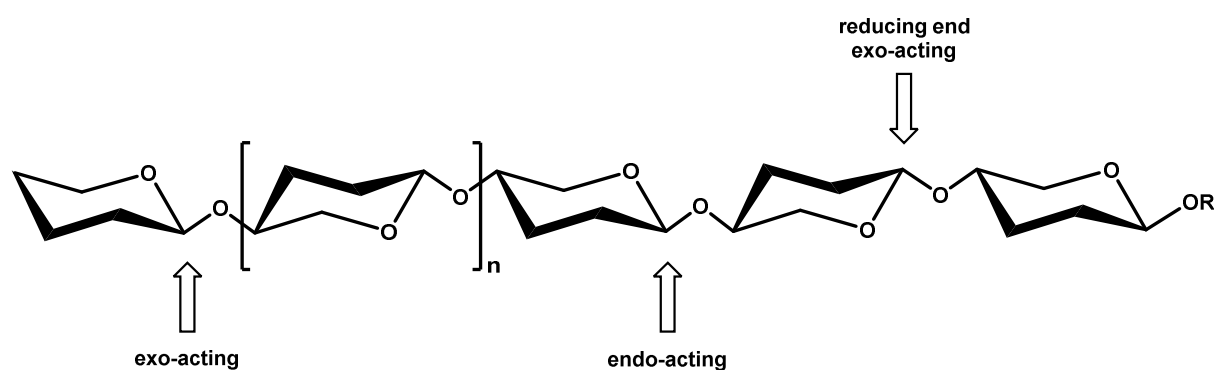


**Figure 7:** Cleaving points on a substrate chain.

### 1.2.1 Hydrolase mechanisms

Another way to categorize glycosyl hydrolases is according to the stereochemical outcome at the anomeric position. If the absolute configuration at the anomeric center is inverted during hydrolysis, the respective glycosidase is referred to as *inverting glycosidase*. In case, the configuration remains, the enzyme is considered a *retaining glycosidase*. In both cases are amino acids like aspartic- or glutamic acid acting as acid and activating base, respectively. The spatial distance between the two carboxyl moieties in the active site is the primary difference between inverting and retaining glycosidases. While during the inverting process the amino acids are located 6-12 Å apart from each other, they are found closer together in retaining glycosidases with an approximate distance of 5 Å.<sup>11,12</sup>

#### Inverting glycosyl hydrolases

During the first step of an inverting mechanism an activated water molecule attacks the anomeric carbon and simultaneously the glycosidic oxygen is protonated. The formed oxocarbenium-ion transition state leads to a direct substitution of the aglycon in which the absolute configuration at the anomeric position becomes inverted.<sup>13,14</sup> In **Figure 8**, it changes from  $\beta$  to  $\alpha$ .

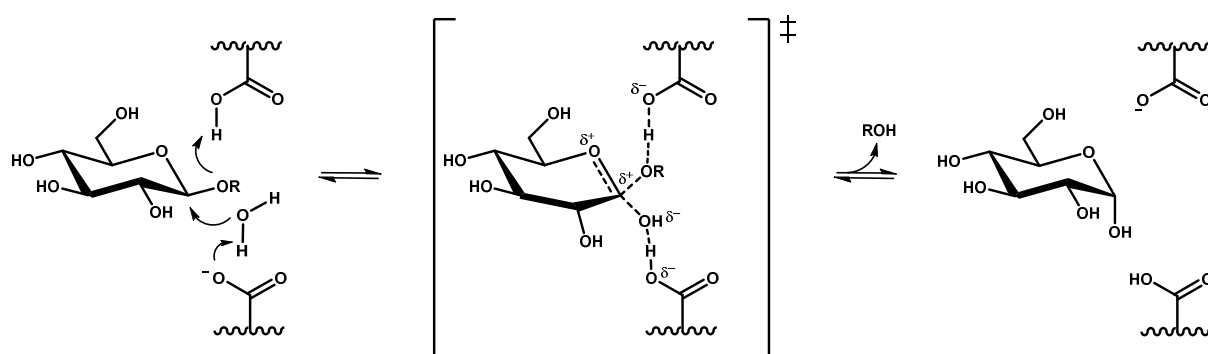


**Figure 8:** Mechanism of an inverting  $\beta$ -glucosidase.<sup>12</sup>

#### Retaining glycosyl hydrolases

Classical double-displacement mechanism

During the first step of the double-displacement mechanism the anomeric carbon is directly attacked by the carboxylic residue forming the first oxocarbenium transition state. Thereby, the protonated aglycon is liberated and the carbohydrate is establishing a covalent linkage to the carboxylic residue with inverted configuration. Furthermore, an activated water molecule attacks the anomeric center which forms the second transition state. At the end, a hydrolyzed carbohydrate moiety with inverted configuration on C-1 is released (**Figure 9**).<sup>13</sup> During this mechanism the water molecule and the aglycon are never part of the same transition state, which explains the shorter distance between the two carboxylic residues.

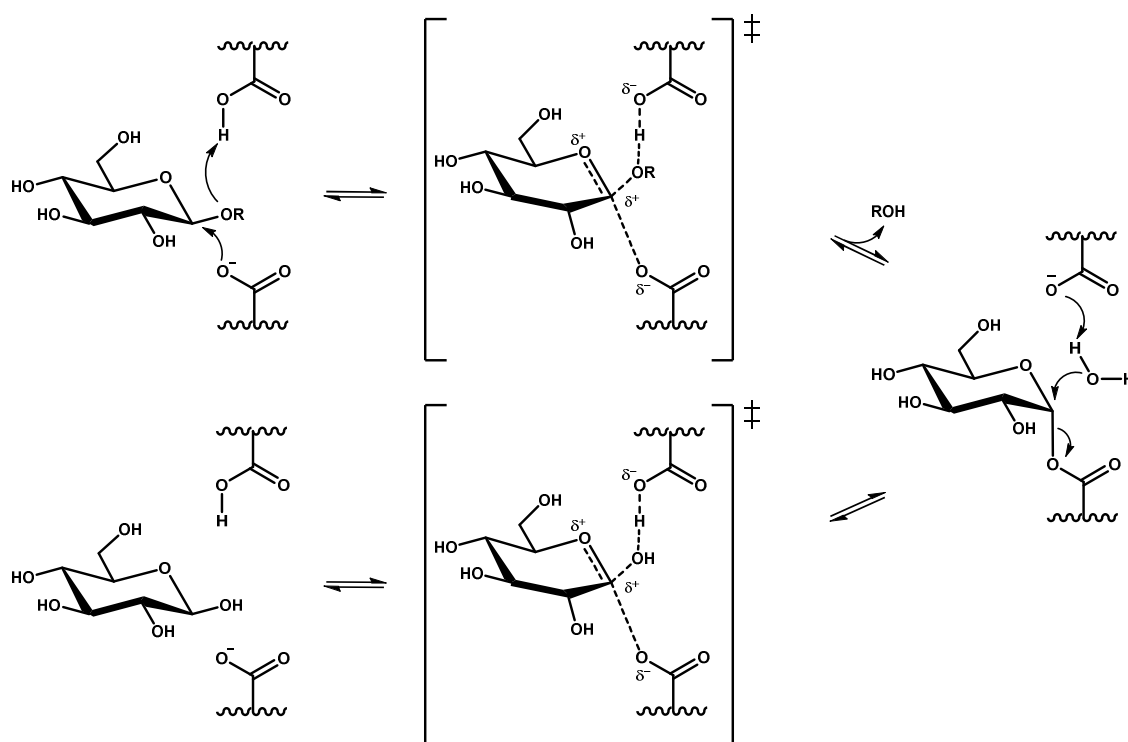


**Figure 9:** Mechanism of a retaining  $\beta$ -glucosidase.<sup>12</sup>

#### Neighbouring-group participation

Moreover, substrates bearing an acetamido group on position C-2 are following a retaining mechanism as well.  $\beta$ -Hexosaminidases Hex A and Hex B, for example, are acting via intramolecular anchimeric assistance of the *N*-acetyl group providing an intermediary oxazolinium ion, which is further attacked by an activated water molecule to provide “free” *N*-acetylhexosamine. Following this mechanism, the second carboxylate do not serve as a catalytic nucleophile, instead it stabilizes the charge development in the transition states (**Figure 10**). However, not all enzymes cleaving substrates bearing a 2-acetamido group are necessarily following the neighbouring group mechanism. There are examples such as *N*-acetyl- $\alpha$ -D-galactosaminidase and *N*-acetyl- $\alpha$ -D-glucosaminidase which are working by the classical double displacement pathway (**Figure 9**).



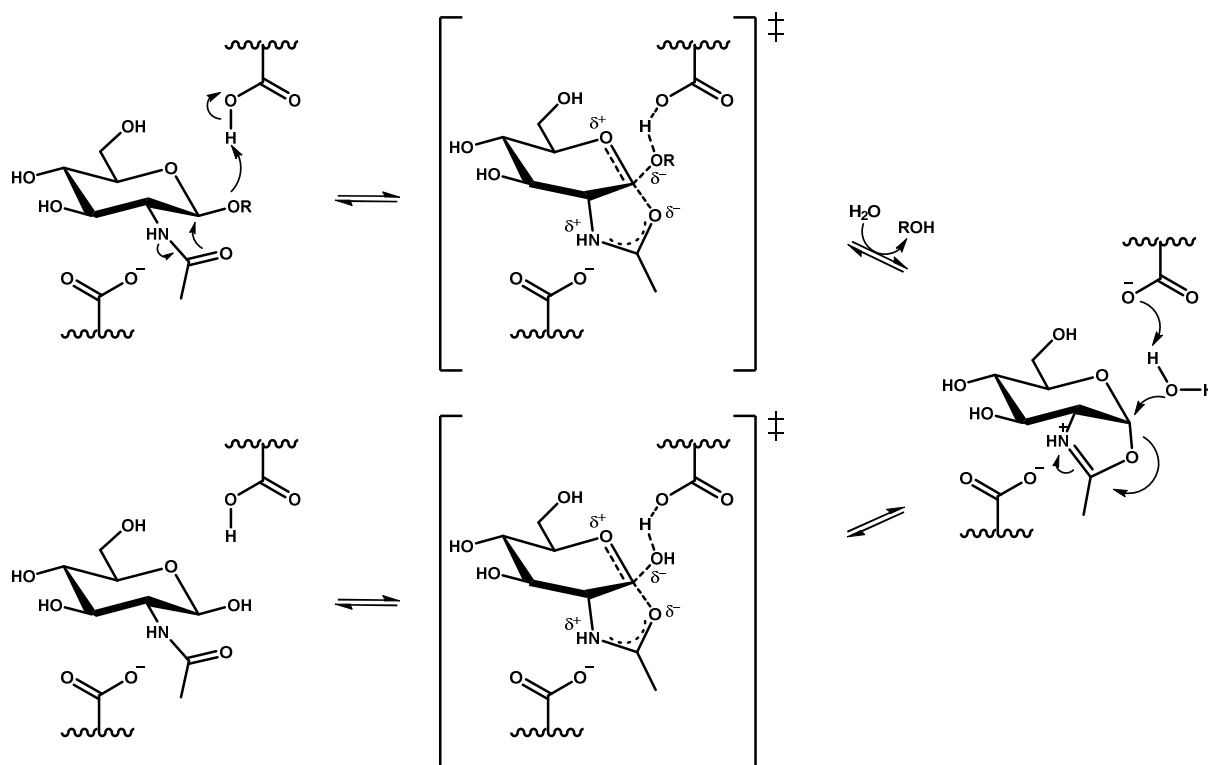


Figure 10: Mechanism based on anchimeric assistance of GH 20 enzymes.<sup>15</sup>

### 1.2.2 Glycosidase inhibitors

Since the importance of glycosidases in metabolic pathways of living organisms has been discovered, small molecules which can influence these types of enzymes, named glycosidase inhibitors, have become interesting. The key idea of carbohydrate chemists is based on the structural resemblance of potential inhibitors to the natural substrates, which should improve the recognition in the active site. These inhibitors can either be synthetically designed or naturally occurring, they can act irreversibly or reversibly and they can be carbohydrate- or non-carbohydrate based.

An example for a naturally occurring reversible glycosidase inhibitor is kushenol A (**6**) (**Figure 11**), a flavonoid derived non carbohydrate structure isolated from *Sophora flavescens*.<sup>16</sup>

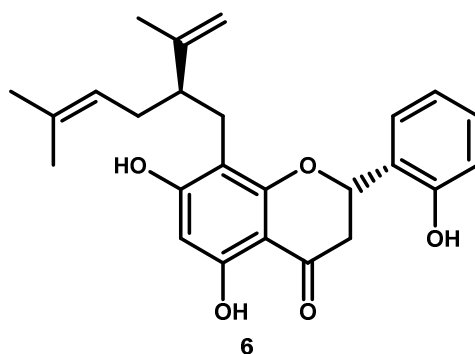
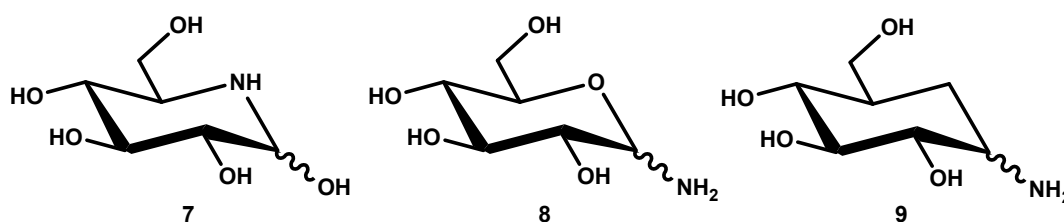


Figure 11: Kushenol A as an example for a non-carbohydrate reversible inhibitor.

However, the most frequently exploited reversible glycosidase inhibitors are analogues of the enzyme's natural substrates with an incorporated trivalent nitrogen. Nojirimycin (**7**), for example, is one of the most prominent inhibitors and has to be assigned to the group of iminosugars, in which the endocyclic oxygen is replaced by a nitrogen atom.<sup>17</sup> Additionally, the nitrogen can be linked glycosidically as an amine, like in glycosylamine (**8**), which belongs to the group of glycosylamines.<sup>18</sup> The class of carbasugars which are linked to an exocyclic nitrogen moiety are called amino-carbasugars (for example validamine (**9**)) and were first isolated from bacteria.<sup>19,20</sup> Examples of reversible glycosidase inhibitors with an incorporated nitrogen group are visualized in **Figure 12**.



**Figure 12:** Examples of nitrogen containing reversible inhibitors.

The mechanistic principle of these nitrogen bearing inhibitors originates from the strong ionic bonds between the positively charged protonated nitrogen and the negatively charged carboxylic acid moiety of the enzyme's active site. The ionic character of nojirimycin (**7**) is demonstrated in **Figure 13**.

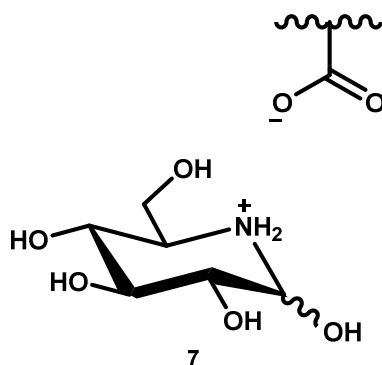


**Figure 13:** Ionic character of nojirimycin (**7**).<sup>21</sup>

In case of irreversible compounds, the carboxylic group of the enzyme's active site binds covalently to the inhibitor and results in complete inactivation of the enzyme. These molecules, for example epoxide- (**10**)<sup>22</sup> or aziridine<sup>23</sup> based sugar derivatives, are used for mechanistic investigations instead of enzyme modulation. The mechanism of an irreversible inhibition is demonstrated in **Figure 14** in which conduritol B-epoxide (**10**) is used as active agent. The structural symmetry of epoxide **10** enables activity towards  $\alpha$ - and  $\beta$ -configured enzymes.<sup>24</sup>

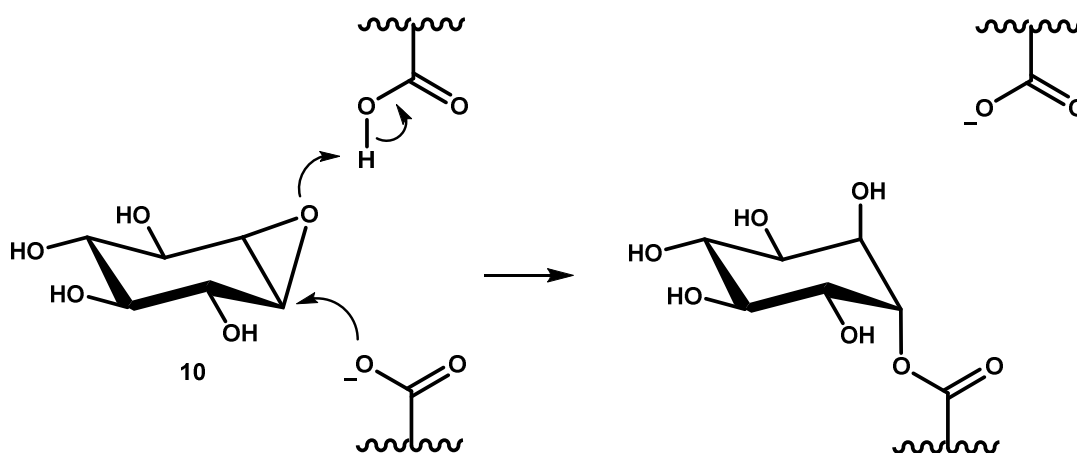


Figure 14: Irreversible inhibition by conduritol B-epoxide (**10**).<sup>25</sup>

### Hexosaminidase inhibitors

Half of the carbohydrate processing enzymes, which are related to lysosomal storage diseases, are involved in the catalytic removal of *N*-acetyl-D-galactosaminy or *N*-acetyl-D-glucosaminy moieties from degradation-bound glycoconjugates and polysaccharides. Therefore, intensive investigation towards small molecules which are interacting with specific glucosaminidases or galactosaminidases has been already initiated, but, especially for *N*-acetylhexosaminidases Hex A and Hex B just a few inhibitors have been reported so far (Figure 15).<sup>26</sup>

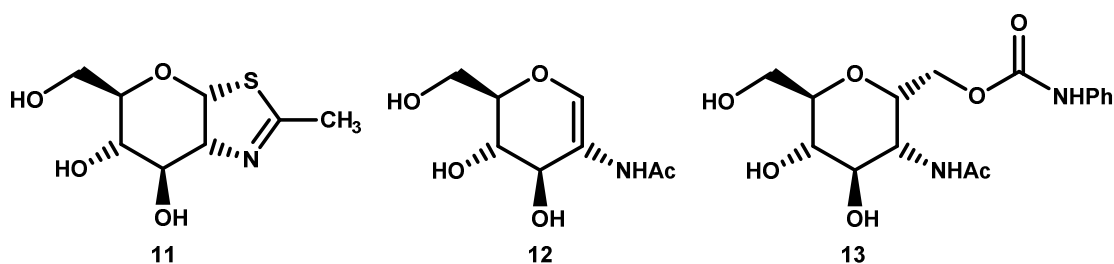


Figure 15: Hexosaminidase inhibitors based on pyranoid carbohydrates.

Compounds such as NAG-thiazole (**11**) and NA-glucal (**12**) are tight binding inhibitors with  $K_i$  values of 2.4  $\mu\text{M}$  and 2.8  $\mu\text{M}$  (SpHexWT) respectively.<sup>27,28</sup> Moreover, the (phenylcarbamoyl)oxime PUGNac (**13**) was identified as an outstanding inhibitor of  $\beta$ -GlcNAcase with a  $K_i$  value of 40 nM with the *M. rouxii* fungal enzyme.<sup>29</sup>

Among *N*-acetylhexosaminidase inhibitors based on the iminosugar structure, 2-acetamido-1,2-dideoxynojirimycin (**14**) and its diastereomers such as the *D-allo* (**16**) and the *D-galacto* (**17**) analogs have to be mentioned. Furthermore, compounds such as LABNac (**18**) and the respective *N*-benzylated version *N*Bn-LABNac (**19**) as well as bicyclic molecules like 6-acetamido-6-deoxycastanospermine (**20**), 6-epi(-)-pochonicine (**21**) and nagstatin (**22**) have been reported (Figure 16).

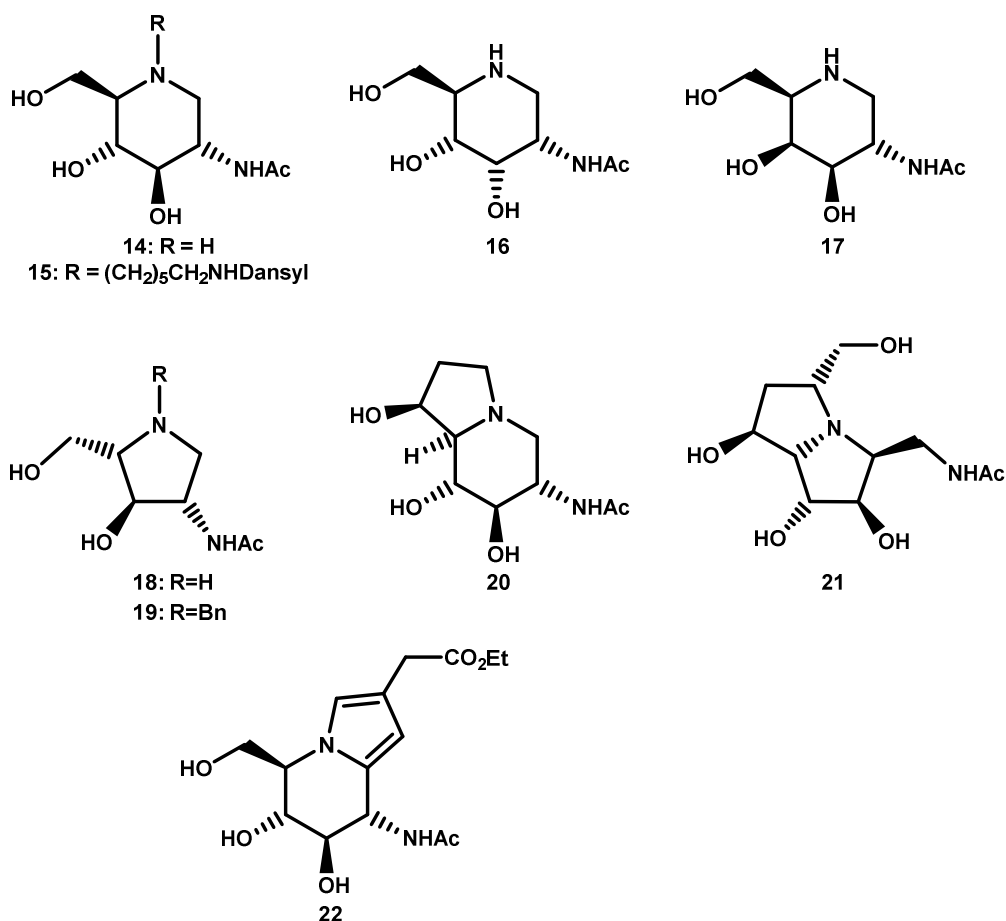
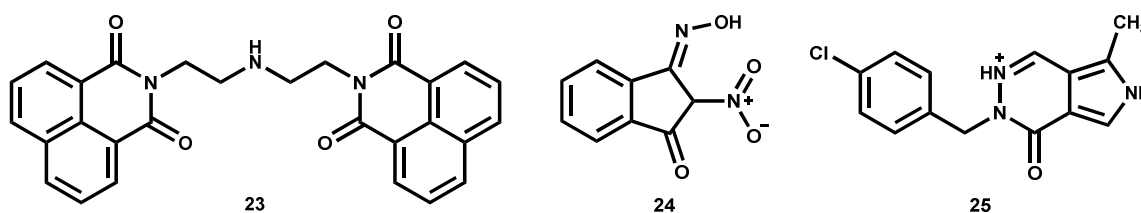


Figure 16: Iminosugar based *N*-acetyl-*D*-hexosaminidase inhibitors.

Table 1: Biological activity of iminosugar based structures.

Comp.	$K_i$ [ $\mu$ M]	$IC_{50}$ [ $\mu$ M]	Enzyme
14	80		$\beta$ - <i>D</i> -hexosaminidase from <i>Streptomyces plicatus</i> <sup>30</sup>
15	1.8		
16	2.6		$\beta$ - <i>N</i> -acetylglucosaminidase from jack bean <sup>31</sup>
17	1.8	2.2	$\beta$ - <i>N</i> -acetylglucosaminidase from jack bean <sup>32</sup>
18		3.4	$\beta$ - <i>N</i> -acetyl- <i>D</i> -glucosaminidase from jack bean <sup>33</sup>
19		5.2	
20		0.5	$\beta$ - <i>N</i> -acetylglucosaminidase from human placenta <sup>34</sup>
21		273	$\beta$ - <i>N</i> -acetylglucosaminidase from jack beans (37°C, pH 5) <sup>35</sup>
22	0.017		<i>N</i> -acetyl- $\beta$ - <i>D</i> -glucosaminidase from hog kidney <sup>36</sup>

Additionally, due to the screening of the Maybridge- and NINDS library, three non-carbohydrate molecules were identified to be *N*-acetyl- $\beta$ -hexosaminidase inhibitors with  $K_i$  values in the low  $\mu\text{M}$  range and, simultaneously, do not inhibit other lysosomal enzymes. Structure **23** acts as a competitive inhibitor with a  $K_i$  value of  $0.8 \mu\text{M}$  and is therefore an important advice on the way to potential pharmacological chaperons for Tay-Sachs and Sandhoff diseases. In **Figure 17**, recently discovered non-carbohydrate  $\beta$ -D-*N*-acetylhexosaminidase inhibitors are illustrated.<sup>27</sup>



**Figure 17:** Non-carbohydrate hexosaminidase inhibitors.

### Carbasugars<sup>37</sup>

The year 1966 was an important year for many carbohydrate chemists. Not only the famous 1-deoxynojirimycin (DNJ) (**1**) was synthesized for the first time<sup>3</sup>, also the first synthesis of a carbasugar was reported.<sup>38</sup> In this new class of carbohydrate molecules, formerly known as “pseudosugars”, the ring oxygen is replaced by a methylene group. In **Figure 18**, the first carbasugar achieved via synthesis, 5a-carba- $\alpha$ -D-talopyranose (**26**) and 5a-carba- $\alpha$ -D-galactopyranose (**27**), which was obtained via isolation from bacteria, are visualized.<sup>39</sup>

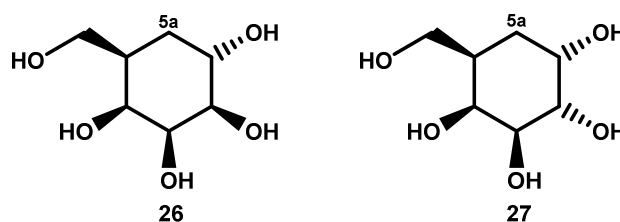


**Figure 18:** First representatives of carbasugars.

Carbasugar structures such as derivatives of cyclohexane or cyclohexene and their nitrogen containing analogues, have been broadly investigated in the past decades.<sup>40</sup> Since their biological activity has been discovered, especially amino sugar compounds, for example, validamines (**28**) and valienamines (**29**) (**Figure 19**), which can be found in nature as parts of more complex molecules like acarbose, have become interesting.<sup>41</sup> Through developments in organic synthesis, a range of derivatives of valienamines and validamines could be synthesized and tested for their biological efficacy. It became apparent, that 1,4-di-epi-D-valienamine- and 1,4-di-epi-D-validamine derivatives are potent inhibitors for  $\beta$ -galactosidases. NOEV (**30**), for example, a benchmark molecule in this area, has a  $K_i$  value

of 0.87  $\mu\text{M}$  with  $\beta$ -galactosidase from bovine liver.<sup>37</sup> Recently, the Glycogroup Graz has successfully synthesized a range of C-5a-modified validamine derivatives. Compound **31** turned out to be a tight binding inhibitor with a  $K_i$  value of 1.9 nM, when tested against Abg ( $\beta$ -glucosidase/ $\beta$ -galactosidase) from *Agrobacterium* sp.<sup>37</sup>

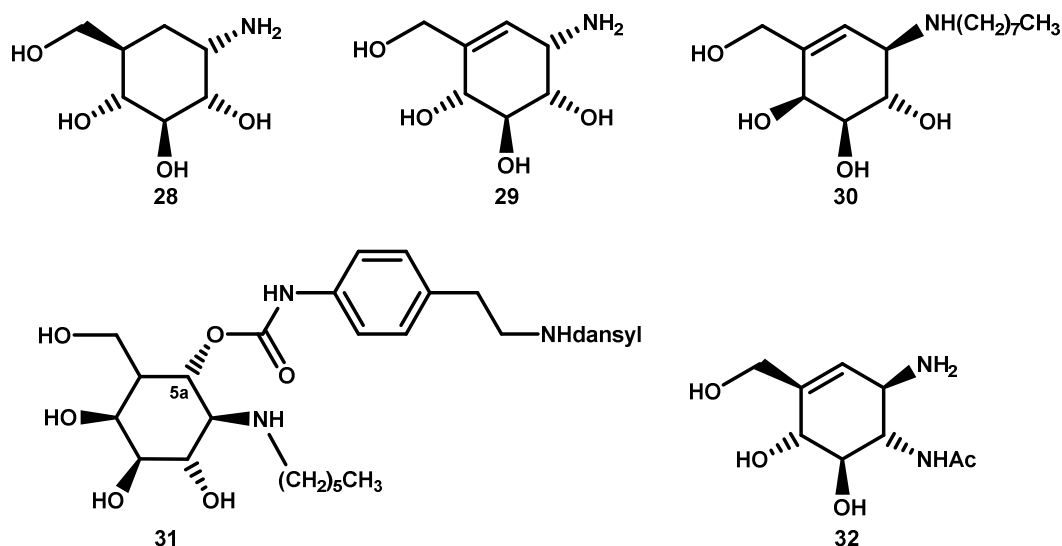


Figure 19: Examples of amino-carbasugars.

In case of hexosaminidase inhibitors based on the carbapyranose structure, the 2-acetamido derivative of 1-epi-valienamine (**32**) has to be mentioned. The compound was tested against the family 20 human placental  $\beta$ -hexosaminidase and achieved a  $K_i$  value of 34  $\mu\text{M}$ .<sup>42</sup>

Akin to the valienamines and validamines mentioned, carbafranoses are, when found in nature, mainly parts of larger molecules, for example, carbanucleosides.<sup>43</sup> Synthetic 5-membered carbasugars with biological activity are shown in **Figure 20**. Structure **33**, first reported by Jäger,<sup>44</sup> and compound **34**,<sup>37</sup> are highly potent inhibitors with  $K_i$  values of 1.0 nM and 1.2 nM respectively against Abg ( $\beta$ -glucosidase/ $\beta$ -galactosidase) from *Agrobacterium* sp.<sup>37,44</sup>

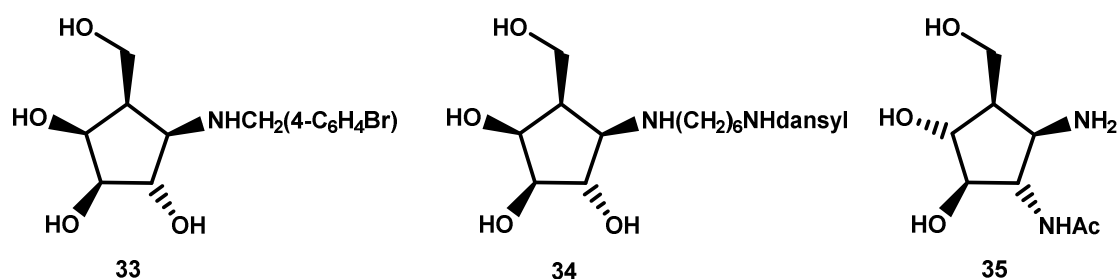


Figure 20: Inhibitors based on the 5-membered carbasugar structure.

Focusing on hexosaminidase inhibitors based on the carbafranoses scaffold, 2-acetamido-1-amino- $\beta$ -D-gluco-cyclopentane **35** was reported as a potent inhibitor of GH 20

hexosaminidases from jack beans and bovine epididymis with  $K_i$  values of 0.39  $\mu\text{M}$  and 0.65  $\mu\text{M}$ , respectively.<sup>44</sup>

### 1.2.3 Glycosphingolipids

Glycosphingolipids (GSLs), for the first time reported in 1884, are important structures of mammalian cell walls.<sup>45</sup> They are generally consisting of a mono- or polysaccharide unit which is *O*-glycosidically linked to a hydrophobic fatty acid *N*-acylated moiety, such as sphingosine or ceramides. In **Figure 21**, the setup of the general structure of glycosphingolipids is visualized.<sup>46</sup>

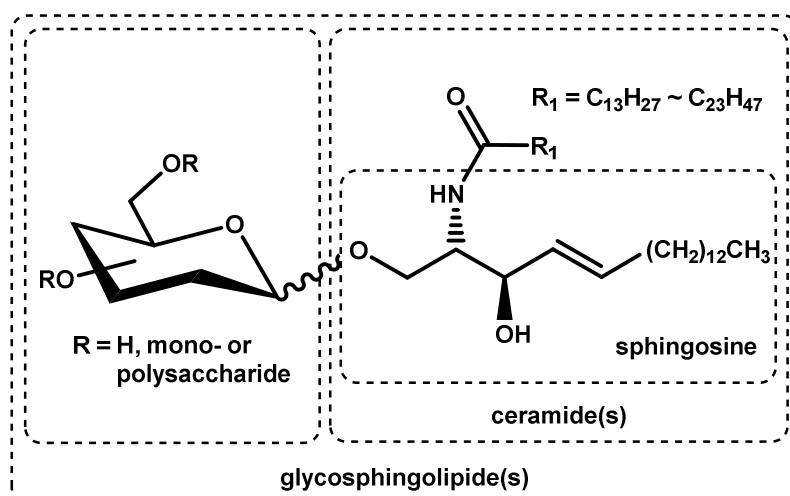


**Figure 21:** General structure of GSLs.

As a result of the high structural variability of GSLs, they can differ in type, number and linkage of the respective sugar moiety as well as in all kinds of lipophilic aglycons, they play a vital role in a range of relevant processes like cell-cell interactions, receptor modulation and signal transduction.

Glycosphingolipids are catabolized in the acidic parts of a cell which are the lysosomes and the late endosomes. This process includes the specific cleavage of carbohydrate units by lysosomal *exo-glycosyl* hydrolases starting from the non-reducing end of the structure. This degradation of GSLs is essential for life whereby disorders in the catabolism of these molecules are associated with various illnesses like the lysosomal storage diseases.<sup>47</sup> An overview of the degradation pathway of glycosphingolipids is given in **Figure 22**.

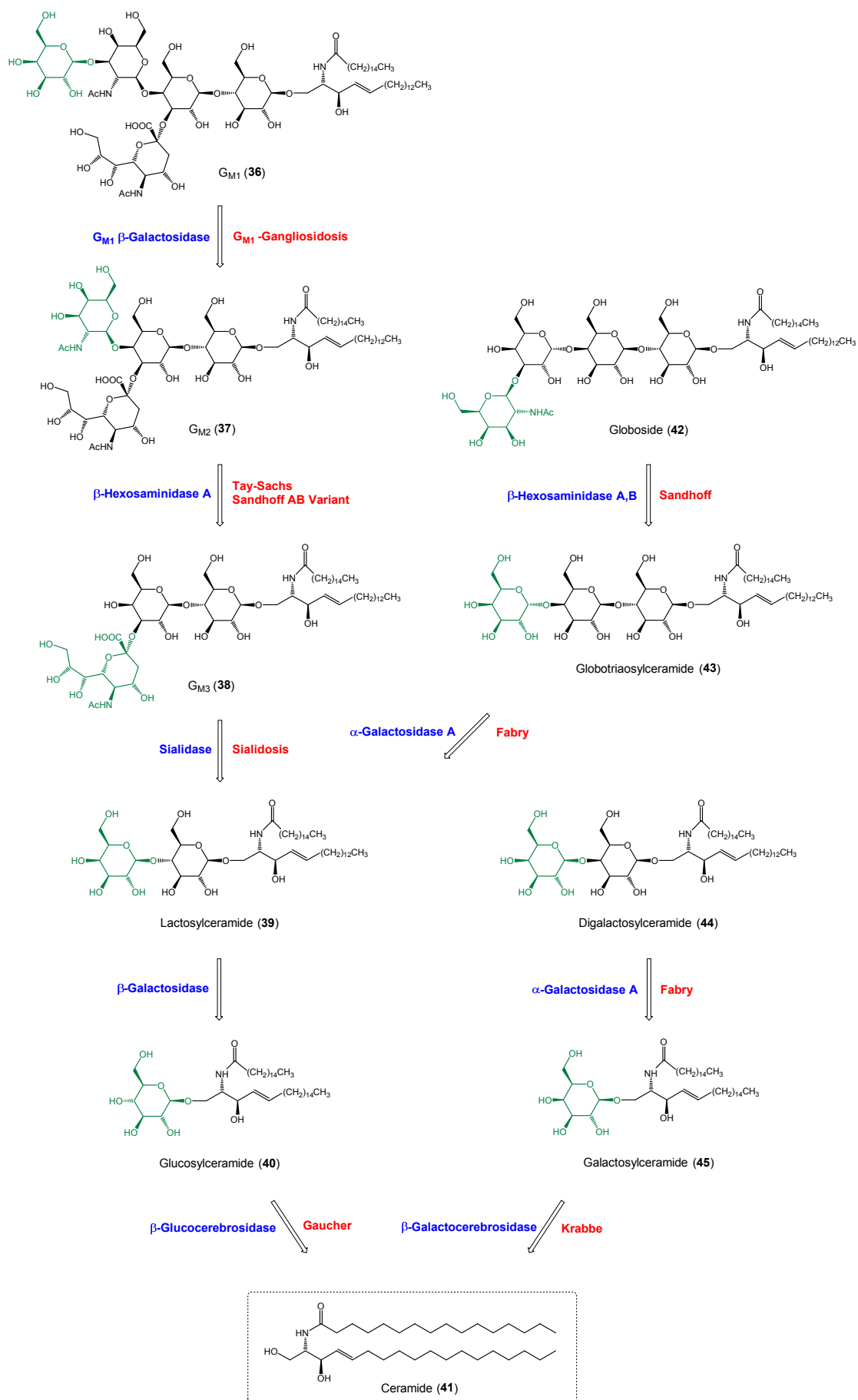


Figure 22: GSLs degradation pathway with glycosidases in blue, observed diseases in case of malfunctioning glycosidases in red and cleaved carbohydrate parts in green.<sup>37,48</sup>



### 1.2.4 Lysosomal storage diseases

Lysosomal storage diseases (LSDs) are a series of metabolic disorders with deficiencies of lysosomal enzymes caused by mutations of specific genes, responsible for their biosynthesis. As a result, macromolecules like GSLs, proteins or lipids, cannot be degraded and are accumulating in the living cell which leads to disruption of intracellular processes to the point of apoptosis.<sup>49</sup>

Approximately 50 different<sup>50</sup> forms of LSDs are known to be related only with the degradation of glycosphingolipids. The probability to be affected with one particular form is rare. The most frequent LSD, Gaucher disease type I for example, has an incidence of 1 to 50.000-200.000 births, however, collectively are GSLs related disorders with 1 of 8000 births the most frequent cause of pediatric neurodegenerative diseases worldwide.<sup>50,51</sup>

Symptoms and progression of the individual disorder can be very different and are depending on the specific disease itself and the age of the patient. Especially as infant, the affects can be enormous, blindness, movement disorder, deafness, delayed development, organ enlargement and neurological pathology are described.<sup>52</sup>

Different therapeutic approaches have been developed in order to deal with the accumulating macromolecules caused by malfunctioning hydrolases. Partially successful treatment has been achieved with enzyme replacement therapy (ERT), where a recombinant version of the defective enzyme is administered to the patient. Via receptor mediated endocytosis, the enzyme can be incorporated by the cell where it acts instead of the misfolded version. The application of ERT is limited to patients without neurological dysfunctions since the recombinant enzyme is not able to cross the blood-brain barrier.<sup>53,54</sup>

The substrate reduction therapy (SRT) focuses on the inhibition of anabolic enzyme activity in order to minimize the substrate of the malfunctioning enzyme. The main advantage over ERT is that SRT agents are able to cross the blood-brain barrier, which allows the treatment of neurological symptoms.<sup>55</sup> Earlier attempts to treat LSDs were made by stem cell transplantation (SCT), with stem cells from a healthy donor. Unfortunately is the SCT therapy limited to a few cases. Promising methods of treatment for the future are the chaperone mediated therapy (CMT) and the gene therapy.

### Chaperon mediated therapy (CMT)

In the last years the chaperon mediated therapy has become one of the most promising attempts for an effective treatment option of lysosomal storage diseases. This method is based on small molecules called “active site specific chaperons” (ASSCs) or “pharmacological chaperons” (PCs), which are, due to their strong interactions with the enzyme’s active site, capable to support correct protein folding within the endoplasmic reticulum (ER). The principle of PC stabilized lysosomal glycosidases was firstly demonstrated by Fan and collaborators in 1999 when they exposed  $\alpha$ -galactosidase A in cells of Fabry patients to deoxygalactonojirimycin in sub-inhibitory concentrations.<sup>56</sup> In 2016, this iminosugar was approved by the European Commission for the treatment of Fabry disease.<sup>57</sup>

Normally, natural occurring chaperon proteins are assisting in correct folding and assembling of macromolecular structures within the endoplasmic reticulum, which are furthermore transported to the Golgi apparatus (**Figure 23-a**).<sup>58</sup>

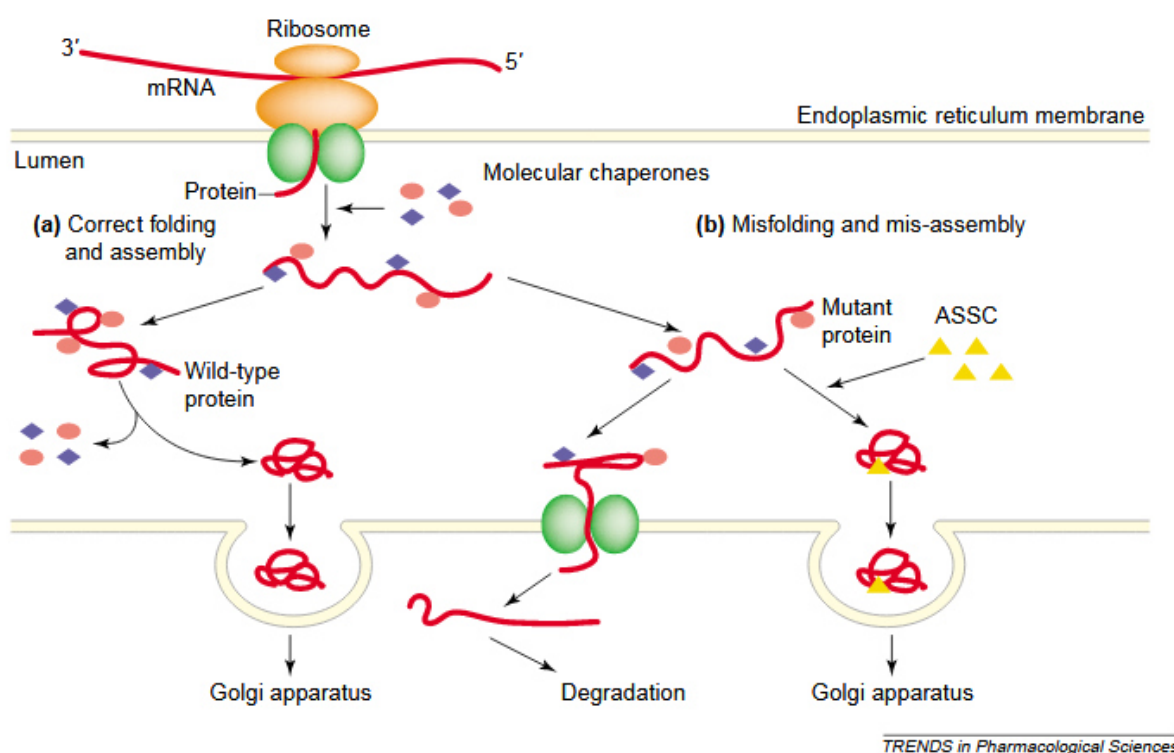


**Figure 23:** Overview about the quality control system and active site specific chaperon assistance in the ER.<sup>58</sup>

In case of structural failure as a result of single mutations in genes, the proteins cannot be folded correctly by natural chaperons and are therefore recognized and decomposed by the endoplasmic reticulum associated degradation pathway (ERAD). During CMT, pharmacological chaperons are interacting with the malfunctioning enzyme’s active site and are therefore assisting the natural chaperons to achieve better folding of the mutant proteins

(**Figure 23-b**).<sup>58</sup> As a result, those proteins are not forced to undergo the ERAD process, instead, they are allowed to pass the Golgi apparatus into the lysosome where the enzyme-ASSC complex dissociates due to lowered pH-values and substrate excess. At the end, a working enzyme is provided which can mitigate the symptoms of lysosomal storage diseases.

Compared to ERT, pharmacological chaperons used in CMT are able to cross the blood-brain barrier, have a good cell permeability and are suitable for oral intake at relatively low cost of production which allows the treatment of neuropathological symptoms of LSD.

## 1.3 Nucleoside processing enzymes

### 1.3.1 Iminosugars

Iminosugars are carbohydrate analogues where a trivalent nitrogen atom is replacing the endocyclic oxygen atom. The exchange endows this class of carbohydrates with additional basic properties which are responsible for the remarkable biological activity.

As already mentioned, 1-deoxynojirimycin (DNJ) (**1**) was the first synthesized structure of this class. It was the result of the race of replacing the ring oxygen with heteroatoms such as nitrogen, sulfur and phosphorus in the early 1960s which was at this time just an academic exercise.<sup>59</sup> The first iminosugar isolated from nature was nojirimycin (**7**), a compound with antibiotic properties.<sup>60</sup> Furthermore, there are also furanose and bicyclic forms of iminosugars such as 1,4-dideoxy-1,4-imino-L-arabinitol LAB and castanospermine and their derivatives (**18**, **19**, **20**, **Figure 16**).

The therapeutic utility of iminosugar based structures are versatile. Besides the usage of pharmacological chaperons, they are used as transition state analogues of nucleoside processing enzymes. These analogues of the transition state are mimicking the structure of the enzyme's substrate at the transition state and are forming a strong bond to the target enzyme. This bond, which can be millions of times more tight in comparison with the original substrate, leads to a stabilization of the normally short-lived transition state to a thermodynamically stable state.<sup>61</sup> A variety of iminosugar based transition state analogues related to nucleoside processing enzymes have been already designed and tested by members of the Ferrier Research Institute and V.L. Schramm and  $K_i$  values in the pico- and femto-molar range have been achieved. An example of such an inhibitor, 5-p-Cl-phenylthio-DADMe-Immucillin-A (**46**) with a  $K_i$  value of 47 fM against 5-Methylthioadenosine/S-Adenosylhomocysteine Nucleosidase (MTAN) from *Escherichia coli*,<sup>62</sup> is shown in **Figure 24**.

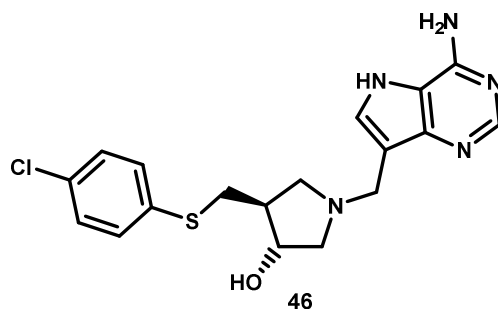


Figure 24: Example of a nucleoside processing enzyme inhibitor.

### 1.3.2 Nucleoside- and nucleotide analogues

Most common DNA and RNA occurring nucleosides are glycosylamines, which means they are consisting of a glycosyl group and an amino moiety connected via a  $\beta$ -*N*-glycosidic bond. The glycosyl group is made up of a ribofuranose (RNA) or 2-deoxyribofuranose (DNA) and the amino moiety of a nucleobase. Nucleotides have in comparison to nucleosides one to three phosphate groups linked to the sugar moiety through the 5'-hydroxy-group. These structures are the molecular building blocks of DNA and RNA which comprise the genetic information of all living organisms. In **Figure 25** structural elements of nucleotides are illustrated, including the primary nucleobases. The purine bases adenine (**47**) and guanine (**48**) and pyrimidine base cytosine (**49**) occur in both RNA and DNA, while uracil (**50**) just in RNA and thymine (**51**) just in DNA.<sup>63</sup>

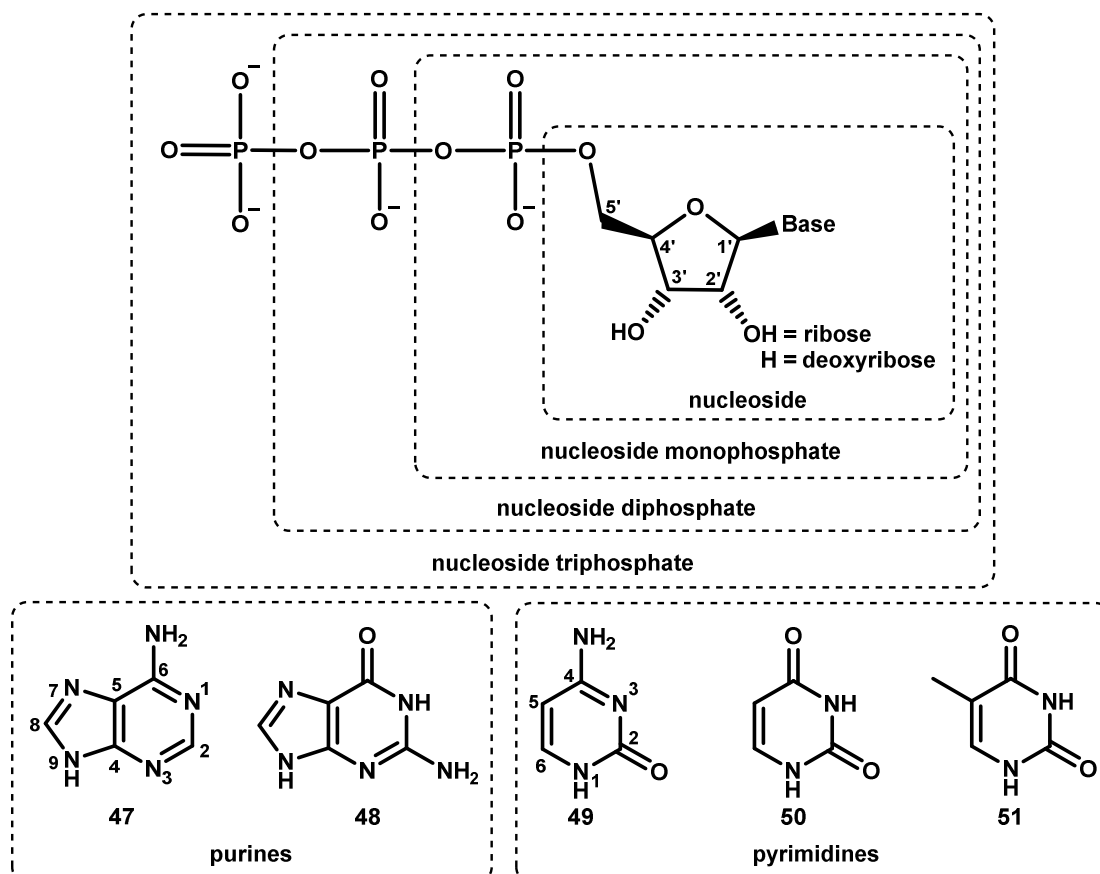


Figure 25: Structural elements of nucleotides.<sup>63</sup>

Developments of nucleoside- and nucleotide analogues as potential anti-viral drugs started in the early 1970s. Acyclovir (**52**), a derivative of guanine, discovered by Elion, is acting as an analogue of endogenous deoxyguanosine to block viral DNA polymerase which leads to elimination of the virus.<sup>64</sup> Nowadays, the class of analogues of nucleosides/tides account for more than 50 % of the drugs used for the treatment of viral infections like HIV or Hepatitis. An example of an already FDA approved molecule is MK-0608 (**53**), an analogue of adenosine, which inhibits viral RNA replication of the Hepatitis C virus.<sup>65</sup>

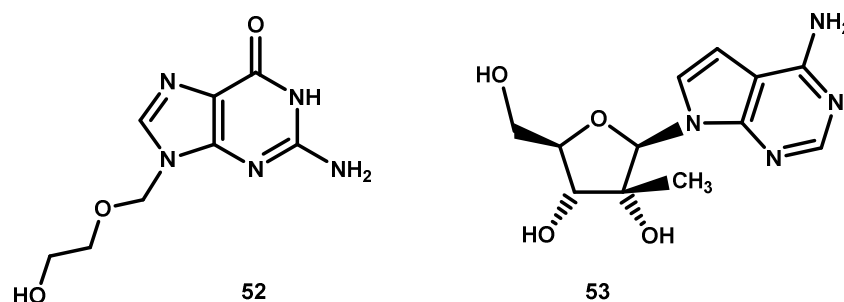


Figure 26: Examples of anti-viral agents.

### Iminosugar based nucleoside- and nucleotide analogues

In case of analogues of nucleosides/tides based on iminosugars, the ring oxygen is replaced by nitrogen and the connection between the sugar structure and the basic moiety is accomplished by a C-glycosidic bond. These structures are known as iminoribitol-C-nucleosides or colloquially as “immucillins”. An already commercially available example is Immucillin-H (**54**), also known as forodesine, which is an effective inhibitor of purine nucleoside phosphorylases and nucleoside hydrolases. The first synthesis of Immucillin H was achieved by Tyler and Furneaux from Victoria’s Ferrier Research Institute in 1998.<sup>66</sup> In April 2017, the drug has been approved in Japan under the trade name Mundesine<sup>®</sup> for the treatment of relapsed peripheral T-cell lymphoma, after 19 clinical trials.<sup>67,68</sup>

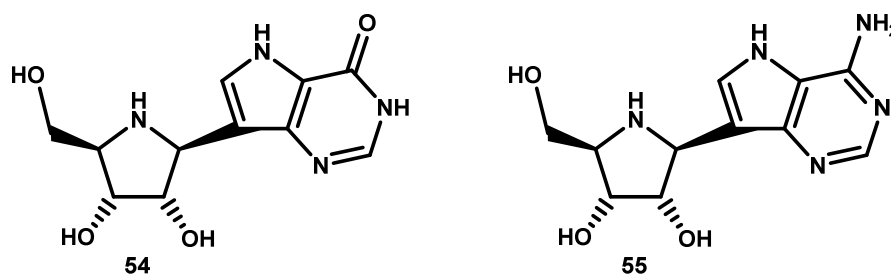


Figure 27: Immucillin-H (**54**) and Immucillin-A (**55**).

Another representative of this class which has recently become interesting is Immucillin-A (**55**), also known as galidesivir. Since the WHO recognized the Ebola virus (EBOV) as a high priority target, a range of compounds have been screened to become anti-viral agents.<sup>69</sup> One of these structures was Immucillin-A, which showed antiviral activity against a series of RNA

viruses like Marburg virus (MARV), EBOV, and Zika virus (ZIKV). It is assumed that the compound is incorporated into the viral RNA strand where it inhibits the RNA polymerase by non-obligate RNA chain termination. The anti-viral agent is furthermore highly selective for viral RNA polymerase, whereas human DNA and RNA is not affected.<sup>70</sup>

### Prodrugs and ProTides

The therapeutic effect of nucleoside analogues depends on the stepwise addition of phosphate groups by cellular kinases to form active nucleoside triphosphates. But, since nucleoside triphosphates have a poor chemical stability and a high polarity which hinders them from being transported across the cell membranes, they cannot be used as drugs directly. Furthermore, during the activation of nucleosides, the first phosphorylation step has often been recognized as the limiting step. Therefore, chemists designed “protected” monophosphate nucleosides which are, in comparison to “free” nucleoside monophosphates (**Figure 28-1**), capable to cross the biological barriers. Afterwards, the protecting groups are degraded and the free nucleoside monophosphate can be further phosphorylated (**Figure 28-2**).<sup>71</sup>

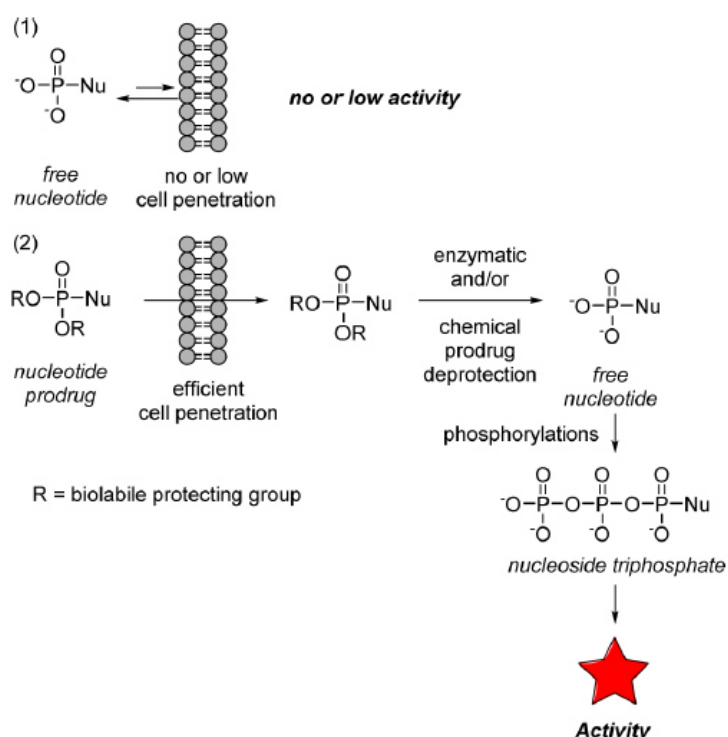


**Figure 28:** Biological process of nucleoside monophosphate prodrugs.

The use of phosph(on)ate prodrugs has not only proved to improve the activity of parent compounds, it also created new potent structures which are otherwise inactive in their nucleoside form as a result of a lack of monophosphorylation.<sup>71</sup>

There are a few different techniques available for the synthesis of prodrugs. One of the most applied, is the Prodrug Nucleotide (ProTide) technology discovered by McGuigan and co-workers in the early 1990s.<sup>71</sup> This technique uses aryloxyphosphoramidates which are composed of a phosphorus atom bearing an amino acid alkyl ester and an aryloxy group. The mode of action of these aryloxyphosphoramidates starts with crossing the cell membrane and further hydrolysis via esterase or cathepsin A to get carboxylate **A**. After spontaneous intramolecular cyclisation, a 5-membered ring **B** is formed, from which the aryl-group is released. Through water-mediated hydrolysis, the cyclic intermediate undergoes chemical ring opening leading to phosphoramidate diester **C**. Finally, the nucleoside monophosphate is freed after cleavage of **C** via phosphoramidase or histidine triad nucleotide-binding protein-1 (HINT-1) (**Figure 29**).<sup>71</sup>

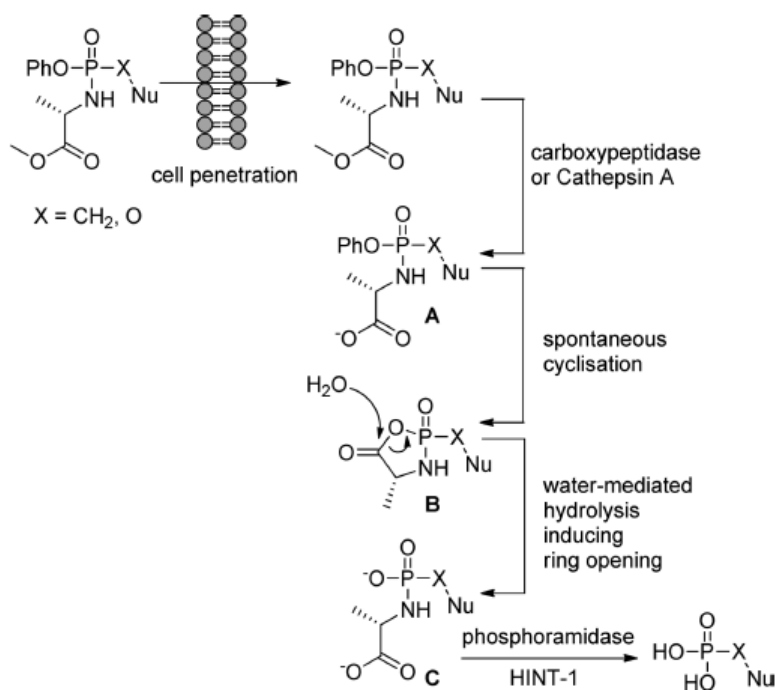


**Figure 29:** Mode of action of aryloxyphosphoramidate prodrugs.<sup>71</sup>

A disadvantage of this technique is caused through the different substituents on the phosphorus atom which provides an additional chiral center. The resulting diastereomers may have different biological properties and can be hard to separate via silica-gel chromatography. In this case, an asymmetric approach using a chiral auxiliary has to be considered.

An already commercially available therapeutic example of a nucleoside using the prodrug technology is the anti-viral agent Sofosbuvir<sup>®</sup> (**56**) (**Figure 30**). It is used against all hepatitis C virus (HCV) genotypes over a relatively short treatment period of 8-12 weeks compared to the previous “standard of care” treatment over one year including combined intake of interferon and ribavirin. Sofosbuvir<sup>®</sup>, which is an inhibitor of RNA-dependent RNA

polymerase, was approved by the FDA as an antiviral component in the treatment of chronic HCV infections, in 2013.<sup>65</sup>

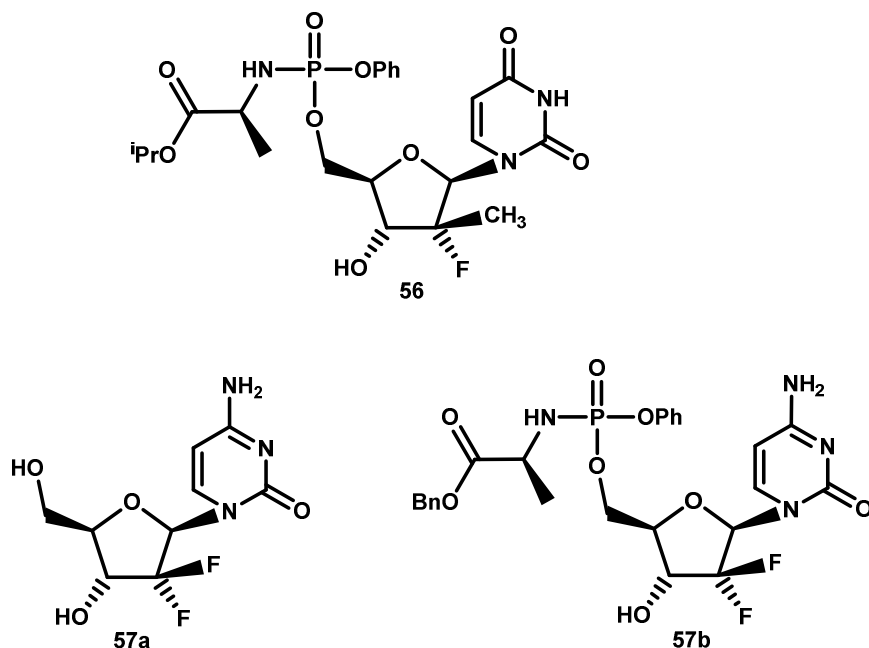


**Figure 30:** Examples of nucleosides bearing an arylphosphoramidate-group.

Another example of medical efficacy enhancement by the prodrug technique can be shown with gemcitabine (**57a**) (**Figure 30**). This nucleoside analogue has been the standard treatment for pancreatic cancer since its approval by the FDA in 1996. However, as a result of struggling with cancer resistances, a series of gemcitabine phosphoramidates have been tested such as structure (**57b**). This compound showed high efficacy against a range of cancers and simultaneously circumvents resistance mechanisms. Current clinical phase I/II studies of ProTide (**57**) showed good results to become a new drug for cancer treatment in the future.<sup>72</sup>

### 1.3.3 RNA viruses

Viruses are very small infectious particles with a typical size between 20 to 300 nm. They consist of an outer cover, made up of proteins and sometimes additional lipid-membranes, which is protecting the RNA- or DNA-core (genome). For the reproduction, viruses are completely depending on cells (animal, bacterial or plant), where sometimes enzymes are needed for the first step of viral replication. Viruses are usually classified via the Baltimore method, which is based on the structure of their genome and their method of replication and not on the diseases they cause. As a result, there are RNA- and DNA-viruses where each type can be single-stranded (ss) or double stranded (ds). Furthermore, single stranded RNA-viruses are divided into (+)- and (-)-sense RNA.<sup>73</sup>



Especially RNA viruses like the Human Immunodeficiency Virus (HIV), Hepatitis C virus (HCV), Ebola virus (EBOV) and Zika virus (ZIKV) are remaining a constant global threat. Hence, large amounts of money have been provided on the investigation of RNA viruses and their replication which relies on RNA-dependent RNA polymerases (RdRps). These polymerases are using RNA precursors along with other related proteins, encoded by the host or virus, to synthesize RNA structures. This RdRp directed RNA replication exhibits a high error frequency due to low fidelity and since viral RNA polymerases lack the proofreading ability of DNA polymerases. As a result of the lower accuracy, phosphorylated potential anti-viral nucleosides are utilized by the viral RNA polymerase which results in either the termination of chain elongation, the accumulation of mutations or apoptosis. The RdRp has a high sequence homology across a range of viruses, thus, nucleosides can be active against several viruses.<sup>73,74</sup>

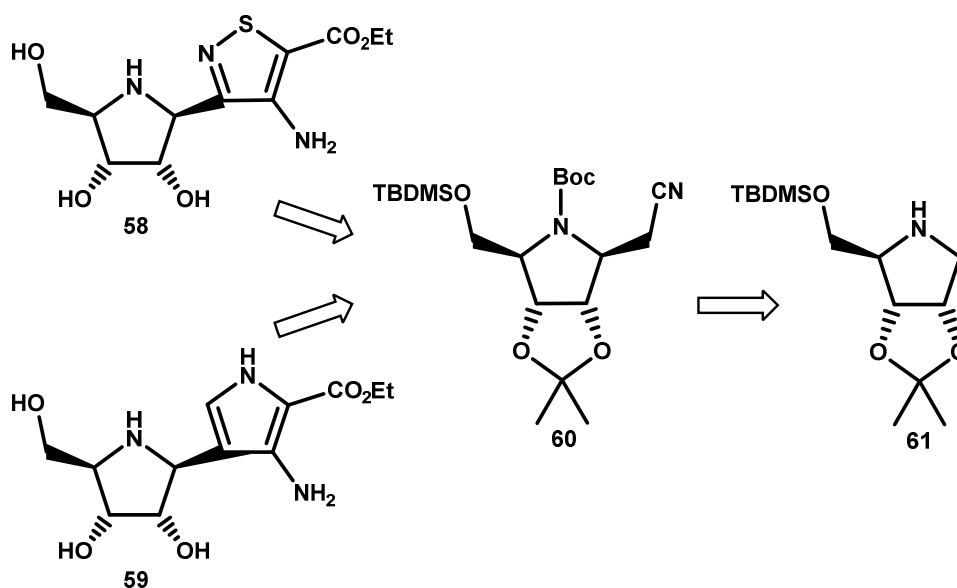
## 2 Problem statement and aim of this work

In general, this work has been focused on the synthesis, the isolation as well as the characterization of biologically active organic compounds.

### 2.1 Iminosugar nucleoside analogues as potential anti-viral agents

Since the WHO has identified the Ebola virus (EBOV) as a high priority target, a series of compounds have been screened to become an anti-viral agent. One of these structures Galidesivir (**55**), also known as Immucillin A, was the first example of an iminoribitol-C-nucleoside with anti-viral activity. Subsequent testing of Immucillin A derivatives showed similar activities and made the Galidesivir scaffold a promising starting point.<sup>69,70</sup> The efficacy of such nucleosides strongly depends on the stepwise addition of phosphate groups through cellular kinases. Thus, techniques such as the ProTide technology by McGuigan and co-workers were elaborated, which are exploiting aryloxyphosphoramidates to create “protected” monophosphate nucleotides.<sup>71</sup> The task of this project has been to synthesize new potentially anti-viral structures based on the Galidesivir scaffold. Additionally, it has been planned to produce prodrugs of these compounds and compare their biological activities with the “free” nucleosides.

The target molecules **58** and **59** have been planned to be synthesized from acetonitrile adduct **60**, which was prepared via oxidation and subsequent addition of nucleophilic acetonitrile to iminoribitol derivative **61**. To achieve the respective prodrug compounds, the nucleosides are coupled with phosphoramidate structures in the presence of an organic base.



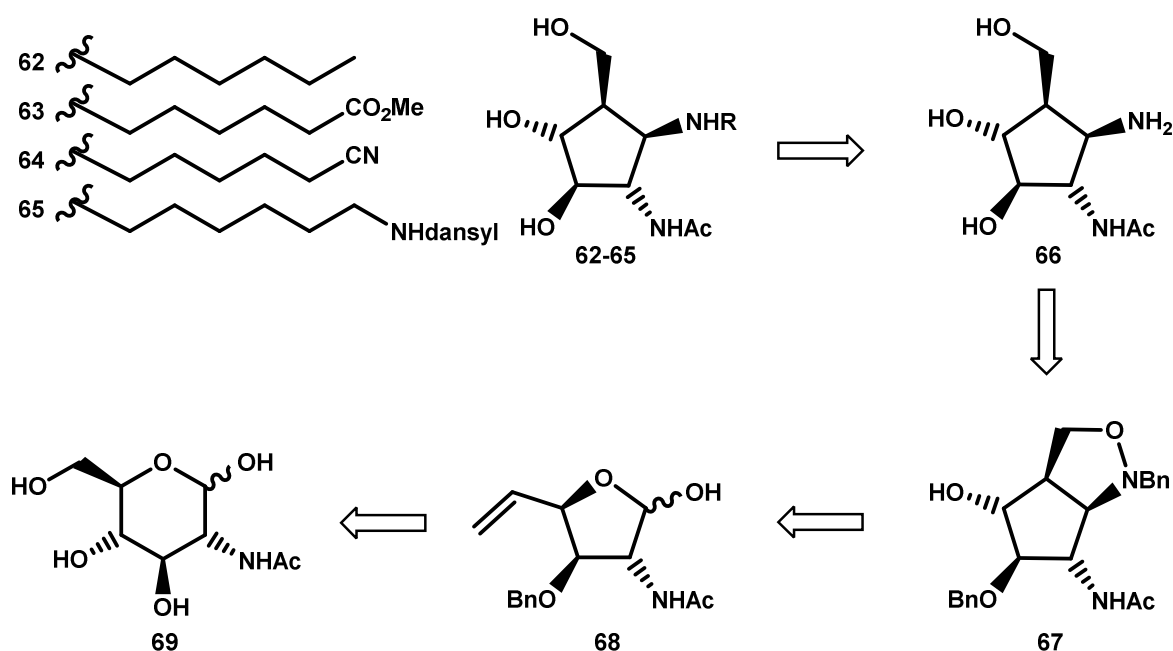
**Scheme 1:** Retrosynthetic considerations for the synthesis of iminoribitol-C-nucleosides.

## 2.2 Furanoid carbasugars as GH 20 hexosaminidase inhibitors

The aim of the second project has been focused on the synthesis of new powerful inhibitors of human lysosomal hydrolases in order to identify novel pharmacological compounds for the treatment of lysosomal storage diseases by chaperon-mediated therapy.

Approximately half of the almost sixty lysosomal storage diseases described in literature, are the result of a lack or catalytic incompetence of carbohydrate processing enzymes such as glycosidases or phosphorylases. Moreover, 50 % of the carbohydrate processing enzymes are involved in the chemical manipulation of *N*-acetyl-D-glucosaminy or *N*-acetyl-D-galactosaminy residues from degradation-bound polysaccharides and glycoconjugates.<sup>27</sup>

Focusing on hexosaminidase inhibitors based on the carba-furanose scaffold, 2-acetamido-1-amino- $\beta$ -D-gluco-cyclopentane was already reported as potent inhibitor of GH 20 hexosaminidases from jack beans and bovine epididymis with  $K_i$  values of 0.39  $\mu$ M and 0.65  $\mu$ M, respectively.<sup>44</sup> Consequently, a set of furanoid carbasugars has been planned to be synthesized, starting from *N*-acetyl-D-glucosamine (**69**), following a [2+3] cycloaddition based approach. The primary amine of structure **66** has been planned to be selectively mono-alkylated using bromoalkyl or iodoalkyl structures in the presence of a weak base. Furthermore, it has been planned to screen these new compounds (**62-66**) for their activity as  $\beta$ -*N*-acetyl-D-hexosaminidase inhibitors.



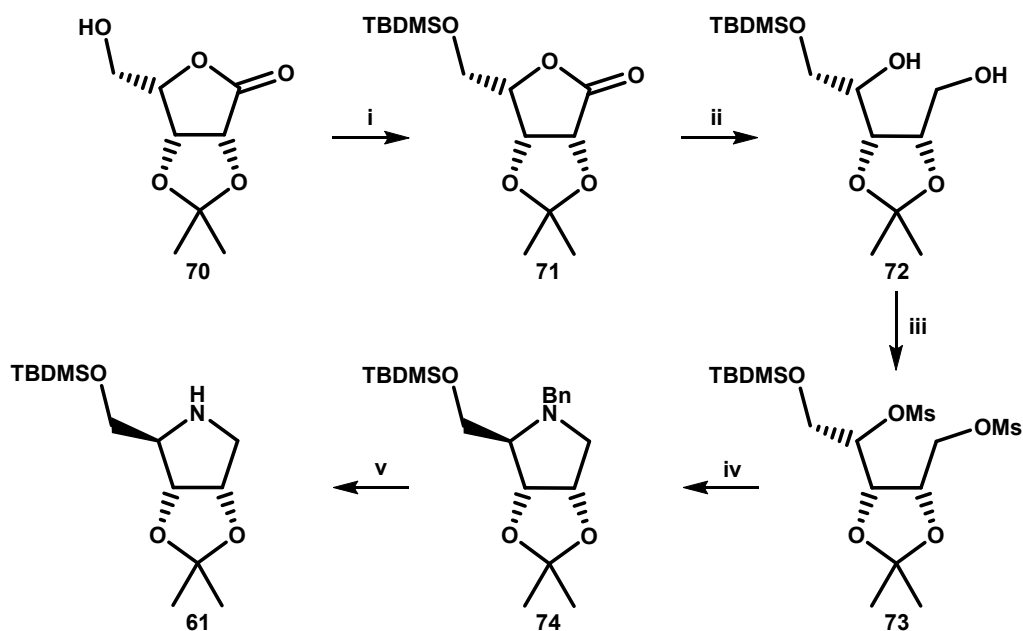
**Scheme 2:** Retrosynthetic overview for the synthesis of alkylated furanoid carbasugars.

## 3 Results and discussion

### 3.1 Iminoribitol-C-nucleosides

#### 3.1.1 Synthesis of acetonitrile adducts

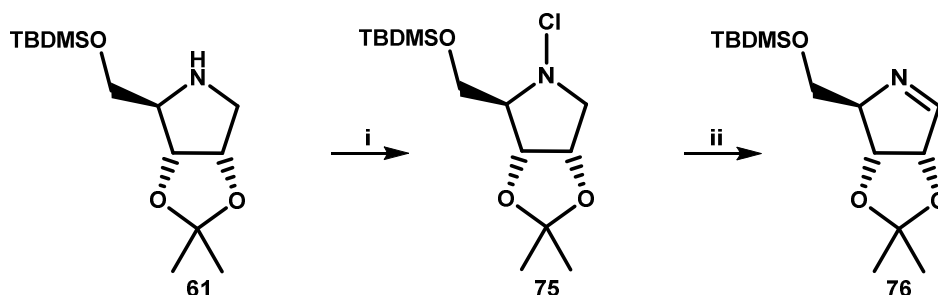
The synthesis for the first project started with protected iminoribitol **61**, which had been produced by the staff of the Ferrier Research Institute (FRI). Since **61** is a key starting material for the preparation of all kinds of Immucillins, a quick overview about possible synthetic pathways, is described. The proposed synthesis starts with commercially available 2,3-O-Isopropylidene-L-lyxono-1,4-lactone (**70**) following a 5-step reaction cascade (**Scheme 3**) patented by BioCryst Pharmaceuticals Inc in 2014.<sup>75</sup>



**Scheme 3:** Possible reaction sequence to iminoribitol **61**; i) TBDMSO, imidazole; ii) NaBH<sub>4</sub>, MeOH; iii) Mesityl chloride, DMAP; iv) BnNH<sub>2</sub>; v) H<sub>2</sub>, Pd/C.

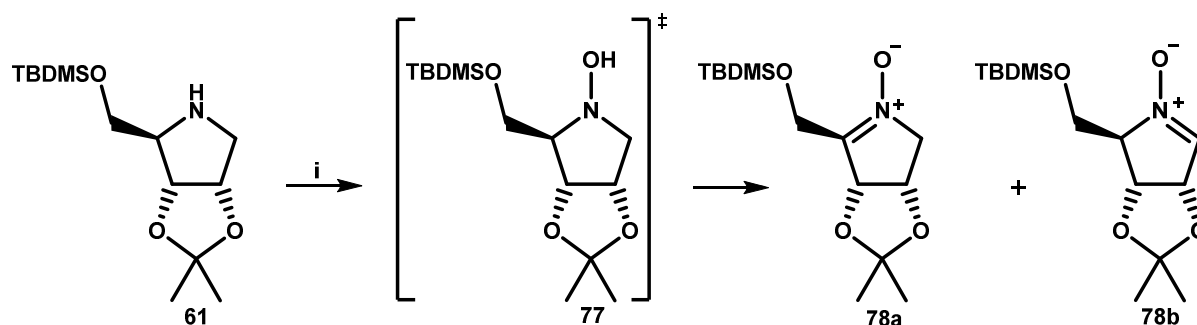
This cascade starts with the silylation of the 5-hydroxy group with TBDMSO and imidazole to afford protected substance **71**. The ring opening can be achieved by reducing the lactone with sodium borohydride to get diol **72**, followed by a sulfonylation of the hydroxy groups to achieve the methanesulfonate **73**. Treatment with benzylamine substitutes the primary mesylate group followed by an intramolecular nucleophilic reaction to displace the second methanesulfonyl group, which includes inversion of configuration of C-4. As a last step, *N*-benzyl iminoribitol **74** is hydrogenated over Pd/C to afford the desired protected iminoribitol compound **61**.

The first synthetic approaches to “immucillins” were realized via electrophilic imine **76**. The production of intermediate **76**, starting from iminoribitol **61**, needed low reaction temperatures ( $-78^{\circ}\text{C}$ ) and provided relatively low yields (**Scheme 4**).<sup>76</sup> Thus, BioCryst modified the production using phase transfer catalysts which led to better yields at temperatures close to ambient conditions ( $-15^{\circ}\text{C}$ ).<sup>77</sup>



**Scheme 4:** Original approach for the synthesis of imine (**76**); i) NCS, pentane; ii) LiTMP, THF,  $-78^{\circ}\text{C}$ .

However, as a result of the limited stability of **76**, the addition of further alkyl- or aryllithium derivatives, either failed or gave poor yields. In comparison to the imine **76**, the corresponding nitrone **78** exhibits higher electrophilic reactivity while being much more stable.<sup>78</sup> Initial studies used selenium dioxide and hydrogen peroxide in acetone for oxidation, but the possibility to form unstable acetone peroxides, has let us look for another option.<sup>78,79</sup> Finally, the conversion of the iminoribitol structure **61** to the corresponding nitrone **78** (**Scheme 5**), was achieved by using a methyltrioxorhenium/hydrogen peroxide (MTO/ $\text{H}_2\text{O}_2$ ) system, which is suitable for all kinds of secondary amines.<sup>80</sup>

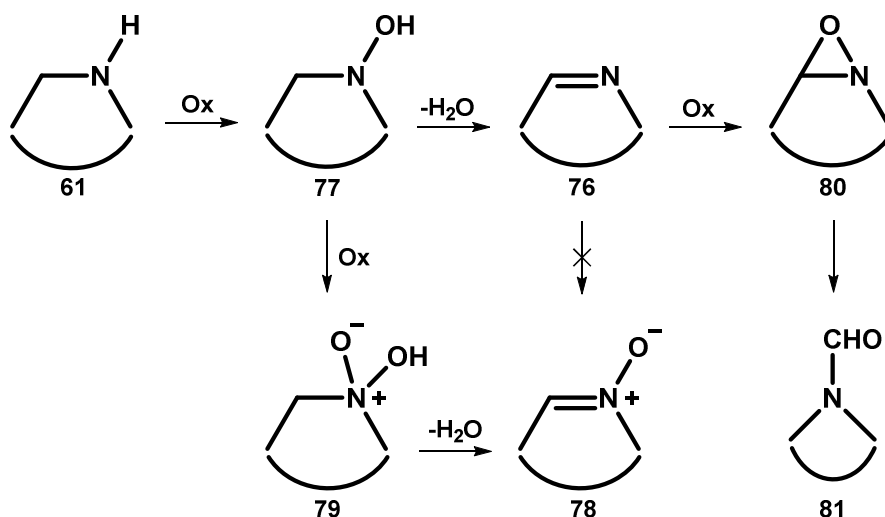


**Scheme 5:** Synthesis of **78**; i) MTO (0.2 mol %),  $\text{H}_2\text{O}_2$  (30%) in DCM, rt, then MeOH, 15 min, dropwise addition of **61** in DCM,  $0^{\circ}\text{C}$ .

During the oxidation, the starting material (**61**) is converted into two possible nitrone-regioisomers (**78a-b**) via a hydroxylamine-intermediate (**77**). This reaction was executed at a 10 g scale, where after separation of the unwanted isomer **78a** via recrystallization and silica-gel chromatography, desired isomer **78b** was isolated in excellent yield (85 %).

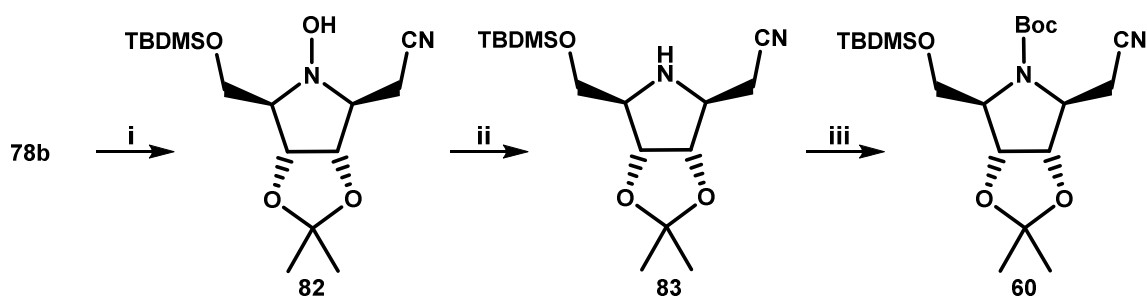
The following mechanism (**Scheme 6**), was proposed for the oxidation of secondary amines into nitrones using mCPBA as oxidant. It is assumed, that the mechanism proceeds in at

least two stages via the already shown hydroxylamine intermediate **77**. Further oxidation of the hydroxylamine (**77**) leads to hydroxylamine *N*-oxide (**79**), which then, dehydrates to the desired nitrone (**78**). Otherwise, in case of a dehydration of the hydroxylamine (**77**), an imine (**76**) is formed, which can be either oxidized to an oxaziridine (**80**) or to a nitrone (**78**). However, the formation of a nitrone (**78**) via an imine intermediate (**76**) was ruled out in a second experiment, in which just the aldehyde (**81**) was identified if starting from an imine (**76**).<sup>81</sup>



**Scheme 6:** Proposed reaction mechanism for the oxidation of secondary amines.<sup>81</sup>

Furthermore, the desired nitrone regioisomer **78b** underwent stereoselective addition by lithiated acetonitrile forming hydroxylamine **82**. After reduction of **82** using activated zinc-dust, amine **83** was protected by treatment with di-*tert*-butylcarbonate, to provide desired structure **60** (**Scheme 7**).

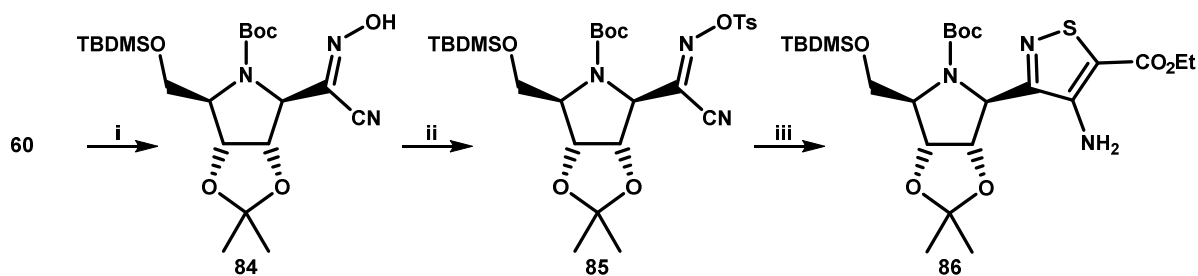


**Scheme 7:** Synthesis of acetonitrile adduct (**60**); i) <sup>n</sup>BuLi, CH<sub>3</sub>CN, THF; ii) Zn-dust, CH<sub>3</sub>COOH; iii) (Boc)<sub>2</sub>O, DCM.

Since acetonitrile adduct **60** was a key compound for all proposed targets, this three-step procedure was performed several times with an overall average yield of 69%. Structure **60** was obtained in high purity and its NMR data were identical to those reported in literature.<sup>82</sup>

### 3.1.2 Synthesis of isothiazole-C-nucleosides

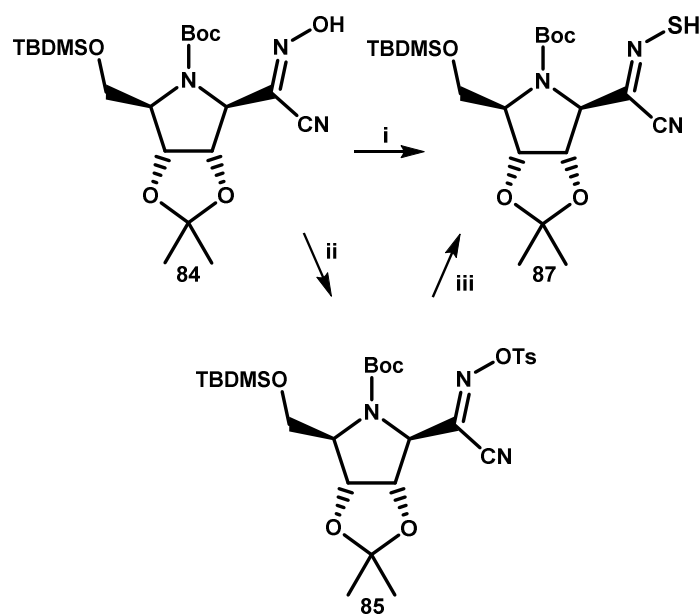
For the preparation of isothiazole structure **86** (Scheme 8), oxime **84** was synthesized by treating acetonitrile adduct **60** with tert-butyl nitrite and potassium tert-butoxide under anhydrous conditions.



**Scheme 8:** Planned sequence for the synthesis of **86**; i)  $\text{KO}^t\text{Bu}$ ,  $^t\text{BuONO}$ , THF; ii) TsCl, DIPEA, DCM; iii)  $\text{HSCH}_2\text{CO}_2\text{Et}$ , TEA, EtOH.

Subsequently, structure **84** was O-tosylated employing *p*-toluenesulfonyl chloride (TsCl) and Hünig's base, to obtain tosyloximino compound **85**. For the cyclisation, structure **85** was treated with ethylthioglycolate and triethylamine at 0°C. According to the literature,<sup>83</sup> this reaction should perform following a straight addition/elimination mechanism and concomitant spontaneous cyclisation in the presence of a base (DBU). The principle was proven several times, also with sugar structures such as D-ribofuranose.<sup>84</sup> Unfortunately, even after numerous attempts, isothiazole structure **86** could not be obtained.

Another approach for the production of the desired isothiazole system (**86**), started with the conversion of oxime **84** to the corresponding thiooxime **87**. This route was tried via two different ways. On the first one, Lawesson's reagent<sup>85,86</sup> was used to get the thiooxime (**87**) directly from oxime **84**, in the second approach, the tosyloximino structure (**85**) was intended to be converted into the desired thiooxime (**87**) exploiting sodium hydrosulfide (Scheme 9).



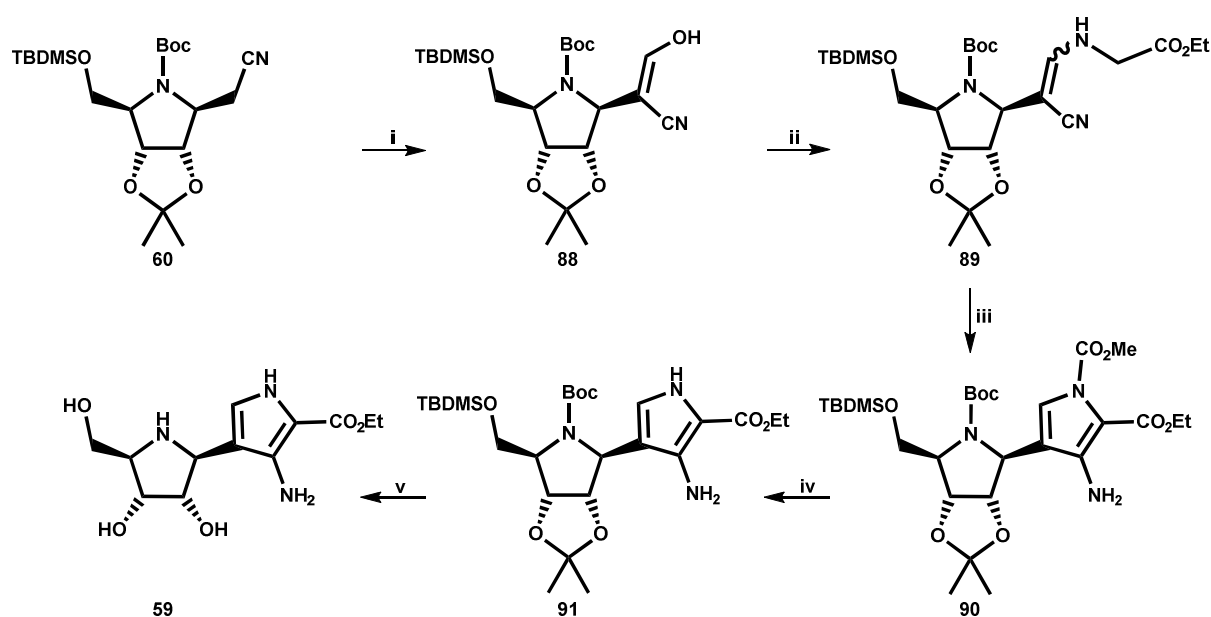
**Scheme 9:** Synthesis of thiooxime **87**; i) Lawesson's reagent, toluene; ii) TsCl, DIPEA, DCM; iii) NaHS, EtOH.

Unfortunately, none of the attempts for synthesizing the desired thiooxime structure **87** were successful and this section of the project had to be abandoned.

### 3.1.3 Synthesis of pyrrole-C-nucleosides

The synthesis of pyrrole-C-nucleosides, started with the treatment of acetonitrile adduct **60** (**Scheme 10**) with ethyl formate and sodium hydride under argon atmosphere. The obtained enol **88** was converting to an isomeric mixture of enamine **89**, by using glycine ethylester in the presence of sodium acetate. During the first synthesis of immucillins, the subsequent cyclisation was induced by benzyl chloroformate and DBU, followed by hydrogenolysis to remove the CBz protecting group.<sup>82</sup> In our case, hydrogenolysis was not necessary, by using a methyloxycarbonyl protecting group instead, which was simply removed by adding methanol and DBU. After deprotection of structure **91** with hydrochloric acid and methanol, pyrrol-compound **59** was isolated as crystals of high purity (93 %). Structure **59** was analysed via NMR spectroscopy, mass analysis and HPLC and thus, was ready for biological testing.

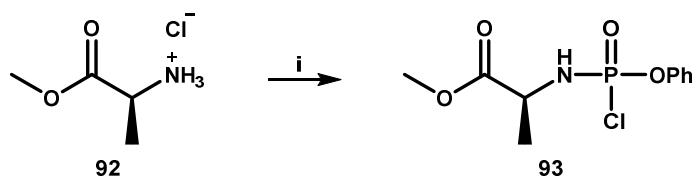




**Scheme 10:** Synthesis of pyrrole-C-nucleoside **59**; i) EtOCHO, NaH, THF; ii) glycine ethylester HCl, NaOAc, MeOH; iii) CICO<sub>2</sub>Me, DBU, DCM; iv) DBU, MeOH; v) HCl, MeOH.

### 3.1.4 Synthesis of phosphorochloridates

During the development of ProTides, L-Alanine was fixed as amino acid, since this has given the best biological activity while of the same time being processed well by enzymes.<sup>87</sup> Thus, commercially available L-Alanine methyl ester hydrochloride (**92**) was used as starting material for the synthesis of phosphorochloridate compound **93** (**Scheme 11**). Under anhydrous conditions at -70°C, a mixture of phenyl dichlorophosphate and amino ester **92** was treated with triethylamine. While in the literature<sup>87</sup> yields around 90 % are reported, we only obtained 40 %. However, no further modification was performed and as a result of low stability, structure **93** was used in the next reaction immediately after analysis. NMR spectra obtained (<sup>31</sup>P, <sup>1</sup>H and <sup>13</sup>C) were identical to those reported in the literature.<sup>87</sup>

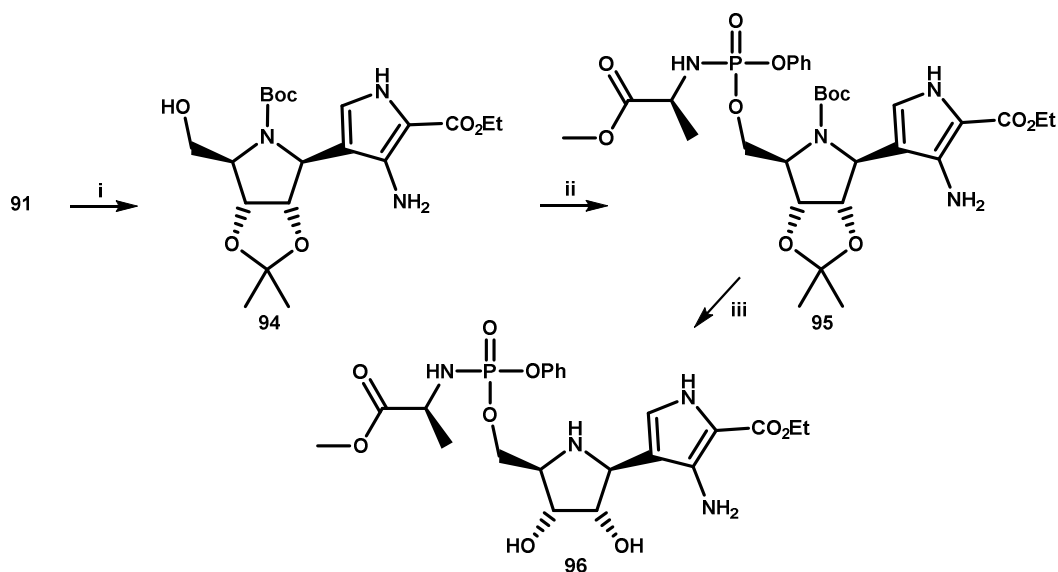


**Scheme 11:** Synthesis of phenyl (methoxy-L-alaninyl) phosphorochloridate **93**; i) PhOPOCl<sub>2</sub>, TEA, DCM, -70°C.

### 3.1.5 Synthesis of pyrrole-C-nucleoside prodrug

For the synthesis of prodrug structures, the protecting group of C-5 has to be split off. So, as shown in **Scheme 12**, structure **91** was treated with tetrabutylammonium fluoride at ambient conditions. The following coupling reaction between the phosphorochloridate compound **93** and structure **94** was carried out using *N*-methylimidazole as base (yield 49 %). According to

the literature, yields are varying between 11 to 80 %, which is strongly dependent on the kind of nucleobase, temperature, solvent and ProTide type.<sup>71</sup>



**Scheme 12:** Synthesis of pyrrole-C-nucleoside prodrug **96**; i) *n*-Bu<sub>4</sub>NF, THF; ii) NMI, THF; iii) TFA, THF.

In the final reaction, coupling product **95** was fully deprotected employing trifluoroacetic acid in THF. Unfortunately, workup after 12 hours revealed, that not only the protecting groups had been split off, but also some coupling product was cleaved. However, desired prodrug compound **96** was isolated as a mixture of diastereomers (yield 56 %) in high purity (98 %).

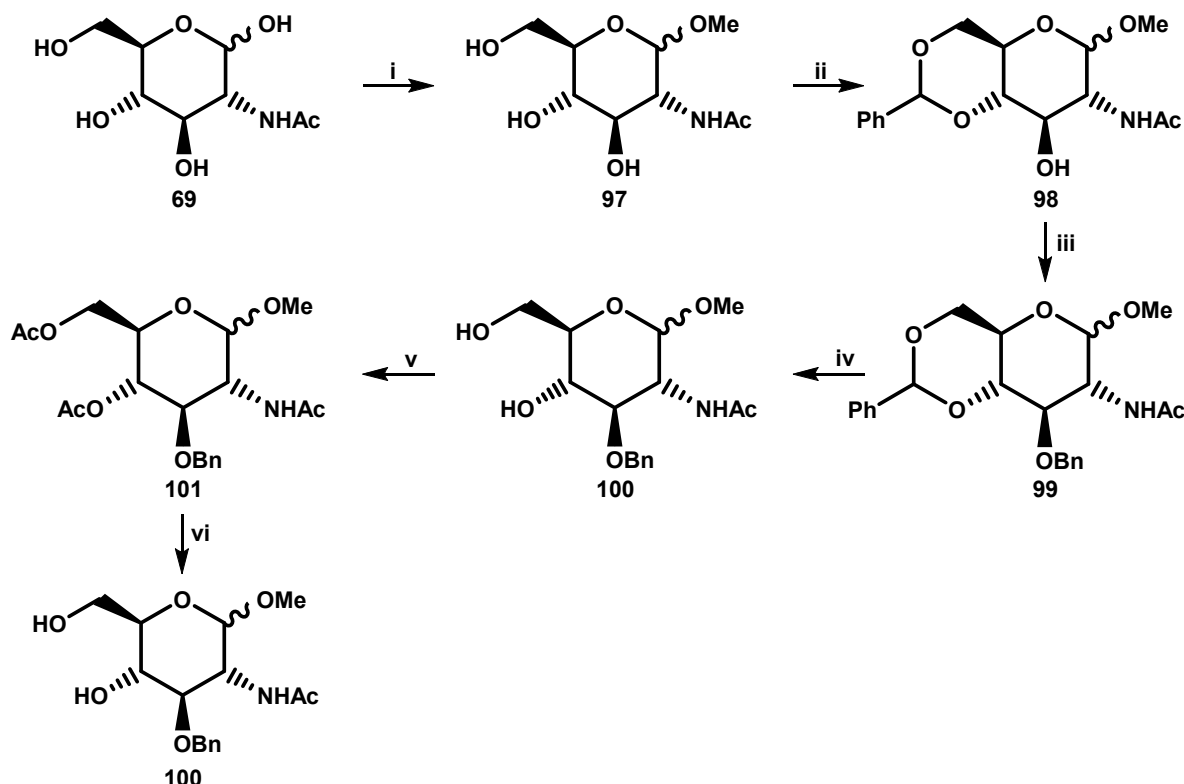
### 3.1.6 Biological evaluation

The biological evaluation of pyrrole-C-nucleoside **59** and its corresponding prodrug **96** is currently in progress. Results on their activity will be presented near future.

## 3.2 Synthesis of *N*-substituted 3-acetamido-4-amino-5-hydroxymethylcyclopentanetriols

### 3.2.1 Synthesis of 2-acetamido-3-*O*-benzyl-2-deoxy-D-glucopyranoside **100**

The synthesis of furanoid carbasugars was realized via a simple sequence of steps (**Scheme 13**), starting from commercially available *N*-acetyl-D-glucosamine (**69**).

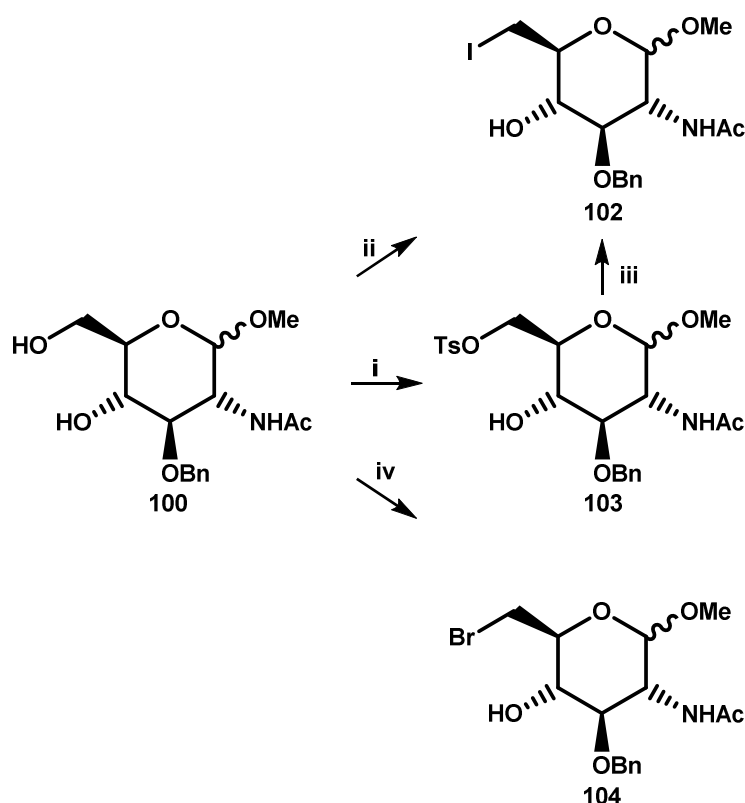


**Scheme 13:** Synthesis of compound **100**; i) IR-120, MeOH, reflux; ii)  $C_6H_5CH(OMe)_2$ , pTSA, DMF, 70°C; iii) BnBr, KOtBu, THF; iv) HCl, THF/H<sub>2</sub>O; v) Ac<sub>2</sub>O, DMAP, pyridine; vi) NaH, MeOH.

The first step, a Fischer glycosylation was carried out by Patrick Weber (Glycogroup Graz) according to the procedure reported in literature.<sup>88</sup> The following reactions were simple protecting and deprotecting steps, which were realized via in-house methods: Firstly, positions C-4 and C-6 were protected by an *O*-benzyliden-group, exploiting benzaldehyde dimethyl acetal and *p*-toluenesulfonic acid. After *O*-benzylation of position *O*-3 with benzylbromide in the presence of potassium tert-butoxide, the *O*-benzyliden group was removed, using hydrochloric acid, affording crude compound **100**. As a result of the high polarity of this substance (**100**), it was assumed to be hard to purify via silica gel chromatography. Thus, product **100** was *O*-acetylated using acetic anhydride in the presence of 4-dimethylaminopyridine. Consequently, further purification of less polar product **101** by silica gel chromatography was performed without any problems. After saponification, the desired compound **100** was obtained.

### 3.2.2 Conversion of the 6-hydroxy group into the corresponding alkyl halide

For the introduction of the iodo substituent at position C-6, Garegg's method<sup>89</sup> was used (**Scheme 14**). In this reaction, the primary alcohol reacts selectively with a mixture of iodine, triphenylphosphane and imidazole to form the 6-deoxyiodo compound **102**. During the following purification process, sodium thiosulfate was used to remove remaining unreacted iodine. Nevertheless, subsequent silica gel chromatography proved to be difficult, since the polarity-differences between the acetamido-product and by-products were not sufficient. Unfortunately, after several purification attempts, it was still not possible to afford 6-deoxyiodo-compound **102** as a pure substance.



**Scheme 14:** i)  $I_2$ ,  $PPh_3$ , imidazole, THF, reflux; ii)  $TsCl$ , TEA, DCM; iii)  $n-Bu_4NI$ , MeCN, reflux; iv)  $CBr_4$ ,  $PPh_3$ , pyridine, DCM.

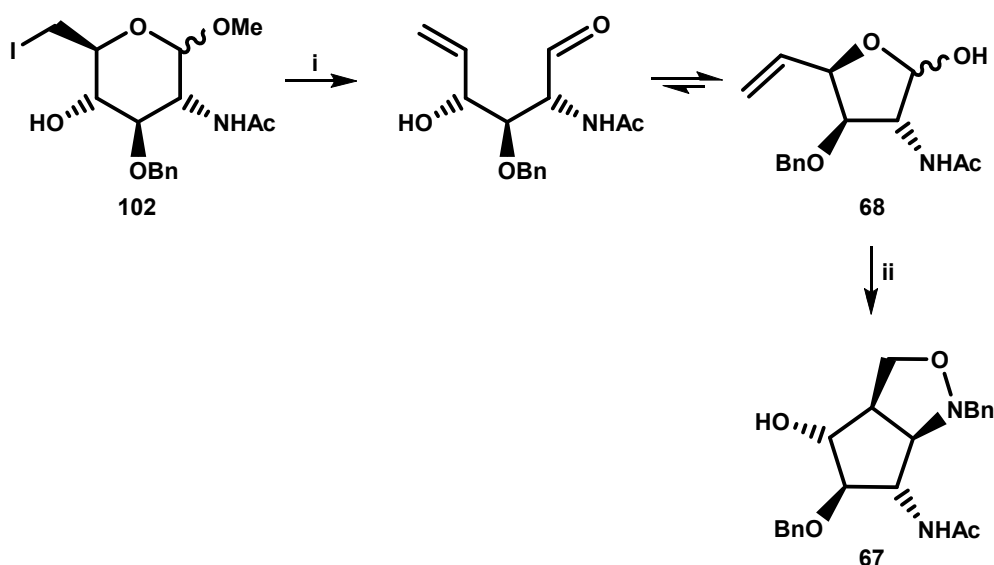
To avoid the triphenylphosphane oxide, the second attempt started with the tosylation of C-6 employing 4-toluenesulfonyl chloride and trimethylamine at ambient conditions. Subsequently, tosylate structure **103** was treated with tetrabutylammonium iodide, which afforded the 6-deoxyiodo structure **102** (70% over two steps). The third attempt for the implementation of a halide on C-6 was carried out following Appel's reaction<sup>90</sup> conditions. The primary alcohol reacted selectively with a mixture of tetrabromomethane, triphenylphosphane and pyridine, to form the 6-bromo compound **104**. Compared with Garegg's conditions, the inconvenient triphenylphosphane oxide was formed as well,

however, I did not have to deal with the typical side products of the Garegg reaction. Unfortunately, the desired 6-deoxybromo compound **104** could not be isolated.

### 3.2.3 Reductive ring opening and [2+3] cycloaddition

In 1979, Vasella<sup>91</sup> reported the basics about furanoid carbasugar synthesis. He demonstrated the possibility of two different diastereomeric bicycles at the [2+3] cycloaddition. Once the isoxazolidine-ring is above the carbasugar-moiety and once it is under the carbasugar-structure.<sup>91</sup> However, during our synthesis just the first kind of diastereomere was observed. The stereochemistry was later approved by XRD measurements of *N*-Benzyl compound **105** (Figure 31).

Using activated zinc dust, impure 6-iodo structure **102** underwent a reductive ring opening reaction, in which carbasugar precursor **68** was formed. Subsequent treatment with *N*-benzyl-hydroxylamine and pyridine, gave bicyclic isoxazolidine **67**, following an intramolecular [2+3] cycloaddition mechanism (Scheme 15).

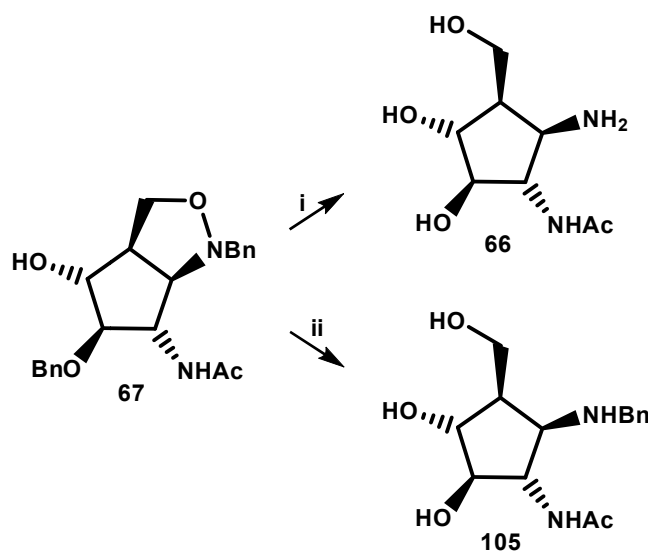


**Scheme 15:** Synthesis of bicyclus **67**; i) Zn, NH<sub>4</sub>Cl, MeOH; ii) BnNHOH, pyridine, MeOH.

### 3.2.4 Hydrogenolysis

The reductive isoxazolidine cleavage and subsequent hydrogenolytic deprotection were performed using Pearlman's catalyst under hydrogen atmosphere to provide structure **66** (Scheme 16). Unfortunately, due to still existing hardly removable iodine containing by-products, the hydrogenation process worked not as smoothly as assumed. It was found, that iodine or halides in general, are known for the deactivation of palladium catalysed hydrogenation or dehydrogenation reactions.<sup>92,93</sup> Nonetheless, on a small scale (less iodine), the hydrogenolysis was successful and the desired 2-acetamido-1-amino-β-D-gluco-

cyclopentane (**66**) was obtained. During another try, employing Pearlman's catalyst in acidic conditions, a partial hydrogenolysis was observed and *N*-benzyl compound **105** was isolated.



**Scheme 16:** Hydrogenation of bicyclus **67**; i)  $H_2$ ,  $Pd(OH)_2$ , MeOH; ii)  $H_2$ ,  $Pd(OH)_2$ , MeOH/AcOH.

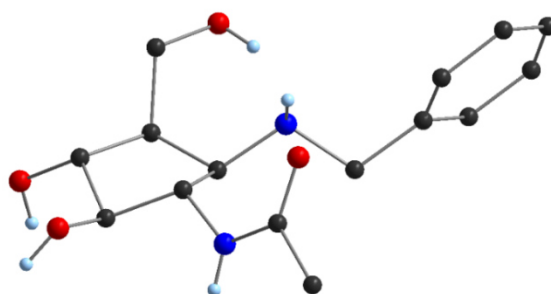
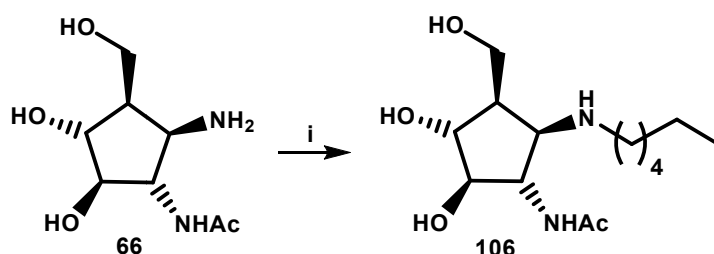


**Figure 31:** Crystal structure of compound **105**.

### 3.2.5 *N*-Alkylation

The reaction of amine **66** with 1-bromohexane in the presence of sodium bicarbonate, led to *N*-Hexyl-2-acetamido-1-amino-β-D-glucocyclopentane (**106**) (**Scheme 17**).



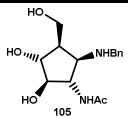
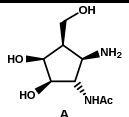
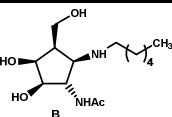
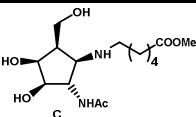
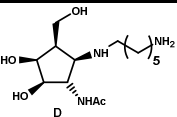
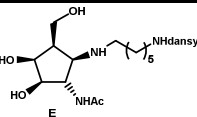
**Scheme 17:** *N*-Alkylation of amine **66**; i) 1-bromohexane,  $NaHCO_3$ , DMF,  $70^\circ C$ .

### 3.2.6 Biological evaluation

Compound **105** was tested as *N*-acetyl- $\beta$ -D-hexosaminidase inhibitor. This biological evaluation was carried out at the laboratories of Stephen G. Withers at the University of British Columbia, Canada. Compound **105** turned out to be a powerful inhibitor of *Streptomyces plicatus* *N*-acetyl- $\beta$ -hexosaminidase (SpHex) with values of  $K_i = 1$  nM and  $IC_{50} = 9.4$  nM. With the same enzyme, 2-acetamido-1,2-dideoxynojirimycin (**14**) exhibited  $K_i = 80$   $\mu$ M.<sup>30</sup>

In relation to recently published<sup>94</sup> biological activities of furanoid carbasugars (**A-E**), inhibitory values of compound **105** are in the same range. Only dansylated compound **E** with a  $K_i$  value of 0.06 nM is more effective (**Table 2**).

**Table 2:** Comparison of inhibitor activities with recently published furanoid carbasugars.<sup>94</sup>

					
1.0	0.7	0.6	0.7	0.7	0.06

$K_i$ -values [nM] of compounds with: SpHex = *Streptomyces plicatus* *N*-acetyl- $\beta$ -D-hexosaminidase

## 4 Conclusion and Outlook

### Aza-sugar nucleoside analogues as potential anti-viral agents

During this project, the synthesis of pyrrole-C-nucleoside **59** and its corresponding prodrug **96**, which are currently tested as potential anti-viral agents, were prepared. The synthesis started with protected iminoribitol compound **61** which was oxidized to the corresponding nitrene **78**. As a result of modified reaction conditions and purification methods, the desired regioisomer **78b** was obtained in excellent yield. After stereoselective addition of lithiated acetonitrile, the first key intermediate **60** was made without any problems. Further steps for the synthesis of pyrrole-C-nucleosides involved the formation of enol **88** with ethyl formate in the presence of sodium hydride, which was then converted to an isomeric mixture of enamine **89**. The cyclisation was initiated via DBU, using methyloxycarbonyl as temporary protecting group, which afforded pyrrol product **91**. The synthesis of the phosphorchloridate structure and the subsequent coupling were successful, however there is still some room for improvement, since the obtained yields are low. Unfortunately, the attempted quite synthesis of isothiazole-C-nucleosides was less successful. Even after a series of trials, it was not possible to isolate the desired sulfur containing structure and, thus the approach was abandoned.

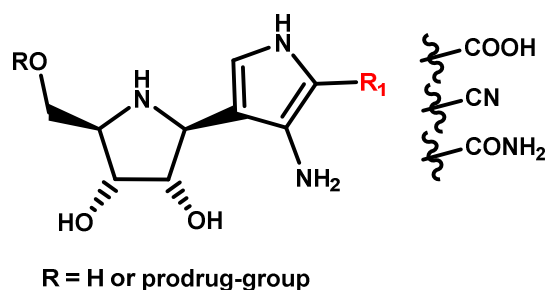


**Figure 32:** Possible modifications of the pyrrole-C-nucleoside structure.

In the future, the functional group on position C-2 could be easily modified multiple times (**Figure 32**). In case of treating the ethyl ester structure with ammonia, the corresponding amide should be formed, while adding KOH or NaOH the carboxylic acid should materialize. To get a nitrile as functional group on position C-2, enol **88** has to be treated with aminoacetonitrile instead of glycine ethyl ester.<sup>82</sup> Furthermore, the phosphoramidate-structure of Immucillin-A would be interesting as well as a new route for the production of isothiazole-C-nucleosides.



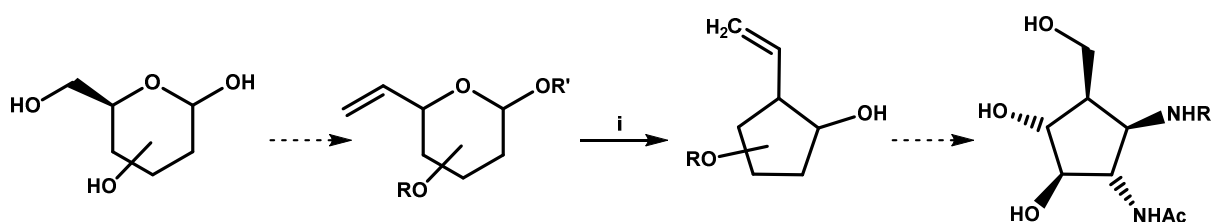
### Potential hexoseaminidase inhibitors

The second project, which was realized in the Glycogroup Graz, was dealing with furanoid carbasugars as potential pharmacological chaperons. During these studies, two potential furanoid inhibitors of *N*-acetyl- $\beta$ -D-hexosaminidase were synthesized.

The project started with a Fischer glycosylation of *N*-acetyl-D-glucosamine, followed by transacetalisation with benzylaldehyde dimethylacetal and *O*-benzylation with benzyl bromide which afforded compound **99** without any problems. After cleavage of the benzylidene protecting group with hydrochloric acid, a deoxyiodination was performed, which led to compound **102**. Furthermore, a reductive ring opening was carried out, followed by a [2+3] cycloaddition, using *N*-benzylhydroxylamine and pyridine. The obtained bicyclus **67** underwent hydrogenolysis in which amine **66** and *N*-benzyl amine **105** were formed. Additionally, amine **66** was alkylated using 1-bromohexane which afforded *N*-hexyl-2-acetamido-1-amino-  $\beta$ -D-gluco-cyclopentane (**106**).

One of the key issues of this project was the removal of iodine containing by-products caused from the reductive ring opening. As a result of the high polarity of acetamido-structures, the purification via silica-gel chromatography became inefficient. This turned out crucial, when reactions were carried out at bigger scale, and iodine containing by-products poisoned the palladium catalysed hydrogenation reaction.<sup>92,93</sup> However, since the procedure worked on lower scale, two inhibitors were successfully synthesized. One of them, structure **105**, has been already tested against *N*-acetyl- $\beta$ -D-hexosaminidase from *SpHex* with values of  $K_i = 1$  nM and  $IC_{50} = 9.4$  nM.

In **Scheme 18**, an alternative route to acetamido-cyclopentanes is described.<sup>37</sup>



**Scheme 18:** Alternative strategy to 2-acetamido carbasugars; i)  $Et_2Zn$ ,  $Pd(Ph_3)_4$ ,  $ZnCl_2$ ,  $THF_{abs}$ .

This route starts with usual protection steps followed by a Swern Oxidation and a Wittig reaction at position C-6. The key step, an intramolecular allylation of the aldehyde moiety can be realized using  $Et_2Zn/Pd(Ph_3)_4$  and  $ZnCl_2$ . The introduction of the 1-amino and 2-acetamido group can be obtained by standard procedures.

## 5 Experimental

The laboratory work for this master's thesis was performed at two different universities. The synthesis of antiviral iminoribitol-C-nucleosides has been carried out in the facilities of the Ferrier Research Institute (FRI) in Wellington, New Zealand under supervision of Gary B. Evans and Peter C. Tyler. The synthesis of potential hexosaminidase inhibitors was performed at the Glycogroup Graz, Austria under supervision of Arnold E. Stütz and Patrick Weber. Data regarding synthesis from New Zealand are labelled with a section sign (§), while information which belongs to the work in Austria is labelled with a double dagger (‡).

### 5.1 General Methods

#### Thin layer chromatography

Analytical thin layer chromatography (TLC) was carried out on aluminium sheets coated with silica gel 60 F<sub>254</sub> (Merck 5554). For the detection of corresponding organic compounds, UV light (254 nm) and one of the following dip reagents was used.

VAN: ‡	Vanillin/sulfuric acid: vanillin (9 g) in H <sub>2</sub> O (900 mL), EtOH (750 mL) and H <sub>2</sub> SO <sub>4</sub> (120 mL).
CAM: ‡	Ceric ammonium molybdate: ammonium heptamolybdate tetrahydrate (100 mL) in 10% H <sub>2</sub> SO <sub>4</sub> (1000 mL) and ceric sulfate (8 g) in 10% H <sub>2</sub> SO <sub>4</sub> (80 mL).
Ehrlich's: §	Ehrlich's reagent: dimethylaminobenzaldehyde (1 g), H <sub>2</sub> SO <sub>4</sub> (25 mL) and methanol (150 mL).
KMnO <sub>4</sub> : §	Sodium permanganate: KMnO <sub>4</sub> (2 g), K <sub>2</sub> CO <sub>3</sub> (13 g), NaOH (3.5 mL) and H <sub>2</sub> O (200 mL).

#### Silica gel chromatography

For the purification of respective products, chromatography was performed either via silica gel chromatography<sup>‡</sup>, or with an automated system with continuous gradient<sup>§</sup>. The stationary phase was consisting of silica gel 35-70  $\mu\text{m}$ <sup>‡</sup> or 40-63  $\mu\text{m}$ <sup>§</sup>. Information about the mobile phase and its composition (v/v) is given at the corresponding reaction.

### Specific rotation

The analytical characterization includes measurements about the optical rotation  $[\alpha]_D^{20}$  of chiral compounds. This was performed using a Perkin Elmer 341 polarimeter at a wave length of 589 nm and a path length of 10 cm at 20°C<sup>‡</sup>.

### Mass analysis

Further definition of the products was done via MALDI-TOF mass spectrometry on a micromass ToFSpec 2E Time-of-Flight mass spectrometer<sup>‡</sup> or in case of substances made in New Zealand a high-resolution electrospray mass spectra (ESI-HRMS) was recorded on a Q-TOF Tandem Mass Spectrometer<sup>§</sup>.

### Nuclear magnetic resonance spectroscopy

NMR spectra were recorded in CDCl<sub>3</sub> (<sup>1</sup>H: center line  $\delta$ = 7.26, <sup>13</sup>C: center line  $\delta$ = 77.16) or MeOH-d<sub>4</sub> (<sup>1</sup>H: center line  $\delta$ = 3.31, <sup>13</sup>C: center line  $\delta$ = 49.00) at 300 MHz<sup>‡</sup> or 500 MHz<sup>§</sup>. Chloroform-d was commonly used for protected substances and methanol-d<sub>4</sub> for unprotected or sparingly soluble compounds. Chemical shifts  $\delta$  are listed in [ppm] and coupling constants J in [Hz]. For final structures or crucial intermediates APT, DEPT, COSY and HSQC spectroscopy were used for unambiguous confirmation of the compounds.

NMR-abbreviations:

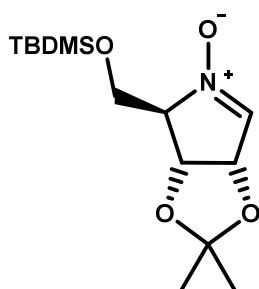
s	singlet	ddd	double double doublet
bs	broad singlet	t	triplet
d	doublet	m	multiblet
dd	double doublet	bm	broad multiblet

## 5.2 Iminoribitol-C-Nucleosides<sup>s</sup>

### 5.2.1 Synthesis of acetonitrile adduct **60**

#### 5-O-*tert*-Butyldimethylsilyl-1,*N*-dehydro-1,4-dideoxy-1,4-imino-2,3-O-isopropylidene-D-ribose *N*-oxide (**78b**)

To a stirred suspension of hydrogen peroxide (21.4 mL, 208 mmol) and methyltrioxorhenium (VII) (35.4 mg, 0.139 mmol) in dichloromethane (60 mL), methanol (10 mL) was added at room temperature. After 15 minutes, neat amine PTA 17-13 **61** (10.0 g, 34.8 mmol) was added dropwise at 0°C. When completed conversion of the starting material was observed (3 hours), the canary yellow reaction mixture was allowed to reach ambient conditions. Furthermore, the reaction was washed with water (20 mL) and brine (20 mL). Combined organic layers were dried (MgSO<sub>4</sub>), filtered and concentrated under reduced pressure. Purification was performed via recrystallization with petrol and silica-gel chromatography which provided nitrone **78b** (8.94g, 29.6 mmol, 85%) and the corresponding regioisomer **78a** (1.11g, 3.68 mmol, 11%), both as a colourless solid.



C<sub>14</sub>H<sub>27</sub>NO<sub>4</sub>Si

MW: 301.46  $\frac{g}{mol}$

TLC: UV, Ehrlich's

R<sub>f</sub>: 0.4 (PE/EA 1:1 v/v)

SCG: (PE/EA 2:1 v/v)

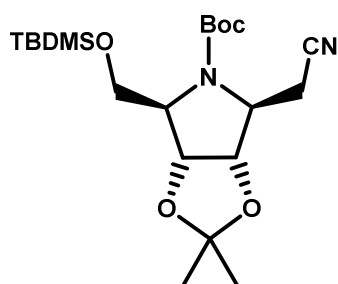
The obtained NMR data were identical with those reported in literature.<sup>78</sup>

#### *N*-*tert*-Butoxycarbonyl-7-O-*tert*-butyldimethylsilyl-2,3,6-trideoxy-3,6-imino-4,5-O-isopropylidene-D-*allo*-heptonitrile (**60**)

(The naming of the following 2 compounds is based on this core structure (**60**))

To a solution of *n*-butyllithium (18.8 mL, 44.5 mmol, 2.36  $\frac{mol}{L}$  in hexane) in dry THF (60 mL), acetonitrile (2.48 mL, 47.4 mmol) was added dropwise at -70°C. After 30 minutes, nitrone **78b** (8.94 g, 29.6 mmol) dissolved in dry THF (25 mL) was added over a period of 10 minutes, keeping the temperature below -65°C. After completed conversion (45 minutes), the slightly yellow reaction was quenched with water (5 mL) and partitioned between petrol (100 mL) and water (150 mL). Combined organic layers were dried (MgSO<sub>4</sub>), filtered and concentrated under reduced pressure. Resulting crude hydroxylamine **82** was dissolved in acetic acid (50.0 mL, 0.872 mmol) and treated with zinc dust (5.82 g, 88.9 mmol). The reaction was stirred for 15 hours with occasional cooling to keep the temperature below

30°C. After completed consumption of intermediate **82**, solids were filtered and solvents were removed *in vacuo*. The residue was dissolved in dichloromethane (40 mL) and washed with NaHCO<sub>3</sub> (30 mL, saturated), dried (MgSO<sub>4</sub>), filtered and concentrated which provided crude amine **83**. A solution of crude amine **83** dissolved in dichloromethane (40 mL), was treated with di-*tert*-butyl-dicarbonate (7.84 g, 35.6 mmol) at room temperature. After completed protection (90 minutes), water (10 mL) was added and the resulting mixture was washed with NaHCO<sub>3</sub> (20 mL, sat.). The combined organic layers were dried (MgSO<sub>4</sub>), filtered and concentrated under reduced pressure. Purification on silica-gel provided title compound **60** (8.68 g, 20.4 mmol, 69%) as colourless syrup.



C<sub>21</sub>H<sub>38</sub>N<sub>2</sub>O<sub>5</sub>Si

MW: 426.63  $\frac{g}{mol}$

TLC: UV, Ehrlich's

R<sub>f</sub>: 0.6 (PE/EA 7:3 v/v)

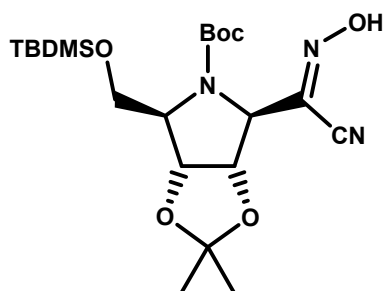
SCG: (PE/EA 20:1 v/v)

<sup>1</sup>H and <sup>13</sup>C NMR spectra were identical with those reported in literature.<sup>78</sup>

## 5.2.2 Synthesis of isothiazole-C-nucleosides

### 2-Hydroxyimino-60 (**84**)

To a solution of acetonitrile adduct **60** (0.211 g, 0.495 mmol) in dry THF (6 mL), *tert*-butyl nitrite (0.18 mL, 1.5 mmol) and potassium *tert*-butoxide (0.74 mL, 0.74 mmol, 1  $\frac{mol}{L}$  in THF) were added slowly at 0°C. After completed conversion (1 hour), the reaction was washed with water (10 mL) and brine (10 mL). Combined organic layers were dried (MgSO<sub>4</sub>), filtered and concentrated under reduced pressure. Purification by silica gel chromatography, provided oxime **84** (0.189 g, 0.415 mmol, 84%) as a yellow syrup.



C<sub>21</sub>H<sub>37</sub>N<sub>3</sub>O<sub>6</sub>Si

MW: 455.63  $\frac{g}{mol}$

TLC: UV, Ehrlich's

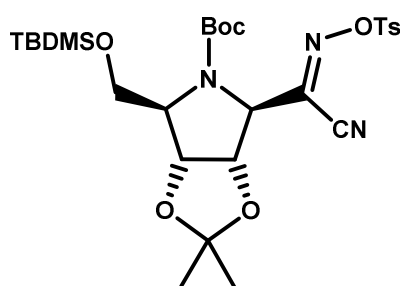
R<sub>f</sub>: 0.55 (PE/EA 2:1 v/v)

SCG: (PE/EA 10:1 v/v)

The obtained NMR data were identical with those reported in literature.<sup>65</sup>

**2-Tosylhydroxyimino-60 (85)**

A solution of compound **84** (0.082 g, 0.180 mmol) in dry dichloromethane (7 mL) was treated with *N,N*-diisopropylethylamine (0.13 mL, 0.720 mmol) and *p*-toluenesulfonyl chloride (0.053 g, 0.270 mmol). After completed conversion (30 minutes), the reaction was quenched with water (5 mL) and washed with HCl (15 mL, 10%) and NaHCO<sub>3</sub> (15 mL, saturated). Combined organic layers were dried (MgSO<sub>4</sub>), filtered and concentrated *in vacuo*. Purification via column chromatography gave desired structure **85** (0.097 g, 0.159 mmol, 88%) as colourless syrup.



$$\text{C}_{28}\text{H}_{43}\text{N}_3\text{O}_8\text{Si}$$

$$\text{MW: } 609.81 \frac{\text{g}}{\text{mol}}$$

$$\text{TLC: UV, Ehrlich's}$$

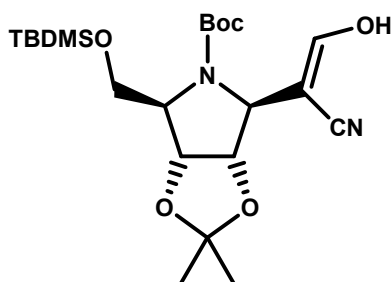
$$\text{R}_f: 0.35 \text{ (PE/EA 4:1 v/v)}$$

$$\text{SCG: (PE/EA 10:1 v/v)}$$

<sup>1</sup>H and <sup>13</sup>C NMR spectra were identical with those reported in literature.<sup>65</sup>

**5.2.3 Synthesis of pyrrole-C-nucleosides****(1S)-*N*-tert-Butoxycarbonyl-7-*O*-tert-butylidimethylsilyl-2-cyano-2,3,6-trideoxy-3,6-imino-4,5-*O*-isopropylidene-*D*-allo-hept-1-enitol (88)**

To a solution of acetonitrile adduct **60** (2.15 g, 5.04 mmol) in dry THF (12 mL), ethyl formate (4.14 mL, 50.4 mmol) and sodium hydride (0.806 g, 20.2 mmol, 60% dispersion) were added at room temperature. After completed conversion of the starting material (2.5 hours), the orange reaction was quenched with water (5 mL) and washed with water (20 mL) and brine (20 mL). The organic layer was dried (MgSO<sub>4</sub>), filtered and concentrated under reduced pressure. The residue was chromatographically purified to obtain the desired enol **88** (1.81 g, 3.98 mmol, 79%) as colourless foam.



$$\text{C}_{22}\text{H}_{38}\text{N}_2\text{O}_6\text{Si}$$

$$\text{MW: } 454.64 \frac{\text{g}}{\text{mol}}$$

$$\text{TLC: UV, Ehrlich's}$$

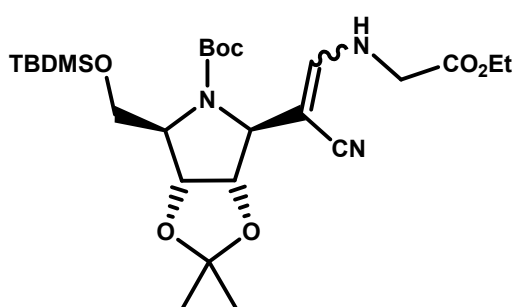
$$\text{R}_f: 0.1 \text{ (PE/EA 4:1 v/v)}$$

$$\text{SCG: (PE/EA 8:1 v/v)}$$

The obtained NMR data were identical with those reported in literature.<sup>82</sup>

**(1S)-N-tert-Butoxycarbonyl-7-O-tert-butyldimethylsilyl-2-cyano-1,2,3,6-tetra-deoxy-1-N-(ethoxycarbonylmethylamino)-3,6-imino-4,5-O-isopropylidene-D-allo-hept-1-enitol (89)**

Glycine ethyl ester hydrochloride (0.487 g, 3.45 mmol) and sodium acetate (0.567 g, 6.91 mmol) were added to a stirred solution of enol **88** (0.314 mg, 0.691 mmol) dissolved in methanol (5 mL). After stirring for 18 hours at room temperature, the reaction was washed with water (20 mL) and brine (20 mL). Combined organic layers were dried ( $\text{MgSO}_4$ ), filtered and concentrated under reduced pressure. Crude enamine **89**, afforded as a mixture of isomers, was directly used in the next step without any further purification or characterization.



$\text{C}_{26}\text{H}_{45}\text{N}_3\text{O}_7\text{Si}$

MW:  $539.75 \frac{\text{g}}{\text{mol}}$

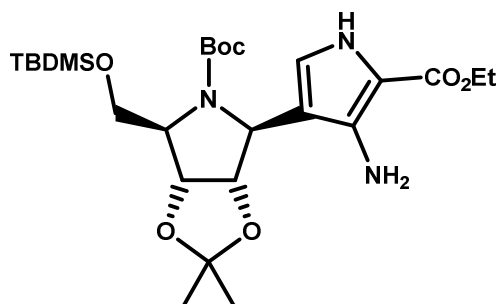
TLC: UV, Ehrlich's

$R_f$ : ---

SCG: ---

**(1S)-1-(3-Amino-2-ethoxycarbonylpyrrol-4-yl)-N-tert-butoxycarbonyl-5-O-tert-butyldimethylsilyl-1,4-dideoxy-1,4-imino-2,3-O-isopropylidene-D-ribitol (91)**

To a stirred solution of crude enamine **89** (0.398 g, 0.737 mmol) in dry dichloromethane (13 mL), DBU (0.68 mL, 4.4 mmol,) and methyl chloroformate (0.17 mL, 2.2 mmol) were added. The reaction was kept under reflux for 19 hours until full conversion was achieved. Furthermore, the reaction mixture containing protected intermediate **90**, was treated with methanol (20 mL). After completed deprotection (6 hours), the reaction was washed with HCl (15 mL, 10%) and  $\text{NaHCO}_3$  (15 mL, saturated), the combined organic layers were dried ( $\text{MgSO}_4$ ), filtered and the volatiles were removed *in vacuo*. The crude residue was purified over silica gel chromatography which afforded pyrrole compound **91** (0.282 mg, 0.523 mmol, 71%) as colourless syrup.



$\text{C}_{26}\text{H}_{45}\text{N}_3\text{O}_7\text{Si}$

MW:  $539.75 \frac{\text{g}}{\text{mol}}$

TLC: UV, Ehrlich's

$R_f$ : 0.35 (PE/EA 7:3 v/v)

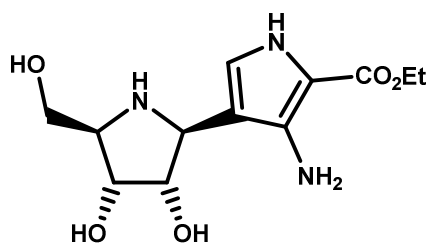
SCG: (PE/EA 5:1 v/v)

**<sup>1</sup>H NMR** (500 MHz, CDCl<sub>3</sub>) δ = 6.46 (s, 1H, H-5'), 4.98 (s, 1H, H-1), 4.75 and 4.26 (d, 1H, H-2,3), 4.08 (dd, 2H, CH<sub>2</sub>CH<sub>3</sub>), 4.03 (bs, 1H), 3.60 (s, 1H), 3.36 (bs, 1H), 1.46 and 1.41 [2s, 6H, C(CH<sub>3</sub>)<sub>2</sub>], 1.31 [s, 9H, OC(CH<sub>3</sub>)<sub>3</sub>], 1.21 (t, 3H, CH<sub>2</sub>CH<sub>3</sub>), 0.84 [s, 9H, Si(CH<sub>3</sub>)<sub>3</sub>CH<sub>3</sub>], 0.00 and -0.02 [2s, 6H, Si(CH<sub>3</sub>)<sub>2</sub>].

**<sup>13</sup>C NMR** (125 MHz, CDCl<sub>3</sub>) δ = 171.4, 161.8, 155.5, 140.1 (C), 120.0 (C-5'), 112.6, 111.9, 106.7 (C), 84.3, 82.5 (C-2,3), 80.4 [OC(CH<sub>3</sub>)<sub>3</sub>], 66.3, 63.0 (C-1,4), 60.5, 59.6 (C-5, CH<sub>2</sub>CH<sub>3</sub>), 28.6 [OC(CH<sub>3</sub>)<sub>3</sub>], 27.5, 25.7 [C(CH<sub>3</sub>)<sub>2</sub>], 26.0 [SiC(CH<sub>3</sub>)<sub>3</sub>], 18.3 [SiC(CH<sub>3</sub>)], 14.8 (CH<sub>2</sub>CH<sub>3</sub>), -5.29[Si(CH<sub>3</sub>)<sub>2</sub>].

**(1S)-1-(3-Amino-2-ethoxycarbonylpyrrol-4-yl)-1,4-dideoxy-1,4-imino-D-ribose (59)**

The deprotection was performed by treating a solution of **91** (0.10 g, 0.19 mmol) in methanol (1 mL) with hydrochloric acid (1 mL, conc.). After full conversion, the solvent was removed under reduced pressure. The residue was diluted in hydrochloric acid (1 mL, conc.) and was concentrated again. Furthermore, the residue was portioned between water (5 mL) and dichloromethane (5 mL). The water phase was concentrated *in vacuo* and after purification by column chromatography, product **59** (0.045 g, 0.16 mmol, 85%, purity: 93%) was obtained as colourless solid.



C<sub>12</sub>H<sub>19</sub>N<sub>3</sub>O<sub>5</sub>

MW: 285.30  $\frac{g}{mol}$

TLC: UV, Ehrlich's

R<sub>f</sub>: 0.45 (40% of NH<sub>3</sub> (7 N) in CHCl<sub>3</sub>)

SCG: (CHCl<sub>3</sub>/MeOH/NH<sub>3</sub> 40:9:0.1 v/v)

**<sup>1</sup>H NMR** (500 MHz, MeOH-d<sub>4</sub>) δ = 6.77 (s, 1H, H-5'), 4.27 (q, 2H, COOCH<sub>2</sub>CH<sub>3</sub>), 3.98-3.92 (m, 3H, H-1,2,3), 3.69 (dd, 2H, H-5), 3.14 (q, 1H, H-4), 1.34 (t, 3H, COOCH<sub>2</sub>CH<sub>3</sub>).

**<sup>13</sup>C NMR** (125 MHz, MeOH-d<sub>4</sub>) δ = 162.1 (COOEt), 140.5 (C-3'), 120.1 (C-5'), 111.6, 106.9 (C-2',4'), 76.1, 72.0, 65.5 (C-2,3,4), 62.0 (C-5), 59.0 (COOCH<sub>2</sub>CH<sub>3</sub>), 58.7 (C-1), 13.6 (COOCH<sub>2</sub>CH<sub>3</sub>).

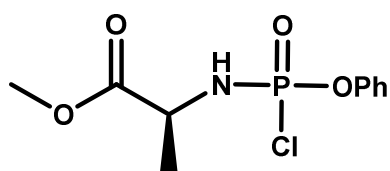
**MS:** Calcd for [C<sub>12</sub>H<sub>19</sub>N<sub>3</sub>O<sub>5</sub>H]: m/z 286.1403 [M+H]<sup>+</sup>; Found [M+H]<sup>+</sup> 286.1396.



## 5.2.4 Synthesis of the phosphoramidate compound **93**

### Phenyl (Methyl-L-alaninyl)phosphorchloridate (**93**)

Triethylamine (1.8 mL, 13 mmol) was slowly added to a solution of dichlorophosphoryloxybenzene (0.90 mL, 5.7 mmol) and methyl (2S)-2-aminopropanoate hydrochloride (**92**) (0.81 g, 5.8 mmol) in dry dichloromethane (50 mL) at -70°C. Over a time period of 12 hours, the reaction was allowed to warm to room temperature gradually. After full conversion, the mixture was treated with diethyl ether (20 mL) and the precipitating triethylammoniumchloride salt was filtered. After removing all volatiles under reduced pressure, the crude material was purified by silica gel chromatography, which afforded desired phosphoramidate **93** (0.66 g, 2.4 mmol, 42%) as colourless oil.



$C_{10}H_{19}ClNO_4P$

MW:  $277.64 \frac{g}{mol}$

TLC: UV, Ehrlich's

$R_f$ : 0.5 (PE/EA 1:1 v/v)

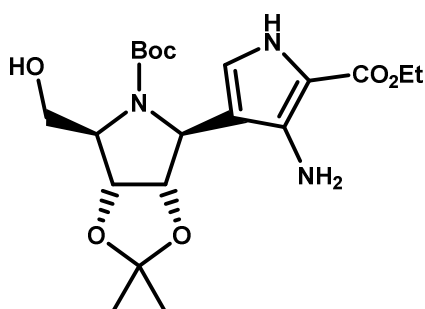
SCG: (PE/EA 2:1 v/v)

The obtained NMR data were equivalent to those reported in literature.<sup>87</sup>

## 5.2.5 Synthesis of pyrrole-C-nucleoside prodrug

### (1S)-1-(3-Amino-2-ethoxycarbonylpyrrol-4-yl)-N-tert-butoxycarbonyl-1,4-dideoxy-1,4-imino-2,3-O-isopropylidene-D-ribose (**94**)

A solution of pyrrol derivative **91** (0.175 g, 0.324 mmol) in dry THF (2 mL) was treated with tetrabutylammonium fluoride (0.7 mL, 0.7 mmol,  $1 \frac{mol}{L}$  in THF). After full conversion (20 minutes), the reaction mixture was washed with water (5 mL) and brine (5 mL), dried ( $MgSO_4$ ), filtered and concentrated under reduced pressure. After purification by column chromatography, compound **94** (0.101 g, 0.237 mmol, 73%) was used in the next step without any characterization.



$C_{20}H_{31}N_3O_7$

MW:  $425.48 \frac{g}{mol}$

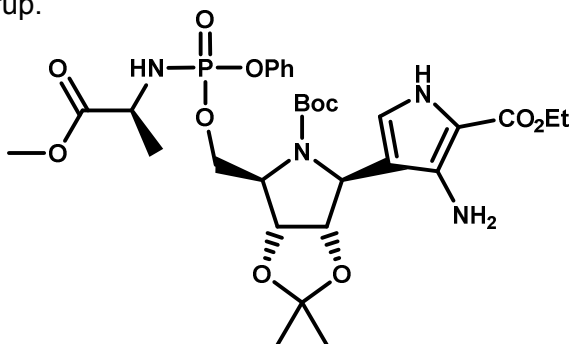
TLC: UV, Ehrlich's

$R_f$ : 0.15 (PE/EA 1:1 v/v)

SCG: (PE/EA 4:1 v/v)

**94 5-(Phenyl methyl-L-alanyl)-phosphate (95)**

A solution of phosphoramidate compound **93** (0.40 g, 1.4 mmol) in dry THF (2 mL) was added to a stirred mixture of **94** (0.051 g, 0.12 mmol) and 1-methylimidazole (0.19 mL, 2.40 mmol) in dry THF (1 mL). After completed conversion (48 hours), the reaction was washed with HCl (10 mL, 10%) and NaHCO<sub>3</sub> (10 mL, saturated). Combined organic layers were dried (MgSO<sub>4</sub>), filtered and concentrated under reduced pressure. Purification over silica gel chromatography provided coupling product **95** (0.039 g, 0.059 mmol, 49%) as a syrup.

C<sub>30</sub>H<sub>49</sub>N<sub>4</sub>O<sub>11</sub>PMW: 666.66  $\frac{g}{mol}$ 

TLC: UV, Ehrlich's

R<sub>f</sub>: 0.85 (DCM/EA/MeOH 2:2:1 v/v)

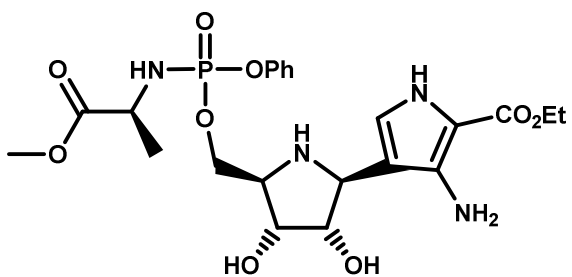
SCG: (DCM/EA/MeOH 80:2:1 v/v)

<sup>31</sup>P NMR (202 MHz, MeOH-d<sub>4</sub>) δ = 3.7, 3.4 (2s).

MS: Calcd for [C<sub>30</sub>H<sub>49</sub>N<sub>4</sub>O<sub>11</sub>PH]: m/z 667.2744 [M+H]<sup>+</sup>; Found [M+H]<sup>+</sup> 667.2747.

**59 5-(Phenyl methyl-L-alanyl)-phosphate (96)**

To a solution of compound **95** (0.045 mg, 0.068 mmol) in THF (0.5 mL), trifluoroacetic acid (1 mL, 13.0 mmol) was added at room temperature. After completed deprotection (12 hours), the reaction mixture was concentrated *in vacuo*. The resulting residue was purified by column chromatography to obtain the desired title compound **96** (0.020 g, 0.038 mmol, 56%, purity: 98%, approximate 1 to 1 mixture of diastereomers) as colorless solid.

C<sub>22</sub>H<sub>31</sub>N<sub>4</sub>O<sub>9</sub>PMW: 526.48  $\frac{g}{mol}$ 

TLC: UV, Ehrlich's

R<sub>f</sub>: 0.4 (EA/MeOH/NH<sub>4</sub>OH 7:2:1 v/v)SCG: (EA/MeOH/NH<sub>4</sub>OH 17:2:1 v/v)

<sup>1</sup>H NMR (500 MHz, MeOH-d<sub>4</sub>) δ = 7.35 (dt, 2H, Ph), 7.23-7.16 (m, 3H, Ph), 6.74 (d, 1H, H-5'), 4.30-4.17 (m, 4H), 4.04-3.86 (m, 4H), 3.70 (s, 3H, OCH<sub>3</sub>), 3.67-3.61 (m, 1H), 1.37-1.30 (m, 6H, CH<sub>3</sub>, CH<sub>2</sub>CH<sub>3</sub>).

$^{13}\text{C}$  NMR (125 MHz, MeOH- $d_4$ )  $\delta$  = 175.7, 175.4, 165.0, 163.5, 163.1 (C), 130.8, 130.1, 126.2, 123.7, 123.2, 122.9, 121.6, 112.1, 108.8 (CH), 77.9, 76.8, 76.7, 73.0, 71.6, 65.2, 64.9 (CH), 68.6, 60.4 ( $\text{CH}_2$ ), 52.8, 52.4, 51.6, 51.5 (CH,  $\text{CH}_3$ ), 20.4, 15.0 ( $\text{CH}_3$ ).

$^{31}\text{P}$  NMR (202 MHz, MeOH- $d_4$ )  $\delta$  = 4.1, 3.9 (2s).

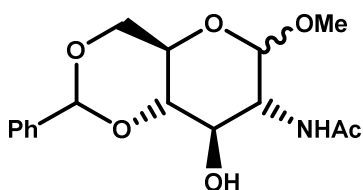
MS: Calcd for  $[\text{C}_{22}\text{H}_{31}\text{N}_4\text{O}_9\text{PH}]$ :  $m/z$  527.1907  $[\text{M}+\text{H}]^+$ ; Found  $[\text{M}+\text{H}]^+$  527.1904.

### 5.3 Synthesis of *N*-Substituted 3-Acetamido-4-amino-5-hydroxymethylcyclopentane-1,2,6-triols

#### 5.3.1 Synthesis of 3-Acetamido-4-amino-5-hydroxymethylcyclopentanetriol (66)

##### (2R,3R,4S,5R)-Methyl 2-acetamido-4,6-O-benzylidene-2-deoxy-D-glucopyranoside (98)

A solution of compound **97** (10.8 g, 45.9 mmol) in DMF (120 mL), was treated with benzaldehyde dimethyl acetal (20.7 mL, 138 mmol) and *p*-toluenesulfonic acid (cat. amounts). After full conversion (stirred under reduced pressure at 70°C), the reaction mixture was treated with  $\text{NaHCO}_3$  (140 mL, saturated) and the product precipitated as colorless sediment. The solid was filtrated, washed with diethyl ether (15 mL) and dried under reduced pressure which afforded the 4,6-O protected compound **98** (14.8 g, 45.9 mmol) as colourless solid. The product was used in the next reaction without any purification or characterization.



$\text{C}_{16}\text{H}_{21}\text{NO}_6$

MW:  $323.35 \frac{\text{g}}{\text{mol}}$

TLC: UV, CAM

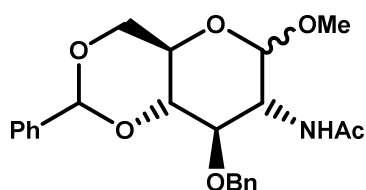
$R_f$ : 0.65 (EA/MeOH 4:1: v/v)

SCG: ---

##### (2R,3R,4S,5R)-Methyl 2-acetamido-3-O-benzyl-4,6-O-benzylidene-2-deoxy-D-glucopyranoside (99)

To a suspension of **98** (14.8 g, 45.9 mmol) in THF (200 mL), potassium tert-butoxide (7.73 g, 68.9 mmol) and benzyl bromide (6.55 mL, 55.1 mmol) were added at 0°C. The reaction was allowed to warm to room temperature and after full conversion (90 minutes), the reaction mixture was treated with water (90 mL) (removing benzyl bromide excess) and partitioned between EA (60 mL) and water (30 mL). The combined organic layers were dried ( $\text{Na}_2\text{SO}_4$ ),

filtered and concentrated under reduced pressure which provided crude **99** as yellow solid. The residue was used in the next reaction step without any purification or characterization.



$C_{23}H_{27}NO_6$

MW:  $413.47 \frac{g}{mol}$

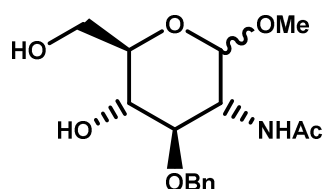
TLC: UV, CAM

$R_f$ : 0.45 (C/EA 1:4: v/v)

SCG: ---

### (2R,3R,4S,5R)-Methyl 2-acetamido-3-O-benzyl-2-deoxy-D-glucopyranoside (**100**)

To a solution of crude **99** (45.9 mmol) in THF (100 mL), water (10 mL) and HCl (2 mL, conc.) were added at room temperature. After 18 hours, full conversion of the starting material was observed (TLC). Furthermore, pyridine was added (until pH 7 was reached) and the mixture was concentrated under reduced pressure which provided crude **100** as yellow syrup. To get better properties in terms of chromatography, crude **100** (45.9 mmol) dissolved in pyridine (150 mL) was treated with DMAP (cat. amounts) and acetic anhydride (28.0 mL, 298 mmol) at 0°C. After completed diacetylation (30 minutes), the reaction was quenched with MeOH (10 mL) and concentrated *in vacuo*. The resulting residue was dissolved in DCM (20 mL), washed with HCl (10 mL, 1/6 v:v) and NaHCO<sub>3</sub> (10 mL, saturated), dried (Na<sub>2</sub>SO<sub>4</sub>), filtered and concentrated. By purification of the remaining residue on silica gel, the desired compound **101** (9.72 g, 23.7 mmol, 52% over 3 steps) was isolated as colorless solid. The subsequent saponification was realized by dissolving the acetylated product **101** (9.72 g, 23.7 mmol) in MeOH (200 mL) and adding sodium hydride (cat. amounts). After full conversion (15 minutes), the reaction was treated with IR 120, filtrated and all volatiles were removed under reduced pressure which provided **100** (6.34 g, 19.5 mmol, 82%) as colourless solid.



$C_{16}H_{23}NO_6$

MW:  $325.36 \frac{g}{mol}$

TLC: UV, CAM

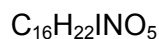
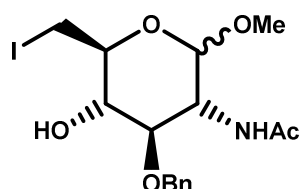
$R_f$ : 0.3 (EA/MeOH 10:1: v/v)

SCG: ---

The obtained NMR data were equivalent to those reported in literature.<sup>95</sup>

**(2R,3R,4S,5S)-Methyl 2-acetamido-3-O-benzyl-2,6-dideoxy-6-iodo-D-glucopyranoside (102)**

The iodine was introduced by dissolving compound **100** (1.1 g, 3.2 mmol) in THF (40 mL) and adding triphenylphosphane (1.1 g, 4.2 mmol), imidazole (0.7 g, 9.7 mmol) and iodine (0.98 g, 3.87 mmol). The reaction was stirred for 25 minutes under reflux until the starting material fully converted to a less polar product. After adding diethyl ether (40 mL), the precipitated triphenylphosphane oxide was filtered and the solvent was washed with NaHCO<sub>3</sub> (30 mL, saturated, thiosulfate). Combined organic layers were dried (Na<sub>2</sub>SO<sub>4</sub>), filtered and concentrated under reduced pressure. The resulting residue was purified by silica gel chromatography which afforded 6-iodo compound **102** (1.9 g) and some by-products (iodine and triphenylphosphane oxide) as yellowish syrup.



$$MW: 435.26 \frac{g}{mol}$$

TLC: UV, CAM

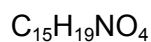
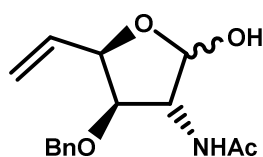
R<sub>f</sub>: 0.7 (EA/MeOH 10:1: v/v)

SCG: C/EE 1:2: v/v

The obtained NMR data were equivalent to those reported in literature.<sup>96</sup>

**(2R,3R,4R)-2-Acetamido-3-O-benzyl-2,5,6-trideoxy-D-xylo-hex-5-enofuranose (68)**

A suspension of zinc dust (2.11 g, 32.3 mmol) and ammoniumchloride (1.73 g, 32.3 mmol) in MeOH (30 mL) was stirred vigorously for 15 minutes. The starting material **102** (3.23 mmol) in MeOH (10 mL) was added dropwise and after 75 minutes, TLC confirmed full conversion. After filtration, the volatiles were removed under reduced pressure which provided crude **68** as syrup. The residue was used in the next step directly, without any purification or characterization.



$$MW: 277.32 \frac{g}{mol}$$

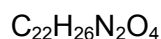
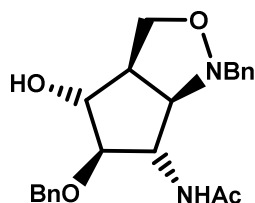
TLC: UV, CAM

R<sub>f</sub>: 0.75 (EA/MeOH 4:1: v/v)

SCG: ---

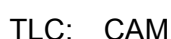
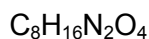
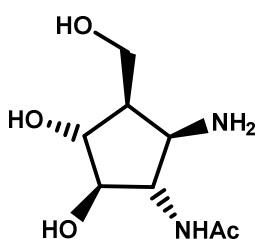
**(1R,2R,3S,4R,5R)-3-Acetamido-5,6-anhydro-2-O-benzyl-4-(N-benzyl)hydroxylamine-5-hydroxymethylcyclopentane-1,2-diol (67)**

To a solution of crude substance **68** (3.2 mmol) dissolved in MeOH (50 mL), *N*-benzylhydroxylamine (0.52 g, 3.2 mmol) and pyridine (1.04 mL, 12.9 mmol) was added at room temperature. After completed conversion (18 hours), the solvent was removed under reduced pressure. Purification on silica gel provided bicyclus **67** (0.75 g, 2.0 mmol, 61% over 3 steps) as yellowish syrup. The product was used in the next step without further characterization.



**(1R,2R,3S,4R,5R)-3-Acetamido-4-amino-5-hydroxymethylcyclopentane-1,2,6-triol (66)**

A suspension of bicyclus **67** (0.75 g, 2.0 mmol) in MeOH (10 mL), was treated with pearlman's catalyst (cat. amounts) under hydrogen atmosphere. After full conversion of the starting material (2 hours), the reaction mixture was filtrated and concentrated *in vacuo* which provided substance **66** (0.215 g, 1.05 mmol, 95%) as colorless syrup.



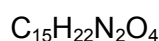
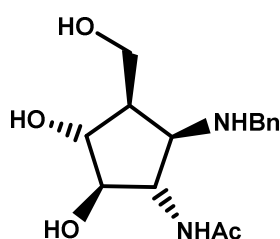
$^1H$  NMR (300 MHz,  $D_2O$ )  $\delta$  = 3.86-3.72 (m, 5H, H-2, H-3, H-4), 3.38-3.30 (m, 1H, H-1), 2.17-2.06 (m, 1H, H-5), 2.01 (s, 3H,  $CH_3$ -Ac);

$^{13}C$  NMR (75.5 MHz,  $D_2O$ )  $\delta$  = 175.5 ( $\underline{C}$ -Ac), 78.9, 75.7, 60.3 (C-2, C-3, C-4), 59.5 (C-6), 53.5 (C-1), 45.9 (C-5), 22.8 ( $\underline{C}H_3$ -Ac);

### 5.3.2 N-Alkylated products of **66**

#### (1R,2R,3S,4R,5R)-N-(1-Benzyl)-3-acetamido-4-amino-5-hydroxymethylcyclopentane-1,2,6-triol (**105**)

Bicyclus **67** (0.75 g, 2.0 mmol) in MeOH (20 mL) was stirred with pearlman's catalyst under hydrogen atmosphere at acidic conditions (HCl, conc.). After completed reaction (90 minutes), the mixture was filtrated and concentrated under reduced pressure. The resulting residue was purified by silica gel chromatography which afforded *N*-benzyl compound **105** (0.25 g, 0.85 mmol, 43%) as colorless solid.



$$MW: 294.35 \frac{g}{mol}$$

TLC: UV, CAM

R<sub>f</sub>: 0.5 (CHCl<sub>3</sub>/MeOH/NH<sub>4</sub>OH 3:1:0.01 v/v/v)

SCG: (CHCl<sub>3</sub>/MeOH/NH<sub>4</sub>OH 3:1:0.01 v/v/v)

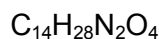
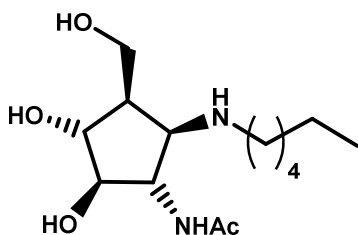
$$[\alpha]_D^{20} = + 30.7 \left( c 0.985 \frac{g}{100 mL}, MeOH \right)$$

<sup>1</sup>H NMR (300 MHz, D<sub>2</sub>O) δ = 7.43-7.25 (m, 5H, H-Ar), 3.91 (t, 1H, J<sub>1,2</sub> 8.4 Hz, H-2), 3.82 (d, 2H, J<sub>5,6</sub> 8.1 Hz, H-6), 3.80-3.64 (m, 4H, H-3, H-4, CH<sub>2</sub>-Bn), 3.16 (t, 1H, H-1), 2.17 (dt, 1H, H-5), 1.96 (s, 3H, CH<sub>3</sub>-Ac)

<sup>13</sup>C NMR (75.5 MHz, D<sub>2</sub>O) δ = 173.9 (C-Ac), 138.7 (ipso.-Ar), 128.7, 128.3, 127.5 (Ar), 79.6 (C-3), 75.2 (C-4), 59.5 (C-6), 58.9 (C-2), 57.4 (C-1), 50.6 (CH<sub>2</sub>-Ar), 45.3 (C-5), 22.2 (CH<sub>3</sub>-Ac)

#### (1R,2R,3S,4R,5R)-N-(1-Hexyl)-3-acetamido-4-amino-5-hydroxymethylcyclopentane-1,2,6-triol (**106**)

A solution of structure **66** (31.0 mg, 0.159 mmol) in DMF (2 mL) was stirred with NaHCO<sub>3</sub> (0.050 g, 0.60 mmol) and 1-bromohexane (32.0 μL, 0.224 mmol) at 70°C. After 18 hours, the reaction mixture was concentrated under reduced pressure and after purification via silica gel chromatography (2x), *N*-hexyl structure **106** (0.017 mg, 0.058 mmol, 39%) was isolated as colorless solid.



$$MW: 288.39 \frac{g}{mol}$$

TLC: CAM

R<sub>f</sub>: 0.6 (CHCl<sub>3</sub>/MeOH/NH<sub>4</sub>OH 8:4:1 v/v/v)

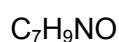
SCG: (CHCl<sub>3</sub>/MeOH/NH<sub>4</sub>OH 8:1:0.01 v/v/v)

<sup>1</sup>H NMR (300 MHz, MeOH-d<sub>4</sub>) δ = 3.96-3.76 (m, 4H, H-2, H-4, H-6), 3.70 (dd, 1H, J<sub>2,3</sub> J<sub>3,4</sub> 8.1 Hz, H-3), 3.32-3.24 (m, 1H, H-1), 2.88-2.70 (m, 2H, H-1'), 2.17-2.07 (m, 1H, H-5), 1.99 (s, 3H, CH<sub>3</sub>-Ac), 1.55 (dt, 2H, H-2'), 1.38-1.28 (m, 6H, H-3', H-4', H-5'), 0.91 (t, 3H, H-6');

<sup>13</sup>C NMR (75.5 MHz, MeOH-d<sub>4</sub>) δ = 174.3 (C-Ac), 80.6 (C-3), 76.5 (C-4), 62.9 (C-1), 60.5 (C-2, C-6), 49.5 (C-1'), 46.9 (C-5), 29.6 (C-2'), 32.7, 17.7, 23.6 (C-3', C-4', C5'), 22.6 (CH<sub>3</sub>-Ac), 14.3 (C-6');

### 5.3.3 Synthesis of *N*-benzylhydroxylamine

To a solution of benzaldehyde (10.0 g, 94.2 mmol) in MeOH (80 mL), hydroxylamine hydrochloride (7.20 g, 104 mmol) and sodium hydroxide (34.6 mL, 104 mmol, 3  $\frac{mol}{L}$ ) were added at room temperature. After 2.5 hours, the reaction was concentrated *in vacuo* and the resulting white residue was partitioned between EA (20 mL) and water (20 mL). The organic layer was dried (Na<sub>2</sub>SO<sub>4</sub>), filtrated and the volatiles were removed under reduced pressure. Furthermore, the resulting residue and sodium cyanoborohydride (8.90 g, 142 mmol) were added to a solution of acetyl chloride (7.40 mL, 104 mmol) in MeOH (100 mL) at 0°C. After 16 hours the mixture was neutralized by adding sodium hydride (3  $\frac{mol}{L}$ ) and concentrated under reduced pressure. The residue was dissolved in EA (20 mL), washed with water (20 mL), dried (Na<sub>2</sub>SO<sub>4</sub>), filtrated and concentrated *in vacuo*. Purification on silica gel provided *N*-benzylhydroxylamine (5.40 g, 43.8 mmol, 47%) as yellowish solid.

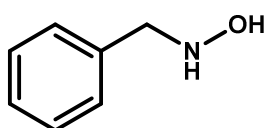


$$MW: 123.16 \frac{g}{mol}$$

TLC: UV, CAM

R<sub>f</sub>: 0.6 (C/EA 1:1 v/v)

SCG: (C/EA 3:1)



The NMR data were identical to those reported in literature.<sup>97</sup>



## 6 References

- [1] J. B. Laursen, J. Nielsen, *Chem. Rev.*, **2004**, *104*, 1663-1685.
- [2] P. Compain, O. R. Martin, *Iminosugars: from synthesis to therapeutic applications*. John Wiley & Sons, Ltd, **2007**.
- [3] A.E. Stütz, *Iminosugars as Glycosidase Inhib.*, Wiley-VCH Verlag GmbH & Co. KGaA, Weinheim, FRG, **1999**.
- [4] J. J. Clayden, N. Greeves, S. Warren, P. Wothers, *Organic Chemistry*, **2001**.
- [5] „Kohlenhydrate“, In *Römpf Online Chemielexikon*, Thieme-Verlag.
- [6] R. K. Singla, V. G. Bhat, *Indo Global Journal of Pharmaceutical Sciences*, **2011**, *1* (4), 281-286
- [7] H. A. L. Wiggers, *Ann. der Pharm.* **1832**, *1*, 129-182.
- [8] Z. Yu-Tao, S. Hai-Ying, A. Wei, *World J. Gastroenterol.*, **2016**, *22*, 2483-2493.
- [9] <http://www.enzyme-database.org/> (02.15.2018).
- [10] G. Davis, B. Henrisat, *Structure*, **1995**, *3*, 853-859.
- [11] D. L. Zechel, S. G. Withers, *Acc. Chem. Res.*, **2000**, *33*, 11-18.
- [12] V. L. Y. Yip, S. G. Withers, M. L. Sinnott, S. Roseman, H. Schachter, R. A. Laine, C. R. Bertozzi, L. L. Kiessling, J. B. Lowe, J. D. Marth, et al., *Org. Biomol. Chem.*, **2004**, *2*, 2707.
- [13] M. L. Sinnott, *Chem. Rev.*, **1990**, *90*, 1171-1202.
- [14] J. D. McCarter, G. Stephen Withers, *Curr. Opin. Struct. Biol.*, **1994**, *4*, 885-892.
- [15] Adopted from: <http://www.cazypedia.org/index.php/> (02.15.2018).
- [16] J. H. Kim, Y. B. Ryu, N. S. Kang, B. W. Lee, J. S. Heo, I. Y. Jeong, K. H. Park, *Biol. Pharm. Bull.*, **2006**, *29*, 302-305.
- [17] S. Inouye, T. Tsuruoka, T. Ito, T. Niida, *Tetrahedron*, **1968**, *24*, 2125-2144.
- [18] H. Y. L. Lai, B. Axelrod, *Biochem. Biophys. Res. Commun.*, **1973**, *54*, 463-468.
- [19] Y. Kameda, S. Horii, *J. Chem. Soc. Chem. Commun.*, **1972**, *0*, 746.
- [20] Y. Kanieda, N. Asano, M. Teranishi, K. Matsui, *J. Antibiot. (Tokyo)*, **1980**, *33*, 1573-1574.
- [21] D. L. Zechel, S. G. Withers, *Acc. Chem. Res.*, **2000**, *33*, 11-18.
- [22] G. Legler, *Adv. Carbohydr. Chem. Biochem.*, **1990**, *48*, 319-384.
- [23] G. Caron, S. G. Withers, *Biochem. Biophys. Res. Commun.*, **1989**, *163*, 495-499.
- [24] R. Lebl, A pre-commercial de novo synthesis of 5a-C-pentyl-4-epi-isofagomine-a powerful pharmacological chaperone for GM1-gangliosidosis, Graz University of Technology, Austria, **2016**.
- [25] B. P. Rempel, S. G. Withers, *Glycobiology*, **2008**, *18*, 570-586.
- [26] Project proposal for a DOC stipend, P. Weber, *Austr. Acad. Sci.*, Selected Glycosamine Processing Enzymes of the Lysosome: Diseases Caused by Misfolded Mutants and Sugar Mimetics as Potential Correcting Pharmacological Chaperons, Graz University of Technology, Austria, **2016**.
- [27] A. E. Stütz, T. M. Wrodnigg, *Adv. Carbohydr. Chem. Biochem.*, **2016**, *73*, 225-302.
- [28] A. González, G. Vadlamani, B. L. Mark, S. G. Withers, *Chem. Commun.*, **2016**, DOI: 10.1039/C6CC02520J.
- [29] M. Horsch, L. Hoesch, A. Vasella, D. M. Rast, *Eur. J. Biochem.*, **1991**, *197*, 815-818.
- [30] P. Greimel, H. Häusler, I. Lundt, K. Rupitz, A. E. Stütz, C. A. Tarling, S. G. Withers, T. M. Wrodnigg, *Bioorg. Med. Chem. Lett.*, **2006**, *16*, 2067-2070.

- [31] A. de la Fuente, R. Rísquez-Cuadro, X. Verdaguer, J. M. G. Fernández, E. Nanba, K. Higaki, C. Ortiz Mellet, A. Riera, *Eur. J. Med. Chem.*, **2016**, *121*, 926-938.
- [32] D. Best, P. Chairatana, A. F. G. Glawar, E. Crabtree, T. D. Butters, F. X. Wilson, C. Yu, W. Wang, Y. Jia, I. Adachi, A. Kato, G. W. J. Fleet, *Tetrahedron Lett.*, **2010**, *51*, 2222-2224.
- [33] J. S. Sc Rountree, T. D. Butters, M. R. Wormald, S. D. Boomkamp, R. A. Dwek, N. Asano, K. Ikeda, E. L. Evinson, R. J. Nash, G. W. J. Fleet, *ChemMedChem*, **2009**, *4*, 378-392.
- [34] P. S. Liu, M. S. Kang, P. S. Sunkara, *Tetrahedron Lett.*, **1991**, *32*, 719-720.
- [35] R. V. Salunke, N. G. Ramesh, *Eur. J. Org. Chem.*, **2016**, *0*, 654-657.
- [36] T. Aoyagi, H. Suda, K. Uotani, F. Kojima, T. Aoyama, K. Horiguchi, M. Hamada, T. Takeuchi, *The Journal of Antibiotics*, **1992**, *45*, 1404-1408.
- [37] M. Schalli, Carbasugars for  $\beta$ -Galactosidase Related Lysosomal Diseases and for Investigation of G<sub>M1</sub>-Ganglioside Metabolism, Graz University of Technology, Austria, **2017**.
- [38] G. E. McCasland, S. Furuta, L. J. Durham, *J. Org. Chem.*, **1968**, *33*, 2835-2841.
- [39] T. W. Miller, B. H. Arison, G. Albers-Schonberg, *Biotechnol. Bioeng.*, **1973**, *15*, 1075-1080.
- [40] R. Lahiri, A. A. Ansari, J. D. Vankar, *Chem. Soc. Rev.*, **2013**, *42*, 5102-5118.
- [41] S. Horii, T. Iwasa, Y. Kameda, *J. Antibiot.*, **1971**, *24*, 57-58.
- [42] A. Scaffidi, K. A. Stubbs, R. J. Dennis, E. J. Taylor, G. J. Davies, D. J. Vocadlo, R. V. Stick, *Org. Biomol. Chem.*, **2007**, *5*, 3013-3019.
- [43] M. Bessieres, F. Chevrier, V. Roy, L. A. Agrofoglio, *Future Medicinal Chemistry*, **2015**, *7*, 1809-1928.
- [44] M. Kleban, P. Hilgers, J. N. Greul, R. D. Kugler, J. Li, S. Picasso, P. Vogel, V. Jäger, *ChemBioChem.*, **2001**, *5*, 365-370.
- [45] J. L. W. Thudichum, *A Treatise on the Chemical Constitution of the Brain: Based throughout upon Original Researches*, Bailliere, Tindall, And Cox, London, **1884**.
- [46] T. Wennekes, R. J. B. H. N. van den Berg, R. G. Boot, G. A. van der Marel, H. S. Overkleevt, J. M. F. G. Aerts, *Angew. Chem. Int. Ed.*, **2009**, *48*, 8848-8869.
- [47] M. S. Thonhofer, Probes and Potential Drugs for Lysosomal Diseases and Alzheimer's, Graz University of Technology, Austria, **2016**.
- [48] Adopted from: T. Kolter, K. Sandhoff, *Annu. Rev. Cell Dev. Biol.* **2005**, *21*, 81-103.
- [49] B. Winchester, A. Vellodi, E. Young, *Biochemical Society Transactions*, **2000**, *28*, 150-154.
- [50] P. J. Meikle, J. J. Hopwood, A. E. Claque, W. F. Carey, *JAMA*, **1999**, *281*, 249-254
- [51] B. Poorthuis, R. Wevers, W. Kleijer, J. Groener, J. de Jong, S. van Weely, *Hum Gen*, **1999**, *105*, 151-156.
- [52] T. Wrodnigg, A. Stütz, *Current Enzyme Inhibition*, **2012**, *8*, 47-99.
- [53] R. J. Desnick, E. H. Schuchman, *Enzyme Replacement Therapy for Lysosomal Diseases: Lessons from 20 Years of Experience and Remaining Challenges*, Annual Reviews, **2012**.
- [54] D. J. Begley, C. C. Pontikis, M. Scarpa, *Curr. Pharm. Des.*, **2008**, *14*, 1566-1580.
- [55] H. Mellor, J. Nolan, L. Pickering, M. Wormald, F. Platt, R. Dwek, G. Fleet, T. Butters, *Biochemical Journal*, **2002**, *366*, 225-233.
- [56] J. Q. Fan, S. Ishii, N. Asano, Y. Suzuki, *Nat. Med.*, **1999**, *5*, 112-115.
- [57] European Medicines Agency, "Galafold," can be found under [http://www.ema.europa.eu/docs/de\\_DE/document\\_library/EPAR\\_Summary\\_for\\_the\\_public/human/004059/WC500208437.pdf](http://www.ema.europa.eu/docs/de_DE/document_library/EPAR_Summary_for_the_public/human/004059/WC500208437.pdf), **2016**.
- [58] Adopted from: J. Q. Fan, *Trends Pharmacol. Sci.*, **2003**, *24*, 355-360.
- [59] H. Paulsen, K. Todt, *Advanced Carbohydrate Chemistry*, **1968**, *23*, 115-232.
- [60] S. Inouye, T. Tsuruoka, T. Ito, T. Niida, *Tetrahedron*, **1968**, *24*, 2125-2144.

- [61] V. L. Schramm, *ACS Chem. Biol.*, **2013**, *8*, 71-81.
- [62] V. Singh, G. B. Evans, D. H. Lenz, J. M. Mason, K. Clinch, S. Mee, G. F. Painter, P. C. Tyler, R. H. Furneaux, J. E. Lee, L. Howell, V. L. Schramm, *J. Biol. Chem.*, **2005**, *280*, 18265-18273.
- [63] P. Macheroux, Script for Biochemistry I, Graz University of Technology, Austria, **2014**.
- [64] Project proposal, G. B. Evans, Aza-sugar nucleoside analogues as potential anti-viral agents, Ref. ID: 17/031, Ferrier Research Institute, Victoria University of Wellington, New Zealand, **2016**.
- [65] L. Ye, Design and Synthesis of Antiviral Iminoribitol C-Nucleosides, Victoria University of Wellington, New Zealand, **2017**.
- [66] R. W. Miles, P. C. Tyler, R. H. Furneaux, C. K. Bagdassarian, V. L. Schramm, *Biochemistry*, **1998**, *37*, 8615-8621.
- [67] J. Shelton, X. Lu, J. A. Hollenbaugh, J. H. Cho, F. Amblard, R. F. Schinazi, *Chem. Rev.*, **2016**, *116*, 14379-14455.
- [68] <http://investor.shareholder.com/biocryst/releasedetail.cfm?ReleaseID=1019740>, BioCryst Announces Mundipharma Receives Approval for Mundesine® in Japan (03.03.2018).
- [69] <http://www.who.int/csr/resources/publications/ebola/potential-therapies-vaccines/en>, WHO, Potential Ebola therapies and vaccines (03.03.2018).
- [70] T. K. Warren, J. Wells, R. G. Panchal, K. S. Stuthman, N. L. Garza, S. A. Van Tongeren, L. Dong, C. J. Retterer, B. P. Eaton, G. Pegoraro, S. Honnold, S. Bantia, P. Kotian, X. Chen, B. R. Taubenheim, L. S. Welch, D. M. Minning, Y. S. Babu, W. P. Sheridan, S. Bavari, *Nature*, **2014**, *508*, 402-405.
- [71] Adopted from: U. Pradere, E. C. Garnier-Amblard, S. J. Coats, F. Amblard, R. F. Schinazi, *Chem. Rev.*, **2014**, *114*, 9154-9218.
- [72] M. Slusarczyk, M. Huerta Lopez, J. Balzarini, M. Mason, W. G. Jiang, S. Blagden, E. Thompson, E. Ghazaly, C. McGuigan, *J. Med. Chem.*, **2014**, *57*, 1531-1542.
- [73] G. Fuchs, H. G. Schlegel, Allgemeine Mikrobiologie, Georg Thieme Verlag Stuttgart, 8. Auflage, **2007**.
- [74] L. P. Jordheim, D. Durantel, F. Zoulim, C. Dumontet, *Nat. Rev. Drug Discov.*, **2013**, *12*, 447-464.
- [75] Patent, Publication number: WO 2014/078778 A2, Antiviral Azasugar-Containing Nucleosides, **2014**.
- [76] B. A. Horenstein, R. F. Zabinski, V. L. Schramm, *Tetrahedron Lett.*, **1993**, *34*, 7213-7216.
- [77] Patent, Publication number: WO 2016/110527 A1, Process for manufacture of forodesine, **2016**.
- [78] G. B. Evans, R. H. Furneaux, H. Hausler, J. S. Larsen, P. T. Tyler, *J. Org. Chem.*, **2004**, *69*, 2217-2220.
- [79] J. C. Oxley, J. Brady, S. A. Wilson, J. L. Smith, *Journal of Chemical Health and Safety*, **2012**, *19*, 27-33.
- [80] R. W. Murray, K. Iyanar, J. Chen, J. T. Wearing, *J. Org. Chem.*, **1996**, *61*, 8099-8102.
- [81] Adopted from: F. Stappers, R. Broeckx, S. Leurs, L. van den Bergh, J. Agten, A. Lambrechts, D. van den Heuvel, D. de Smaele, *Organic Process Research & Development*, **2002**, *6*, 911-914.
- [82] G. B. Evans, R. H. Furneaux, G. J. Gainsford, V. L. Schramm, P. C. Tyler, *Tetrahedron*, **2000**, *56*, 3053-3062.
- [83] H. Wamhoff, R. Berresse, M. Nieger, *J. Org. Chem.*, **1993**, *58*, 5181-8185.
- [84] Patent, Publication number: US 2012/0157439 A1, Raf inhibitor compounds and methods of use thereof, **2012**.

- [85] M. H. N. Arsanious, S. S. Maigali, L. S. Boulos, *Phosphorus, Sulfur and Silicon*, **2010**, *185*, 57-64.
- [86] N. R. Mohamed, G. A. Elmegeed, H. A. Abd-ElMalek, M. Younis, *Steroids*, **2005**, *70*, 131-136.
- [87] L. Osgerby, Y. C. Lai, P. J. Thornton, J. Amalfitano, C. S. Le Duff, I. Jabeen, H. Kadri, A. Miccoli, J. H. R. Tucker, M. M. K. Muqit, Y. Mehellou, *J. Med. Chem.*, **2017**, *60*, 3518-3524.
- [88] F. Gao, X. Yan, T. Shakya, O. M. Baetting, S. Ait-Mohand-Brunet, A. M. Berghuis, G. D. Wright, K. Auclair, *J. Med. Chem.*, **2006**, *49*, 5273-5281.
- [89] P. J. Garegg, B. Samuelsson, *J. Chem. Soc., Perkin Trans. 1*, **1980**, *0*, 2866-2869.
- [90] R. L. Whistler, A. K. M. Anisuzzaman, *Deoxohalo sugars: Preferential Halogenation of the Primary Hydroxyl Group*, Methods in Carbohydrate Chemistry, Vol. 8, **1980**.
- [91] B. Bernet, A. Vasella, *204 Helv. Chim. Acta*, **1979**, *62*, 1990-2016.
- [92] C. H. Bartholomew, *Applied Catalysis A*, **2001**, *general 212*, 17-60.
- [93] M. D. Argyle, C. H. Bartholomew, *Catalysts*, **2015**, *5*, 145-269.
- [94] P. Weber, S. A. Nasser, B. M. Pabst, A. Torvisco, P. Müller, E. Pascke, M. Tschernutter, W. Windischhofer, S. G. Withers, T. M. Wrodnigg, A. E. Stütz, *Molecules*, **2018**, *23*, 708.
- [95] S. S. Rana, J. J. Barlow, K. L. Matta, *Carb. Res.*, **1983**, *113*, 257-271.
- [96] A. Scaffidi, K. A. Stubbs, R. J. Dennis, E. J. Taylor, G. J. Davies, D. J. Vocadlo, R. V. Stick, *Org. Biomol. Chem.*, **2007**, *5*, 3013-3019.
- [97] S. Pagoti, D. Dutta, J. Dash, *Adv. Synth. Catal.*, **2013**, *355*, 3552-3538.

## 7 Appendix

### 7.1 Abbreviations

Biological terms		General terms	
ASSC	active site specific chaperon	$[\alpha]_D^{20}$	specific optical rotation
CMT	chaperon mediated therapy	APT	attached proton test
DNA	deoxyribonucleic acid	aq.	aqueous solution
EBOV	Ebola virus	cat.	catalytic
EC	enzyme commission number	conc.	concentrated
ER	endoplasmic reticulum	COSY	correlation spectroscopy
ERAD	ER associated degradation	FDA	food and drug administration
ERT	enzyme replacement therapy	FRI	Ferrier research institute
GH	glycosyl hydrolase	HPLC	high performance liquid chromatography
G <sub>M1</sub>	GM1-gangliosidosis	HSQC	heteronuclear single quantum coherence
GSL	glycosphingolipid	MS	mass spectroscopy
HCV	hepatitis C virus	MW	molecular weight
HIV	human immunodeficiency virus	NMR	nuclear magnetic resonance
IC <sub>50</sub>	half max. inhibitory concentration	R <sub>f</sub>	retardation factor
K <sub>i</sub>	enzyme inhibitor dissociation const.	sat.	saturated solution
LSD	lysosomal storage disorder	SCG	silica-gel chromatography
MARV	Marburg virus	TLC	thin layer chromatography
PC	pharmacological chaperon	v/v	Volume/volume
RdRp	RNA-dependent RNA polymerase	WHO	world health organisation
RNA	ribonucleic acid		
SRT	substrate reduction therapy		
ZIKA	Zika virus		
Organic structures			
Ac	acetyl-		
Bn	benzyl-		
Boc	tert-butyloxycarbonyl-		
CBz	carboxybenzyl-		
CN	nitrile-		
Et	ethyl-		
Me	methyl-		
<sup>i</sup> Pr	Isopropyl-		
Ph	phenyl-		
TBDMS	tert-butyl-diemthylsilyl-		
Trit	trityl-		
Ts	tosyl-		

## Reagents and solvents

AcOH	acetic acid
Boc <sub>2</sub> O	di-tert-butyl dicarbonate
C	cyclohexane
CAM	ceric sulfate, ammonium molybdate
DBU	1,8-diazabicyclo[5.4.0]undec-7-en
DCM	dichloromethane
DEAD	diethyl azodicarboxylate
DIPEA	diisopropylethylamine
DMAP	4-dimethylaminopyridin
DMF	dimethylformamide
DMSO	dimethyl sulfoxide
DNJ	1-deoxynojirimycin
EA	ethyl acetate
EtOH	ethanol
HCl	hydrochloric acid
H <sub>2</sub> SO <sub>4</sub>	sulfuric acid
H <sub>2</sub> O <sub>2</sub>	hydrogen peroxide
IR-120	Amberlite IR-120 strongly acidic ion exchange
K <sub>2</sub> CO <sub>3</sub>	potassium carbonate
KMnO <sub>4</sub>	potassium permanganate
LiTMP	lithium tetramethylpiperidide
mCPBA	m-chloroperoxybenzoic acid
MeCN	acetonitrile
MeOH	methanol
MgSO <sub>4</sub>	magnesium sulfate
MTO	methyltrioxorhenium
NaBH <sub>4</sub>	sodium borohydride
NaH	sodium hydride
NaHCO <sub>3</sub>	sodium hydrogencarbonate
NaOAc	sodium acetate
NaOH	sodium hydroxide
Na <sub>2</sub> SO <sub>4</sub>	sodium sulfate
<i>n</i> -BuLi	<i>n</i> -butyllithium
NH <sub>4</sub> Cl	ammonium chloride
NMI	1-methylimidazole
NOEV	<i>N</i> -octyl-4- <i>epi</i> -β-valienamine
NSC	<i>N</i> -chlorosuccinimide
Pd/C	palladium on activated charcoal
Pd(OH) <sub>2</sub> /C	palladium hydroxide on activated charcoal
PE	petroleum ether
pTSA	<i>p</i> -toluenesulfonic acid
t-BuOK	potassium tert-butoxide
TEA	triethylamine
THF	tetrahydrofuran
VAN	vanillin, sulfuric acid

## 7.2 List of publications

### Articles in peer-reviewed journals

#### **“C-5a-substituted validamine type glycosidase inhibitors”**

M. Schalli, A. Wolfsgruber, A. Gonzalez Santana, C. Tysoe, R. Fischer, A. E. Stuetz, M. Thonhofer, S. G. Withers, *Carb. Res.*, **2017**, *440*, 1-9.

#### **“From secondary alcohols to tertiary fluoro substituents: A simple route to hydroxymethyl branched sugars with a fluorine substituent at the branching point“**

M. Schalli, M. Thonhofer, A. Wolfsgruber, H. Weber, R. Fischer, R. Saf, A. E. Stuetz, *Carb. Res.*, **2016**, *436*, 11-19.

### Oral presentations

#### **“Highly Substituted Cyclopentanes as N-Acetyl-Hexosaminidase Inhibitors”**

A. Wolfsgruber, P. Müller, S. A. Nasser, A. E. Stütz, A. Torvisco Gomez, P. Weber, S. G. Withers, T. M. Wrodnigg, A. E. Stütz, 22. Österreichischer Kohlenhydratworkshop, BOKU Wien, 15.-16. February **2018**, Vienna, Austria

#### **“N-Substituted 4-Acetamido-5-amino-1-hydroxymethyl-cyclopentane-diols” (“2-Acetamido-1-amino-β-D-galacto-cyclopentanes”)**

P. Weber, P. Müller, S. A. Nasser, A. E. Stütz, A. Torvisco Gomez, S. G. Withers, A. Wolfsgruber, T. M. Wrodnigg, A. E. Stütz, 22. Österreichischer Kohlenhydratworkshop, BOKU Wien, 15.-16. February **2018**, Vienna, Austria

### 7.3 Curriculum vitae

*Andreas Wolfsgruber, born in Bad Ischl on December 22<sup>nd</sup> 1991 as the son of Franz Wolfsgruber and Hildegard Wolfsgruber (nee Hattinger).*

- Since 04/16      **Master's Programme:** Technical Chemistry, Graz University of Technology. Thesis: Exploratory Studies in the Imino- and Carbasugar area.  
Supervision: Prof. Dr. Arnold E. Stütz
- 04/17 – 07/17      **Visiting Research Student:** Ferrier Research Institute, Victoria University of Wellington. Project title: Synthesis of aza-sugar nucleoside analogues as potential anti-viral agents.  
Supervision: Prof. Peter C. Tyler and Prof. Gary B. Evans
- 10/12 - 04/16      **Bachelor's Programme:** Chemistry, completed at Karl-Franzens University Graz; Thesis: Synthesis of Carbohydrate analogues featuring tertiary fluorine substituents.  
Supervision: Prof. Arnold E. Stütz
- 11/11 – 07/12      **Civilian service:** Upper Austrian life aid (Lebenshilfe Vöcklabruck)
- 09/06 - 06/11      **Secondary School:** HTBLA Wels (Higher technical school), focused on chemistry.